

University of Southern Queensland

Faculty of Engineering and Surveying

Comparison of PV maximum power point.

A dissertation submitted by

Mr Christopher KIRBY

In fulfilment of the requirements of

Bachelor of Engineering (Electrical and Electronic)

October, 2015.

Abstract

Photovoltaic technology began in 1876 with the development of the selenium solar cell, although the limited electrical energy generated was not enough to power any useful machine. Experimentation during the 1950's with alternate materials led to the development of the first silicon based cell. The new silicon cell was selected for use in space exploration to provide a longer lasting energy supply. Modern solar panels are commonly used across the country as part of a distributed electricity supply network.

The electrical power generated by a photovoltaic solar panel will be affected by a large number of factors, ranging from light irradiance level, light angle, location, electrical load on the panels and the configuration of the connection with adjacent panels.

Simulations conducted within Matlab were used to assess the effect of various energy reduction factors when a multiple direction oriented panels are connected in common. The series connected system provided the best level of immunity for the case having unequal levels of shading. The parallel configuration performed better for each of the other cases tested, including mismatched voltage and current specifications, irradiance level, ambient temperature and only angular offset.

The efficiency of a solar panel decreases with increased cell temperature. Natural convection currents surrounding the panel assist with cooling and are increase with a larger panel tilt angle. Experimentation results indicated a linear increase in the panel efficiency of approximately 0.05% per degree tilt increase.

The optimum azimuth and tilt angles vary depending on the installation location. Data obtained using the Homer microgrid modelling package was used to identify the optimum installation angles for four locations throughout Australia. A mathematical model was developed to describe the azimuth and tilt relationship. Further modelling conducted using Homer included a second photovoltaic string. Simulations of different inverter configurations indicated the dual power point tracking provided the best efficiency for all situations. Single power point tracking and separate inverters were able to demonstrate similar efficiencies when components of the installation were matched, and panels were installed on a common orientation.

The goal of this project was to provide information which could assist designers of solar generation installations maximise the electrical energy generated over the life of the system.

The recommendations are the correct inverter selection, prioritisation of the most north facing roof surface, and setting tilt angle relative to the actual installation azimuth will deliver superior energy yields than a generalised installation approach.

University of Southern Queensland

Faculty of Health, Engineering and Sciences

ENG4111/ENG4112 Research Project

Limitations of Use

The Council of the University of Southern Queensland, its Faculty of Health, Engineering & Sciences, and the staff of the University of Southern Queensland, do not accept any responsibility for the truth, accuracy or completeness of material contained within or associated with this dissertation.

Persons using all or any part of this material do so at their own risk, and not at the risk of the Council of the University of Southern Queensland, its Faculty of Health, Engineering & Sciences or the staff of the University of Southern Queensland.

This dissertation reports an educational exercise and has no purpose or validity beyond this exercise. The sole purpose of the course pair entitled “Research Project” is to contribute to the overall education within the student’s chosen degree program. This document, the associated hardware, software, drawings, and other material set out in the associated appendices should not be used for any other purpose: if they are so used, it is entirely at the risk of the user.

Certification of work

I certify the information and work contained within this dissertation, including computer assisted modelling, experimentation, calculated results, analysis and conclusions are entirely my own work, excepting where indication of another source and acknowledgement has been provided.

I further certify this work is original and has not been previously been submitted in any other course or institution.

Christopher Kirby

0050093295

Acknowledgements

This research was conducted under the supervision of Catherine Hills, providing advice and assistance during the course of this dissertation.

I would also like to acknowledge the assistance of the following people,

- Gemma for patience and support throughout the course of my study.
- Madison for patience throughout this dissertation.
- John and Carol Kirby for assistance looking after Madison.
- Andreas Helwig for providing the main project idea and assisting in the development of ideas.
- Les Bowtell for advice regarding convective cooling of panels and assistance to conduct thermal cooling experimentation.
- Wayne Cheary for listening to the endless volumes of information I have reviewed and also for providing advice on avenues of research.
- Antony Zizimou for listening to the information I have reviewed.
- Homer Energy for the use of their microgrid modelling software.

Table of Contents

| | |
|---|-----|
| Abstract | i |
| Limitations of Use..... | iii |
| Certification of work..... | iv |
| Acknowledgements | v |
| Table of Contents | vi |
| List of figures | xii |
| List of tables | xvi |
| 1. Introduction | 1 |
| 2. Literature review..... | 2 |
| 2.1. History of photovoltaic technology..... | 2 |
| 2.2. Construction of photovoltaic systems..... | 3 |
| 2.2.1. Cell construction..... | 3 |
| 2.2.2. Panel construction..... | 4 |
| 2.2.3. Series or parallel connected cells..... | 4 |
| 2.2.4. Inverters..... | 5 |
| 2.3. Principle of photovoltaic operation..... | 5 |
| 2.3.1. PV cell power output..... | 6 |
| 2.3.1.a. Incident solar energy..... | 7 |
| 2.3.1.b. Cell size..... | 8 |
| 2.3.1.c. Light angle..... | 8 |
| 2.3.1.d. Light reflection..... | 10 |
| 2.3.1.e. Panel loading | 11 |
| 2.3.1.f. Panel / Cell design and manufacturing..... | 11 |
| 2.3.1.g. Panel shading..... | 13 |
| 2.3.1.h. Panel efficiency | 13 |
| 2.3.1.i. Panel age..... | 14 |

| | | |
|----------|---|----|
| 2.3.1.j. | Temperature..... | 14 |
| 2.3.1.k. | Installation design..... | 16 |
| 2.3.1.l. | Air mass..... | 16 |
| 2.4. | Inverter design | 17 |
| 2.4.1. | Introduction to converters..... | 17 |
| 2.4.2. | Operation of inverters..... | 17 |
| 2.4.3. | Grid fed inverters..... | 18 |
| 2.4.4. | Single stage inverters..... | 18 |
| 2.4.5. | Multiple stage inverters..... | 18 |
| 2.4.6. | Inverter efficiency..... | 19 |
| 2.4.6.a. | Over voltage..... | 19 |
| 2.4.6.b. | Under voltage | 19 |
| 2.4.6.c. | Over power | 19 |
| 2.4.6.d. | Under power | 20 |
| 2.4.7. | Maximum power point tracking..... | 20 |
| 2.4.7.a. | Perturb and observe..... | 20 |
| 2.4.7.b. | Incremental conductance..... | 21 |
| 2.5. | Modelling..... | 22 |
| 2.5.1. | IV Curve Modelling..... | 22 |
| 2.5.1.a. | IV and PV curves..... | 23 |
| 2.5.1.b. | Location of maximum power point..... | 24 |
| 3. | Project planning..... | 25 |
| 3.1. | Ethics..... | 25 |
| 3.2. | Methodology..... | 25 |
| 3.2.1. | Required resources..... | 25 |
| 3.2.2. | Identification and sourcing of relevant literature..... | 26 |
| 3.2.3. | Modelling multiple interconnected solar panels..... | 26 |

| | | |
|----------|--|----|
| 3.2.4. | Modelling solar panel optimum angle. | 27 |
| 3.2.5. | Modelling multiple string systems..... | 28 |
| 3.2.6. | Selection of installation locations. | 28 |
| 3.2.6.a. | Brooklyn Park, S.A..... | 29 |
| 3.2.6.b. | Toowoomba, Qld..... | 30 |
| 3.2.6.c. | .Darwin, N.T. | 31 |
| 3.2.6.d. | Hobart, Tas. | 32 |
| 3.2.7. | Panel angle effect on cooling..... | 33 |
| 3.2.8. | Development of installation guidelines. | 33 |
| 3.3. | Project timeline..... | 34 |
| 3.4. | Assessment of consequential effects..... | 35 |
| 3.4.1. | Identification of hazards. | 36 |
| 3.4.2. | Risk assessment. | 36 |
| 3.4.3. | Risk matrix scores..... | 37 |
| 3.4.4. | Risk assessment outcomes..... | 37 |
| 3.4.5. | Project hazard identification and risk assessment..... | 38 |
| 4. | Results..... | 39 |
| 4.1. | IV Curve modelling. | 39 |
| 4.1.1. | Differing panel angle. | 40 |
| 4.1.2. | Hard shading panels with varied panel angle. | 42 |
| 4.1.2.a. | Equal shaded area. | 42 |
| 4.1.2.b. | Unequal shaded area: Parallel connected. | 44 |
| 4.1.2.c. | Unequal shaded area: Series connected..... | 47 |
| 4.1.3. | Mismatched panel specifications..... | 50 |
| 4.1.3.a. | Mismatched voltage specifications: Parallel connection..... | 50 |
| 4.1.3.b. | Mismatched voltage specifications: Series connection..... | 52 |
| 4.1.3.c. | Mismatched current specifications: Parallel connection. | 53 |

| | | |
|-------------|--|----|
| 4.1.3.d. | Mismatched current specifications: Series connection..... | 55 |
| 4.1.4. | Varied temperature. | 56 |
| 4.1.4.a. | Varied temperature: Parallel connection | 57 |
| 4.1.4.b. | Varied temperature: Series connection..... | 59 |
| 4.1.5. | Varied irradiance..... | 61 |
| 4.1.5.a. | Varied irradiance: Parallel connection..... | 61 |
| 4.1.5.b. | Varied irradiance: Series connection..... | 63 |
| 4.2. | Thermal cooling experimentation..... | 65 |
| 4.3. | Homer energy modelling. | 67 |
| 4.3.1. | Single string | 67 |
| 4.3.1.a. | Optimum installation angle: 15 degree resolution..... | 68 |
| 4.3.1.b. | Optimum installation angle: 1 degree resolution..... | 69 |
| 4.3.1.c. | Site position effect on optimum installation angle. | 71 |
| 4.3.1.d. | Site position effect on optimum tilt without optimum azimuth. | 73 |
| 4.3.1.e. | Model for determination of optimum tilt and azimuth. | 73 |
| 4.3.1.f. | Single panel model using calculated tilt installation angles..... | 76 |
| 4.3.2. | Dual string modelling. | 78 |
| 5. | Conclusion | 79 |
| 5.1. | Further work. | 80 |
| 6. | References | 81 |
| Appendix A. | Project Specification | |
| Appendix B. | Project timeline | |
| Appendix C. | Derivation of formulas..... | |
| C.1. | Current voltage relationship: IV curve | C1 |
| C.1.1. | Solar panel model | C1 |
| C.1.2. | Solar panel model error..... | C2 |
| C.1.3. | Optimum azimuth | C8 |

| | | |
|-------------|---|-----|
| C.1.4. | Optimum tilt..... | C12 |
| C.1.5. | Optimum tilt correction factor (C)..... | C16 |
| Appendix D. | Matlab code..... | |
| D.1. | Function: Solar_Panel_Model_Par..... | D1 |
| D.2. | Function: Solar_Panel_Model_Ser..... | D2 |
| D.3. | Script: Efficiency_calculator_Par..... | D4 |
| D.4. | Script: Efficiency_calculator_Ser..... | D9 |
| D.5. | Script: Error Search..... | D14 |
| D.6. | Script: Varied_Irradiance_Plot..... | D15 |
| D.7. | Script: Varied_Temperature_Plot..... | D16 |
| Appendix E. | Modelling results..... | |
| E.1. | Optimum installation plots..... | E1 |
| E.1.1. | Brooklyn Park..... | E1 |
| E.1.2. | Toowoomba..... | E3 |
| E.1.3. | Darwin..... | E5 |
| E.1.4. | Hobart..... | E7 |
| E.2. | Location offset plots..... | E9 |
| E.2.1. | Brooklyn Park..... | E9 |
| E.2.2. | Toowoomba..... | E11 |
| E.2.3. | Darwin..... | E13 |
| E.2.4. | Hobart..... | E15 |
| Appendix F. | Hazard identification and risk assessments..... | |
| F.1. | Hazard identification..... | F1 |
| F.1.1. | Solar installations..... | F1 |
| F.1.2. | Project..... | F2 |
| F.2. | Risk matrix scores..... | F2 |
| F.3. | Risk assessment..... | F3 |

| | | |
|-------------|---------------------------------------|----|
| F.3.1. | Solar installations..... | F3 |
| F.3.2. | Project. | F5 |
| Appendix G. | Specification sheets | |
| G.1. | Hareon Solar specification sheet..... | G1 |
| G.2. | Tindo Solar specification sheet..... | G3 |

List of figures

| | |
|---|----|
| Figure 2.1 – Photovoltaic cell cross section..... | 3 |
| Figure 2.2 – Cell, Module, Panel and array relationship | 4 |
| Figure 2.3 – Photovoltaic operation | 6 |
| Figure 2.4 – Solar radiation and electromagnetic spectrum..... | 7 |
| Figure 2.5 – Light reflection characteristics | 10 |
| Figure 2.6 – Generalised IV curve power voltage curve | 11 |
| Figure 2.7 – Generalised IV curve power voltage curve, varied temperature | 14 |
| Figure 2.8 – Perturb and observe flowchart | 21 |
| Figure 2.9 – Incremental conductance flowchart..... | 22 |
| Figure 3.1 – Brooklyn Park site overview | 29 |
| Figure 3.2 – Toowoomba site overview..... | 30 |
| Figure 3.3 – Darwin site overview | 31 |
| Figure 3.4 – Hobart site overview | 32 |
| Figure 4.1a –Parallel MPPT: Panel 1: 0°, Panel 2: 0°-56°..... | 40 |
| Figure 4.1b –Series MPPT: Panel 1: 0°, Panel 2: 0°-56°..... | 41 |
| Figure 4.2a –Parallel MPPT: 1/3 panel shading..... | 43 |
| Figure 4.2b –Series MPPT: 1/3 panel shading..... | 43 |
| Figure 4.3a –Parallel MPPT: Panel 1 @ 2/3 & Panel 2 @ unshaded. | 44 |
| Figure 4.3b – Parallel MPPT: Panel 1 @ 2/3 & Panel 2 @ 1/3 shading..... | 45 |
| Figure 4.4a – Parallel MPPT: Panel 1 unshaded & Panel 2 @ 2/3 shading. | 46 |
| Figure 4.4b – Parallel MPPT: Panel 1 @ 1/3 & Panel 2 @ 2/3 shading..... | 46 |
| Figure 4.5a – Series MPPT: Panel 1 @ unshaded & Panel 2 @ 1/3 shading. | 47 |
| Figure 4.5b – Series MPPT: Panel 1 @ unshaded & Panel 2 @ 2/3 shading. | 48 |
| Figure 4.6a – Series MPPT: Panel 1 @ 2/3 shaded & Panel 2 @ unshaded..... | 49 |
| Figure 4.6b – Series MPPT: Panel 1 @ 2/3 shaded & Panel 2 @ 1/3 shading..... | 49 |

| | |
|--|----|
| Figure 4.7a –Parallel MPPT: Voc @ 29.0V & 30.8V..... | 51 |
| Figure 4.7b – Parallel MPPT: Voc @ 30.8V & 29.0V | 51 |
| Figure 4.8b –Series MPPT: Voc @ 30.8V & 29.0V..... | 53 |
| Figure 4.9a –Parallel MPPT: Isc @ 8.11A & 8.61A..... | 54 |
| Figure 4.9b – Parallel MPPT: Isc @ 8.61A & 8.11A | 54 |
| Figure 4.10a –Series MPPT: Isc @ 8.11A & 8.61A..... | 55 |
| Figure 4.10b – Series MPPT: Isc @ 8.61A & 8.11A..... | 56 |
| Figure 4.11a – Parallel MPPT: T @ 25°C | 57 |
| Figure 4.11b – Parallel MPPT: T @ 15°C | 58 |
| Figure 4.11c – Parallel MPPT: T @ 35°C | 58 |
| Figure 4.12a – Series MPPT: T @ 25°C..... | 59 |
| Figure 4.12b – Series MPPT: T @ 15°C..... | 60 |
| Figure 4.12c – Series MPPT: T @ 35°C..... | 60 |
| Figure 4.13a – Parallel MPPT: G @ 1000W/m ² | 62 |
| Figure 4.13b – Parallel MPPT: G @ 800W/m ² | 62 |
| Figure 4.13c – Parallel MPPT: G @ 400W/m ² | 63 |
| Figure 4.14a – Series MPPT: G @ 1000W/m ² | 64 |
| Figure 4.14b – Series MPPT: G @ 800W/m ² | 64 |
| Figure 4.14c – Series MPPT: G @ 400W/m ² | 65 |
| Figure 4.15 – Normalised cell temperature..... | 66 |
| Figure 4.16 – Tilt angle efficiency..... | 67 |
| Figure 4.17a – Brooklyn Park optimum tilt angle and generated power. | 69 |
| Figure 4.17b – Brooklyn Park optimum tilt angle and generated power. | 70 |
| Figure 4.18 – Optimum tilt angle change per° of latitude versus panel azimuth..... | 73 |
| Figure 4.19 – Optimum azimuth calculated model error. | 75 |
| Figure 4.20 – Optimum tilt calculated model error..... | 76 |

| | |
|--|----|
| Figure 4.21 – Generated power: 2 string 3kW at Azimuth 177..... | 78 |
| Figure C.1a – Varied irradiance model..... | C3 |
| Figure C.1b – Bellini et al. Varied irradiance..... | C4 |
| Figure C.2a – Varied temperature model..... | C4 |
| Figure C.2b – Bellini et al. Varied temperature..... | C5 |
| Figure C.3a – Model V_{OCM} vs irradiance..... | C6 |
| Figure C.3b – Corrected V_{OCM} vs irradiance..... | C6 |
| Figure C.4a – Varied irradiance corrected..... | C7 |
| Figure C.4b – Varied temperature corrected..... | C7 |
| Figure E.1 – Brooklyn Park optimum tilt angle & generated power: 15° resolution | E1 |
| Figure E.2 – Brooklyn Park generated power surface plot: 15° resolution | E2 |
| Figure E.3 – Brooklyn Park optimum tilt angle and generated power: 1° resolution.... | E2 |
| Figure E.4 – Brooklyn Park generated power surface plot: 2° resolution | E2 |
| Figure E.5 – Toowoomba optimum tilt angle and generated power: 15° resolution | E3 |
| Figure E.6 – Toowoomba generated power surface plot: 15° resolution..... | E3 |
| Figure E.7 – Toowoomba optimum tilt angle and generated power: 1° resolution | E4 |
| Figure E.8 – Toowoomba generated power surface plot: 2° resolution..... | E4 |
| Figure E.9 – Darwin optimum tilt angle and generated power: 15° resolution | E5 |
| Figure E.10 – Darwin generated power surface plot: 15° resolution..... | E5 |
| Figure E.11 – Darwin optimum tilt angle and generated power: 1° resolution | E6 |
| Figure E.12 – Darwin generated power surface plot: 2° resolution..... | E6 |
| Figure E.13 – Hobart optimum tilt angle and generated power: 15° resolution | E7 |
| Figure E.14 – Hobart generated power surface plot: 15° resolution..... | E7 |
| Figure E.15 – Hobart optimum tilt angle and generated power: 1° resolution | E8 |
| Figure E.16 – Hobart generated power surface plot: 2° resolution..... | E8 |
| Figure E.17 – Brooklyn Park 5°N generated power surface plot: 2° resolution | E9 |

| | |
|---|-----|
| Figure E.18 – Brooklyn Park 5°S generated power surface plot: 2° resolution..... | E9 |
| Figure E.19 – Brooklyn Park 5°E generated power surface plot: 2° resolution | E10 |
| Figure E.20 – Brooklyn Park 5°W generated power surface plot: 2° resolution..... | E10 |
| Figure E.21 – Toowoomba 5°N generated power surface plot: 2° resolution | E11 |
| Figure E.22 – Toowoomba 5°S generated power surface plot: 2° resolution..... | E11 |
| Figure E.23 – Toowoomba 5°E generated power surface plot: 2° resolution..... | E12 |
| Figure E.24 – Toowoomba 5°W generated power surface plot: 2° resolution | E12 |
| Figure E.25 – Darwin 5°N generated power surface plot: 2° resolution | E13 |
| Figure E.26– Darwin 5°S generated power surface plot: 2° resolution..... | E13 |
| Figure E.27 – Darwin 5°E generated power surface plot: 2° resolution..... | E14 |
| Figure E.28 – Darwin 5°W generated power surface plot: 2° resolution | E14 |
| Figure E.29 – Hobart 5°N generated power surface plot: 2° resolution | E15 |
| Figure E.30 – Hobart 5°S generated power surface plot: 2° resolution..... | E15 |
| Figure E.32 – Hobart 5°W generated power surface plot: 2° resolution | E16 |
| Figure G.1a – Hareon solar specification sheet | G1 |
| Figure G.1b – Hareon solar specification sheet | G2 |
| Figure G.2a – Tindo solar specification sheet | G3 |
| Figure G.2b – Tindo solar specification sheet..... | G4 |

List of tables

| | |
|---|-----|
| Table 4.1 – Optimum installation angles and generated power. | 70 |
| Table 4.2 – Optimum installation at varied site location. | 72 |
| Table 4.3 – Calculated optimum installation angles. | 77 |
| Table B.1 – Project timeline..... | B1 |
| Table C.1 – IV curve input parameters. | C3 |
| Table C.2 – Non optimum tilt angle scaling relative to optimum tilt. | C16 |
| Table F.1 – Risk management score. | F3 |
| Table F.2 – Risk score..... | F3 |
| Table F.3 – Risk assessment: Solar installation. | F4 |
| Table F.4 – Risk assessment: Project. | F5 |

1. Introduction

Solar panels are widely used throughout our community for the generation of electrical power. The aim of this project will be to determine the installation parameters for solar panel installations which maximises the energy generated throughout the life of the installation, and reducing carbon emissions from electrical power generation. Matlab will be used to model the effect of various environmental factors, installation parameters and connection configurations on the output of a small scale solar system. Homer microgrid software will be used to determine the parameters for optimum installation, and the effect of various configurations to the annual power generation. The final section will include guidelines for installation to achieve maximum power generation.

2. Literature review.

The main focus of this project is to optimise the operating efficiency of solar energy systems throughout Australia. There is a large amount of literature available relating to factors which affect the efficiency photovoltaic cells. Standardised test parameters have been adopted by the industry for the testing of solar panels. (National Instruments, 2009a) A majority of the information relating to solar panel efficiency has been sourced from works where the author or sponsoring organisation is involved in research of photovoltaic technology.

2.1. **History of photovoltaic technology.**

The discovery of the photoelectric effect was the result of experiments conducted by William Grylls Adams and Richard Evans Day in 1876. The experimentation involved subjecting selenium to a light source and observing the resulting electrical current produced. The power generated by solar cells manufactured using selenium was insufficient to power any equipment. (Perlin, n.d)

In 1953, scientists at Bell Laboratories produced a silicon based solar cell while researching possible uses of silicon within the electronic industry. The resulting cell generated significantly more power than the selenium cell. The demand for silicon solar cells for power generation applications was limited due to the high cost of manufacturing the cells. (Perlin, n.d)

With the development of earth orbiting satellites and the associated electronic systems, an energy supply lasting longer than conventional batteries was required. Silicon based solar cells provided the solution, leading to a demand for the technology. (Perlin, n.d)

Throughout the 1970's continued development into silicon based solar technology led to a deduction of the per watt unit cost. The cost limited demand for use in remote locations, not serviced through mains power grids. (Perlin, n.d)

Recent years has seen the technology expanded to small scale distributed electricity generation. Each month, over 15000 systems are installed throughout Australia. The total installed capacity exceeded 4GW prior to the end of 2014. (Renew Economy, 2015)

2.2. Construction of photovoltaic systems.

2.2.1. Cell construction.

Polycrystalline photovoltaic cells are manufactured from a thin wafer of boron doped silicon which form a P-type semiconductor. This doping process is achieved by heating the poly-silicon to the melting point, and adding trace amounts of boron. This is then formed into a block before being cut into thin wafers and surface etched to provide a smooth outer surface. A diffusion furnace is then used to create a thin layer of phosphorous on the outside of the wafer to serve as an N-type semiconductor. A conductive material is then attached to the one side of the wafer, removing the N--type material and creating a P plane. Electrical connections are added, enabling the connection of the cell to various other components. (The Florida Solar Energy Centre, 2014b) The cross section of a typical solar cell is shown in figure 2.1. (National Instruments, 2009a) Typical open circuit voltages produced by photovoltaic cells are usually 0.5 – 0.6 V dc, and the current output will be determined by the size of the cell. (The Florida Solar Energy Centre, 2014c)

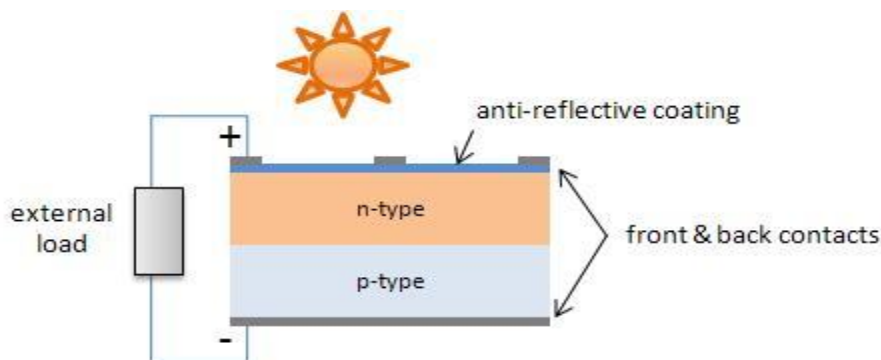


Figure 2.1 – Photovoltaic cell cross section

National Instruments, 2009a

2.2.2. Panel construction.

Photovoltaic modules are constructed by interconnecting a number of cells, and further connected with additional modules to form a panel. These connections may be either series or parallel depending on the output voltage, current or power requirements. (The Florida Solar Energy Centre, 2014a) Both Tindo Solar and Hareon Solar produce panels which have 60 individual cells connected in series, and specification sheets for each manufacturer are located in Appendix G. (Tindo Solar, 2015; Jiangyin Hareon Power Co Ltd, n.d) The connection of multiple panels is referred to as an array. Figure 2.2 shows the relationship between cells, modules, panels and an array. (The Florida Solar Energy Centre, 2014a)

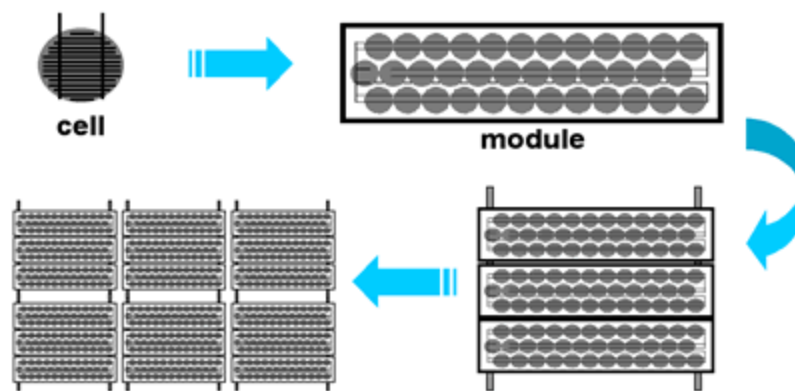


Figure 2.2 – Cell, Module, Panel and array relationship

The Florida Solar Energy Centre, 2014a

2.2.3. Series or parallel connected cells.

The effect of connecting photovoltaic cells in parallel or series it to increase the power generated to levels above the capability of a single cell. Parallel connections are used to increase the current, while the voltage will be common. The current generated by the parallel connected cells must not exceed the rated current input of the inverter. Any imbalance in cell voltage may lead to circulating currents and heating within some of the

cells. (MPPT Solar, n.d a) Cells which are connected in series increase the current, while maintaining a common voltage throughout the series link. The series connected string must be configured so the maximum voltage output does not exceed the specified voltage rating of the inverter. (MPPT Solar, n.d.b)

2.2.4. Inverters.

Inverters are electronic devices which are used to convert DC power into AC for use throughout the home, or exporting to the mains electricity grid. (Ahfock, 2011) Maximum power point tracking is a feature associated with modern solar inverters. This maximises the power generated by a photovoltaic panel. (National Instruments, 2009c)

2.3. Principle of photovoltaic operation

The photovoltaic effect is the principle of converting energy stored within light photons into electrical energy is shown in figure 2.3 (The Florida Solar Energy Centre, 2014c), using silicon based semiconductor materials. Photons within the spectrum of energy emitted by the sun, and colliding with a photovoltaic cell cause an energy increase of the electrons within the outer level of the semiconductor atoms. When this energy reaches a threshold known as the bandgap energy, electrons break away from their atoms moving through the semiconductor forming a flow of current. (National Instruments, 2009a)

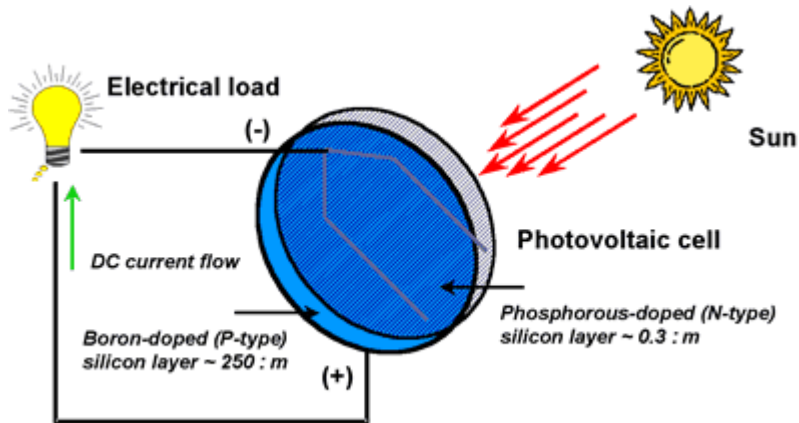


Figure 2.3 – Photovoltaic operation

The Florida Solar Energy Centre, 2014c

2.3.1. PV cell power output.

The power output from a photovoltaic cell is variable, and will be influenced by a large number of factors. (National Instruments, 2009b) These factors include;

- Panel loading,
- Incident solar energy
 - Light spectrum,
 - Current density,
 - Angle to the cell, (National Instruments, 2009b)
- Cell size, (National Instruments, 2009a)
- Panel / Cell design and manufacturing. (National Instruments, 2009b)
- Panel shading, (Sargosis Solar & electric, 2014b)
- Panel efficiency, (National Instruments, 2009b)
- Panel age, (Jordan & Kurtz, 2012)
- Temperature, (National Instruments, 2009b)
- Installation design, (Honsberg & Bowden, 2013k)
- Air mass, (National Instruments, 2009a)
- Optical losses. (Honsberg & Bowden, 2013m)

2.3.1.a. Incident solar energy.

Solar irradiance is a measurement of energy radiated by the sun, measured in watts per square metre. (Honsberg & Bowden, 2013p) Flat plate solar panels are commonly tested using a light energy input equal to 1000 watts per square metre and an air mass of 1.5. (The Florida Solar Energy Centre, 2014a)

Radiated energy which forms part of the electromagnetic spectrum can be described as a wave with defined wavelength, or a particle of energy called a photon. (Honsberg & Bowden, 2013o) Only a small region of the electromagnetic spectrum is visible to the human eye, known as the visible spectrum, and shown in figure 2.4 (Green Rhino Energy Ltd, 2013). The visible spectrum begins at beginning at a wavelength of approximately 400nm for blue light and ending about 700nm for red light. The energy contained within photons vary depending on the wavelength as shown in equation 2.1. (Honsberg & Bowden, 2013o)

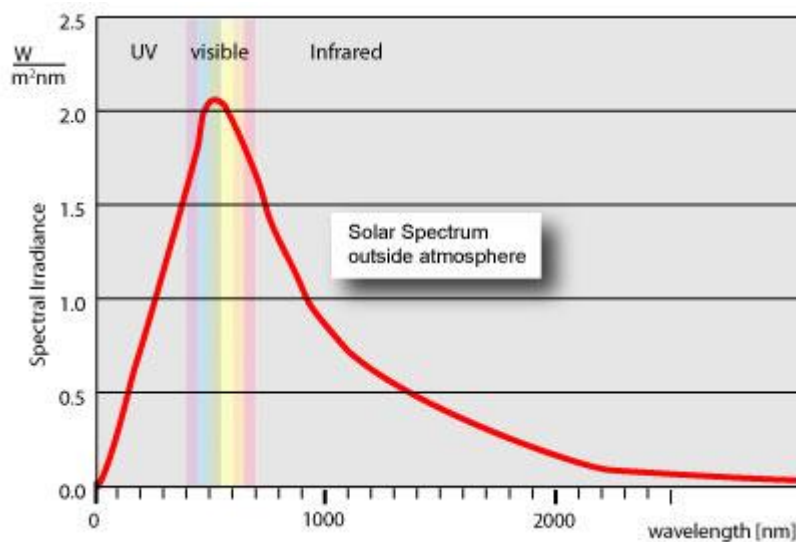


Figure 2.4 – Solar radiation and electromagnetic spectrum

Green Rhino Energy Ltd, 2013

$$E = hf = \frac{hc}{\lambda} \quad (2.1)$$

where h is Planck's constant [$h = 6.626 \times 10^{-34} \text{ Joule. s}$];

c is Speed of light in a vacuum [$c = 2.998 \times 10^8 \text{ m. s}^{-1}$]; and

λ is the light wavelength (Honsberg & Bowden, 2013h)

Photon flux is a term used to define the density of photons from a light source. The greater the number of photons being absorbed into the semiconductor material, the higher the current density within the panel as more electrons available within the conduction band. Multiplying the photon energy together with the photon flux for a given wavelength will provide the available energy for such wavelength. (Honsberg & Bowden, 2013n)

2.3.1.b. **Cell size.**

The energy transmitted through light is defined as being the total radiated energy in watts, distributed evenly across a square metre on a plane perpendicular to the direction of light. The electrical energy generated by the cell will be proportional the area of the collection area. (Green Rhino Energy Ltd, 2013)

2.3.1.c. **Light angle.**

The angle of the light source is a factor which will determine the electrical energy output. Efficiency of the panel will be at maximum when the light source is perpendicular with the surface of the panel, and increasing the angle of incidence of the light leads to the energy being distributed over a larger area, of reduced energy input for the same area.

(Green Rhino Energy Ltd, 2013) The factor of this reduction is described by equation 2.2 (Honsberg & Bowden, 2013s)

$$I(\vartheta) = I_o \cos(\vartheta) \quad (2.2)$$

where I is the intensity of the light source and ϑ is the angular difference between the source of light and perpendicular to the panel. (Honsberg & Bowden, 2013s)

The electromagnetic waves emitted by the sun are not polarised, meaning they are random in rotation about axis of travel. The energy component on the parallel polarisation is equal to the energy component in the perpendicular polarisation plane. (Howell et al, 2010)

The angle at which light reflected from the surface of an object, and light refracted through are perpendicular to each other is called the Brewster angle. This is also the angle at which maximum polarisation will occur. (Encyclopædia Britannica, Inc, 2015a) The energy available to the cell will be greatly reduced due to the polarising effect. The Brewster angle can be defined in terms of the refractive indexes of the two medium which the light is transitioning, and described by equation 2.3. (Howell et al, 2010) Values of refractive index for air is 1.0002 and for crown glass is 1.517. Encyclopædia Britannica, Inc, 2015b)

$$\text{Brewster's angle} \quad \rho = \tan^{-1} \left(\frac{n_2}{n_1} \right) \quad (2.3)$$

Where n is the refractive indexes for each medium.

Substitution of the above refraction values into equation 2.3 provides an angle of 56.6° for light transferring from air into crown glass.

2.3.1.d. Light reflection.

Light energy which is reflected from the surface of a solar panel is lost, providing no benefit to the electrical power output of the panel. The volume of reflected energy from a silicon solar cell may exceed 30% which may be reduced by adding an anti-reflective layer or texturing the surface. The anti-reflective coating is a thin dielectric layer applied to the surface of the cell. The thickness of the layer is designed to reflect light out of phase from the light reflected from the surface of the cell. (Honsberg & Bowden, 2013b) Surface texturing is the process of etching the surface of the cell to produce a rough texture. The angles of the etched surface are intended direct any reflected light back to the cell surface. (Honsberg & Bowden, 2013t)

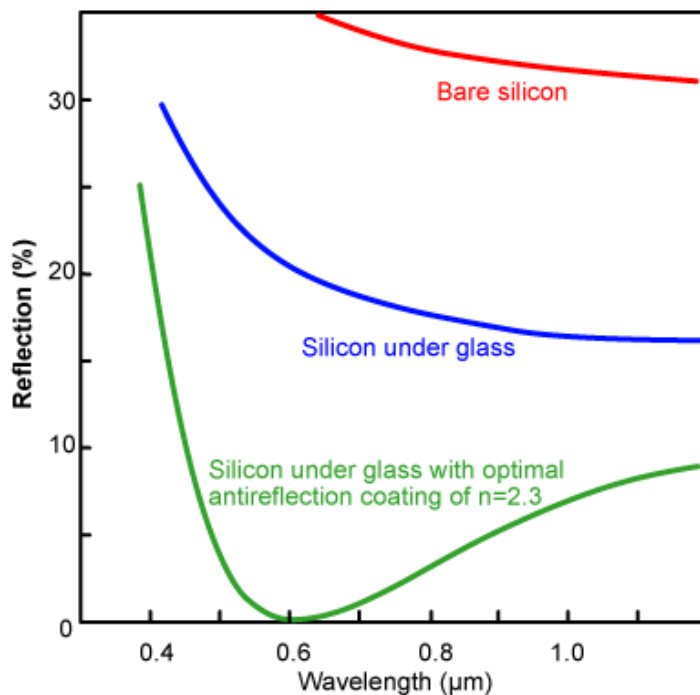


Figure 2.5 – Light reflection characteristics

Honsberg & Bowden, 2013b

The level of reflection is shown in Figure 2.5. The use of properly designed reflection minimisation techniques may reduce the volume of lost energy to negligible levels for a given light wavelength. (Honsberg & Bowden, 2013b)

2.3.1.e. Panel loading

The energy generated by a PV cell is represented by the IV curve. Figure 2.6 shows the relationship between voltage and current at several irradiance values, and can easily be converted to an equivalent voltage power curve shown to the right hand side of the figure. The voltage power curve allows for easy identification of the maximum power point of the panel. (Sargosis Solar & Electric, 2014a) One function of the inverter is varying the load on the PV panels to maintain operation at the maximum power output, and will be discussed in further detail later. (Xue et al 2004)

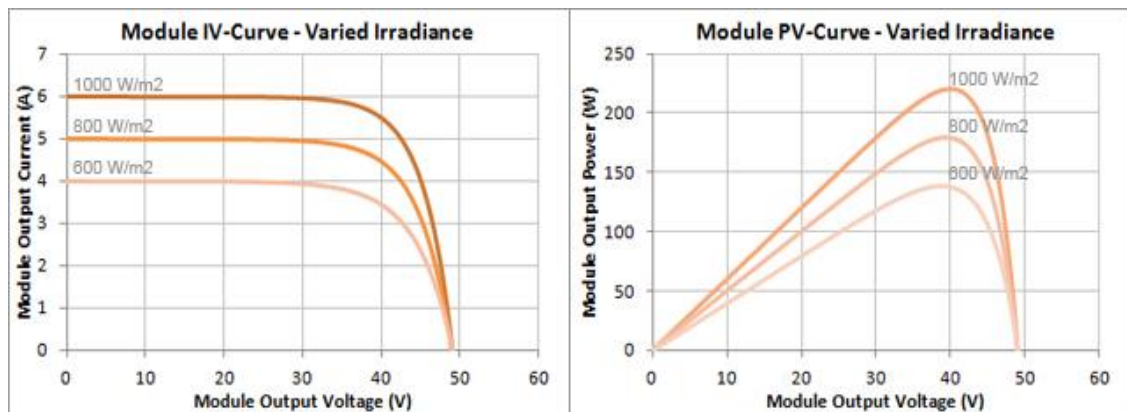


Figure 2.6 – Generalised IV curve power voltage curve

Sargosis Solar & Electric, 2014a

2.3.1.f. Panel / Cell design and manufacturing

Intelligent design and care in manufacturing PV cells can aid in the reduction of internal energy losses. The power output of a PV cell will be at maximum at the point load impedance is equal to the characteristic impedance of the cell. (Honsberg & Bowden,

2013d) Parasitic resistance is the term given to the internal series and (shunt) parallel resistances of a PV cell, reducing the energy output through internal dissipation of power. (Honsberg & Bowden, 2013e)

Cells which have a low shunt resistance are often the result of manufacturing defects. The low resistance creates an additional current path, allowing circulating currents to be generated within the cell. (Honsberg & Bowden, 2013r)

Series resistances are formed by the connection of the semiconductor to the metallic output contacts, as well as current flow through the cell. The voltage drop caused by a series resistance will be proportional to the current, therefore the open circuit voltage will not be affected. (Honsberg & Bowden, 2013q)

Light energy which is reflected, not absorbed or shaded from a PV cell do not add any value to the output power. Reflection is reduced through the addition of anti-reflective coatings to the front surface of a PV panel. (Honsberg & Bowden, 2013m) Etching the front surface of the crystalline wafers produces a rough increases the chance of reflected light being redirected onto another surface of the cell. (Honsberg & Bowden, 2013t) Preventing reflection off the rear of the wafer may be achieved by increasing the thickness, although this may lead to a reduction in the probability the light will generate a current in the cell. (Honsberg & Bowden, 2013m)

Series connected cells can be affected when the output of one or more cells are reduced. Under the condition of a short circuit load, shaded or faulty cells will become reverse biased, dissipating the energy of all other cells as heat. The localised heating may lead to a burnout within the cell. (Honsberg & Bowden, 2013j) Adding a bypass diode reduced the reverse bias voltage of a cell, minimising current, and limiting the effect of local heat dissipation. (Honsberg & Bowden, 2013c)

Circulating currents are formed when differing voltage sources are connected in parallel. When the output from an individual parallel connected cell is reduced, the chance of circulating currents is high. Energy from the circulating current is dissipated within the panel, reducing the power output and potentially damaging the cells. The inclusion of a current blocking diode in series with each parallel connected the cell eliminates the chance of circulating currents from occurring. (Pandit & Chaurasia, 2014)

2.3.1.i. Panel age

Throughout the lifecycle of a PV cell, the efficiency of the cell to convert solar energy into electrical energy is reduced. The rate at which degradation occurs is determined by the construction and materials used to construct the PV cell, as well as the location and climate in which the cell was to be installed. There is no industry standard on what level of reduction is required before the cell is deemed to have failed although for most cell technologies, 20% is considered to be a failure. (Jordan & Kurtz, 2012)

2.3.1.j. Temperature

Temperature changes affect the energy generated by a solar cell. Increases in temperature of a cell lead to a reduction of the band gap energy, leading to an increase of the short circuit current. The intrinsic carrier concentration is determined by the band gap energy, leading to a reduction in the open circuit voltage of the cell. The result of the change to the short circuit current and the open circuit voltage is a decrease in output power. (Honsberg & Bowden, 2013f) The generalised effect of temperature on the IV and PV curves are shown in figure 2.7. (Sargosis Solar & Electric, 2014a)

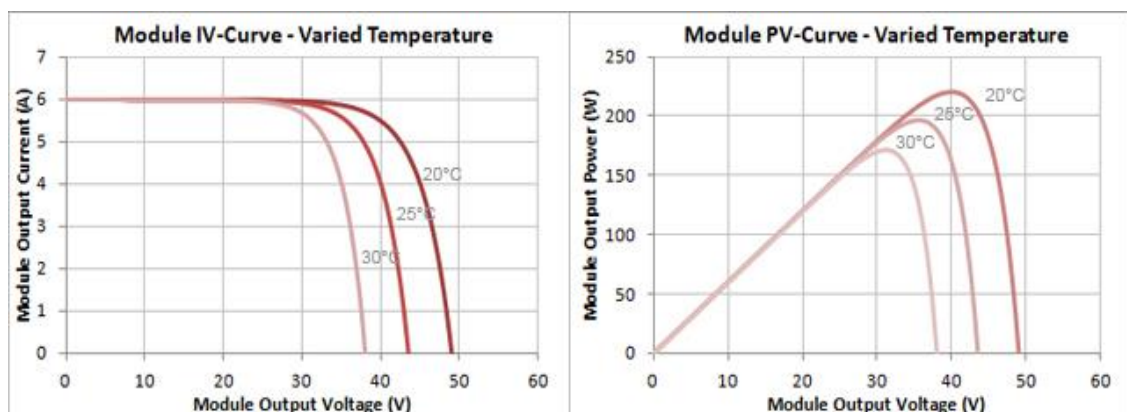


Figure 2.7 – Generalised IV curve power voltage curve, varied temperature

Sargosis Solar & Electric, 2014a

- Radiation will be emitted from any object around us. The power of this radiated energy is determined by the temperature and emissivity of the object. (Honsberg, & Bowden, 2013u)

2.3.1.k. **Installation design**

Mismatch is the situation when one or more cells possess different electrical properties to the remainder of the cells. The effect of mismatch is a reduction of system efficiency and potential for permanent damage to the PV cells. There are numerous causes of mismatch which should be properly assessed during the design of a system, these may include, connection of non-identical cells and panels, shading of a portion of the PV system and connection of differently orientated panels. (Honsberg & Bowden, 2013k)

Parallel connection of solar panels is possible provided the following conditions are met,

- Panel voltage specifications match,
- Panels are installed adjacent and at a common orientation,
- Panels are not subject to uneven shading. (MPPT Solar, n.d. a)

Solar cells are commonly connected in series. Cells which have been shaded present a high resistance to the series connection which may lead to increased heat dissipation. The inclusion of a bypass diode in parallel with a cell, or group of cells will allow current to bypass cells which have been shaded. (MPPT Solar, n.d. b)

2.3.1.l. **Air mass**

Air mass is a relative value used to account for the energy absorbed by particles within our atmosphere. As light passes through earths' atmosphere, air and dust particles absorb some of the energy. The magnitude of energy absorbed is related to the path length of the light. (Honsberg & Bowden, 2013a)

2.4. Inverter design

2.4.1. Introduction to converters.

The development of power electronics has enabled the development of converters which are devices used to convert an electrical input into a more desirable form. Rectifiers, inverters and D.C. to D.C. converters are examples of different types of converters. (Ahfock, 2011)

- Rectifiers are used to convert an alternating current input into a direct current output. The output is dependent on the shape and amplitude of the input. (Ahfock, 2011)
- Inverters are used to convert a direct current input into an alternating current output. The output frequency and voltage are variable. (Ahfock, 2011)
- D.C. to D.C. converters are similar to inverters, except the output is direct current. The voltage is adjustable. (Ahfock, 2011)

2.4.2. Operation of inverters.

Inverters which are commonly used for PV systems normally use a two stage configuration. The first stage of the inverter is used to boost the input voltage, as well as maintaining the PV array at the maximum power point. The conversion from D.C. to A.C. occurs within stage two. (Rosenblatt, L 2015) The inversion process involves the connection of four transistors in a bridge configuration. Switching specific transistors in the correct sequence will provide a square wave output. Adjustment of the switching cycle time and duty cycle will affect the output of the inverter. The addition of frequency filters and the inductance of the load will assist smoothing of the output waveform. The characteristics of the transistors will lead to energy losses of the inverter, consisting of power losses and switching losses. Power losses will be affected by the magnitude of current, and the impedance of the transistor. Switching losses influenced by the time for a transistor to switch from off to on and from on to off, as well as the rate at which the transistor is being switched. (Ahfock, 2011) Single stage inverters perform one voltage change, while multiple stage inverters will perform a larger number of voltage changes. (Xue et al 2004)

2.4.3. Grid fed inverters.

The connection of a PV array to the public utility grid requires the use of an inverter capable of converting the variable direct current power generated by the array into a fixed frequency alternating current supply which is compatible with the grid. This connection is made possible through the use of a grid fed inverter. (Rosenblatt, L 2015) The function of a grid fed inverter is more than performing a voltage conversion. Power delivered to the grid must maintain the same frequency and voltage at the grid while maintaining a sufficiently low level of harmonic distortion. The inverter must be able to protect connected equipment against conditions and energy levels which are outside the normal parameters. (Xue et al 2004)

2.4.4. Single stage inverters.

Single stage inverters provide one point at which voltage change occurs. This stage is responsible for converting the variable dc input from the array to a fixed frequency power output which is compatible with the public utility grid supply, in addition to ensuring isolation between the PV array and the grid and maintaining the operation of the array at the maximum power point. (Xue et al 2004)

2.4.5. Multiple stage inverters.

Inverters which have more than one stage of voltage change are classed as multiple stage. A two stage inverter may provide the required electrical isolation, and convert the variable voltage d.c. from the array into a constant voltage d.c. output. The second stage of the inverter will be used to generate the a.c. output. There are various multi stage inverter configurations which can be used for (Xue et al 2004)

2.4.6. Inverter efficiency.

The voltage and power generated by a solar string may have an adverse effect on the efficiency of an inverter. (Folsom Labs, 2014)

2.4.6.a. Over voltage

The string voltage will be limited by the inverter, preventing any damage due to excessive voltage levels. When the maximum power point voltage for the string is greater than the inverter maximum input voltage, the limiting effect causes the string to operate at a reduced power output. (Folsom Labs, 2014)

2.4.6.b. Under voltage

Inverters will continue to function if the voltage input falls slightly below the nominal operating point, although the generated power will be below the maximum power output of the connected string. Inverters will not function for all voltage levels. Below a minimum voltage threshold, the power supplied from the panels is insufficient to drive the circuitry of the inverter. The inverter does not produce any power under this condition. (Folsom Labs, 2014)

2.4.6.c. Over power

The design of an inverter includes a maximum power rating, and control to prevent this situation from occurring. When the supply from a string begins to exceed this rating, the inverter adjusts the voltage away from the maximum power point, reducing power output. (Folsom Labs, 2014)

2.4.6.d. **Under power**

Data provided by the California Energy Commission indicate the efficiency of an inverter remains relatively constant when the inverter is operating above 30% of full load. The inverter efficiency reduces as the string power is reduced to between 30 - 10%. (Folsom Labs, 2014)

2.4.7. **Maximum power point tracking.**

The power generated by a PV array is dependent on a number of factors, and displayed by the IV curve. The point on the IV curve where the PV array is greatest is called the maximum power point. Environmental factors will influence the solar energy input on a PV array, and hence the output power. The maximum power point does not occur at a fixed position on the IV curve, therefore is unable to be determined in advance. Maximum power point tracking is a function included in modern solar inverters, commonly implemented through constant adjustment of the system operating voltage. There are a number of methods which can be used to monitor and maintain operation at the maximum power point. Two methods of maintaining maximum power are perturb and observe and incremental conductance. (National Instruments, 2009c)

2.4.7.a. **Perturb and observe.**

The Perturb and Observe method maintains the output of the array at the maximum power output by continually monitoring and adjusting the operating voltage or current supplied by the array. After an adjustment of the operating point of the array, the change in power determined. When the result is an increase in power, the process is repeated. Likewise when the result is a decrease in power, the adjustment is performed in the opposite direction. During steady state operation, the continual adjustment of the operating point will lead to oscillation about the maximum power point. The simple implementation for the Perturb and observe method have led to this being the most widely used form of maximum power point tracking. (National Instruments, 2009c)

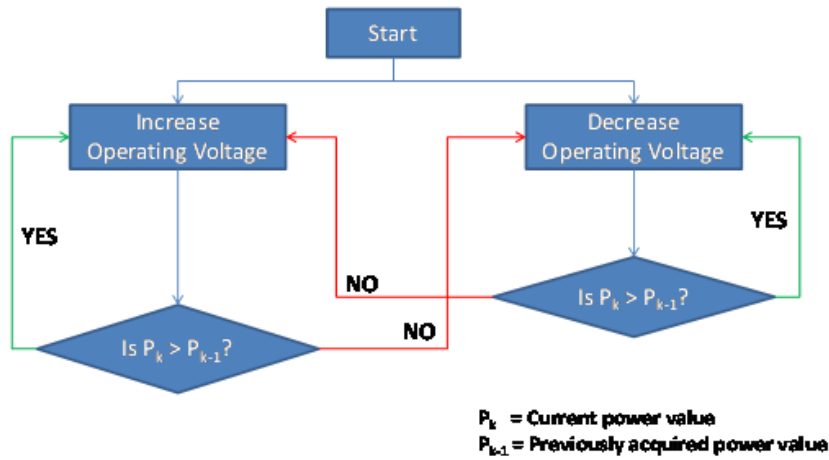


Figure 2.8 – Perturb and observe flowchart

National Instruments, 2009c

2.4.7.b. Incremental conductance.

The incremental conductance operates by monitoring the difference on power output for a difference on system operating voltage. The slope of the power change is assessed, and operating voltage is adjusted accordingly. (National Instruments, 2009c)

- $\frac{dP}{dV} = 0$ No change required, system is at maximum power point.
- $\frac{dP}{dV} > 0$ Increase system voltage.
- $\frac{dP}{dV} < 0$ Decrease system voltage. (National Instruments, 2009c)

The analysis which is performed by the incremental conductance method allows the controller to detect when the maximum power point has been reached, removing the need for the inverter to oscillate about this point. The system responds more accurately to rapid changes in environmental conditions compared to the Perturb and observe method. The

sampling rate of power is reduced compared to the Perturb and Observe as the data processing time is greater. (National Instruments, 2009c)

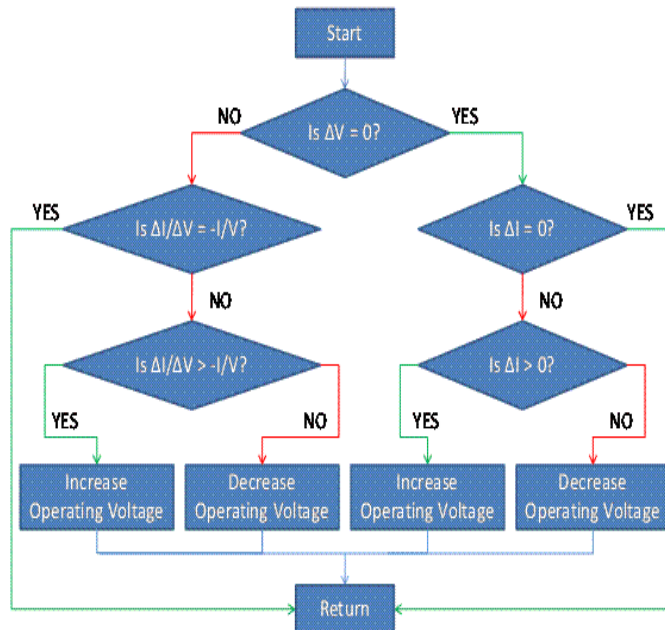


Figure 2.9 – Incremental conductance flowchart

National Instruments, 2009c

2.5. Modelling

2.5.1. IV Curve Modelling

The IV curve of a solar cell is used to display the relationship of current output versus terminal voltage. Multiplying values along the curve by the respective voltage values will provide a power versus voltage curve. (Sargosis Solar & Electric, 2014a) The IV curve modelling will be used to assess the reduction in panel efficiency for the connection of multiple solar panels in both series and parallel connection.

The effect of light reflection will not be considered during the IV curve modelling, as the effect may be reduced to negligible levels by texturing the cell surface and adding anti-reflective coatings. (Honsberg & Bowden, 2013b)

2.5.1.a. IV and PV curves.

Determining the relationship between current and resistance of a solar cell requires knowledge of a number of parameters. (Tayyan, 2006) Equations 2.4a and 2.4b depict the solar cell model developed by Bellini et al. (n.d.). The model allows for the approximation of the relationship between voltage current and power, requiring data which is commonly located on manufacturers datasheets. Tindo solar (2015) and Hareon Solar (Jiangyin Hareon Power Co Ltd, n.d) datasheets located in appendix G provide this data for each respective panel including maximum power point voltage and current, short circuit current and open circuit voltage and normalised to a set of standardised testing conditions. Neither of these sheets provided any information of the internal resistances of the panels.

Current as function of voltage

$$I(V) = I_{SC} \left[1 - C_1 \left(e^{\left(\frac{V}{C_2 \times V_{oc}} \right)} - 1 \right) \right] \quad (2.4a)$$

Voltage as function of current

$$V(I) = C_2 \times V_{oc} \times \ln \left[1 + \frac{\left(1 - \frac{I}{I_{sc}} \right)}{C_1} \right] \quad (2.4b)$$

Power as a function of voltage

$$P(V) = V \times I \quad (2.5)$$

The procedure for this model is located in appendix C, and related Matlab code in Appendix D.

The electrical energy generated by a solar panel will be influenced by a number of factors, including angle of the panel normal to the solar source, irradiance level, ambient air temperature, area of the panel subjected to shading and the voltage and current properties

of the individual panel. The IV curve modelling will be used to assess the efficiency of a system with multiple panels connected in either series or parallel while subjected to different input influences. Equation 2.4a will be used with a common voltage vector to model parallel connected systems, and equation 2.4b will be used for series connected systems with a common current vector. Equation 2.5 will be used to form a power vector.

2.5.1.b. Location of maximum power point.

The process to identify the maximum power point will be derived from the Perturb and observe method as stated by National Instruments (2009c). The voltage vector will be checked for a value matching the calculated maximum power point voltage. The value of the corresponding position on the power vector will be checked and assessed against both adjacent values, indexing the position to the highest value of power. When the selected value of power is greater than both adjacent values, the program loop will be terminated.

3. Project planning.

The successful completion of any major is heavily influenced by the project planning conducted through the early stages of the project. During this phase, the project planner should divide the overall project down into a smaller set of tasks, and develop a methodology for the project completion. Consideration must also be given to the required resources, and their availability. The inclusion of a timeline for the completion of specified tasks will assist in maintaining the project to be completed by the required deadline. (ENG4111 Research project part 1: Project reference book, 2014)

3.1. **Ethics.**

The intention of this project is to improve the annual energy generated by new photovoltaic installations throughout Australia. The installation parameters detailed within are intended to comply with all regulatory requirements, as well as the requirements of the Engineers Australia code of ethics.

3.2. **Methodology.**

The steps required for the investigation of different solar panel and inverter configurations, and the development of optimised installation parameters will be detailed within the following methodology section.

3.2.1. **Required resources.**

MATLAB is a text based computer programming language, specialising in numerical, signal and image processing. The language commonly used throughout various

engineering disciplines, as custom scripts can be written to perform repeated calculations. (Palm, 2009)

Designed by the National Renewable Energy Laboratory, Homer is a software modelling tool specialising in the optimisation of electrical microgrids. The package has the capability to model a variety of supply source options and load profiles. Simulations are conducted to cover each combination of design elements, providing an analysis for the energy generation and consumption together with financial details for each system design option. (Homer Energy, 2015)

3.2.2. Identification and sourcing of relevant literature.

The accuracy of the sourced information is an important factor to maintain the integrity of the finished project. Inaccurate or misleading information may possibly lead to an invalid course of investigation, even an unsubstantiated final outcome. (ENG4111 Research project part 1: Project reference book, 2014)

During the search for information, there will be an emphasis on information sources where the author/s are associated with educational institutions or government. This is intended to remove a potential source of bias, focussing more on information provided by non-commercial sources.

3.2.3. Modelling multiple interconnected solar panels.

The relationship between voltage, current and power will be calculated within MATLAB using the IV curve approximation detailed in appendix C. The combined output from multiple energy sources can be determined by summing the voltage or current for series or parallel connections respectively. The simulation was used to calculate the IV curve for each individual panel, reflecting the output under specific instantaneous installation conditions. The resulting currents will be added along a common voltage vector for parallel and voltage on common current for series connection, along with corresponding

power curves. The slope of each power curve generated are analysed to identify the localised maximum power value. The angle of one panel is indexed, test repeated and power values recorded forming a power to vector relative to angular offset. The resulting information is intended to provide an understanding into the energy losses which are likely to occur when multiple connected panels are installed at differing angles.

3.2.4. Modelling solar panel optimum angle.

Homer Energy will be used to determine the energy produced by a solar energy system with panels orientated at a variety of azimuth and tilt angles at four location throughout Australia. In the first stage of modelling, the azimuth will be assessed at 15° intervals over a complete 360° range, and tilt at 15° intervals and a 90° range. This stage is intended to demonstrate the effect of azimuth and tilt have on the annual energy production of solar systems. The second modelling stage will assess the azimuth and tilt angles over a smaller range at 1° intervals. Energy generation data from Homer will be used to identify the tilt angle providing the highest energy yield over the azimuth vector. The derivation of a polynomial curve function requires knowledge of certain points on the curve. (Larson & Falvo, 2009) The optimum azimuth variable and longitude for each site will form the optimum azimuth function, while the optimum tilt and the site latitude will be used for the tilt function.

3.2.5. Modelling multiple string systems.

Annual energy generation for multi string systems will be determined using Homer. The different inverter configurations will be used for the multi string simulations.

- Single inverter with single channel maximum power point tracking
- Single inverter with dual channel maximum power point tracking
- Two inverters, each with single channel maximum power point tracking

Data extracted from the Homer simulations will be used to determine the conditions required for specific inverter configurations. Changes in different installation angles will also be assessed to determine if the optimum installation angles identified for single string systems can be applied to multiple string systems.

3.2.6. Selection of installation locations.

Multiple sites were selected ranging from Darwin, Northern Territory as a northern location through to Hobart, Tasmania as a southern location. Toowoomba, Queensland and Brooklyn Park, South Australia were included as intermediate locations. The optimum angle of installation is to be determined for each site using solar data available through the Homer energy modelling software, and temperature data from the Australian Bureau of Meteorology for the year 2014. Sites were selected to provide a range of locations covering a large portion of the country, weather data available nearby.

3.2.6.a. Brooklyn Park, S.A.

Site: Brooklyn Apartments, Brooklyn Park.

Location: 34.93°S, 138.55°E (Google, 2015)

Weather data site: 34.95°S, 138.52°E. (Commonwealth of Australia, 2015)

Brooklyn Park is a suburb of Adelaide, located approximately 5km west of the city. Located on approximately 5km south west is the Bureau of meteorology weather monitoring station, providing historic temperature data. (Google, 2015)



Figure 3.1 – Brooklyn Park site overview

Google, 2015

Building Azimuth: 177°

3.2.6.b. Toowoomba, Qld.

Site: USQ, Toowoomba: Engineering (Z block)

Location: 27.60°S, 151.93°E (Google, 2015)

Weather data site: 27.54°S, 151.91°E. (Commonwealth of Australia, 2015)

The University of Southern Queensland is located in Toowoomba, approximately 125km east by road from the city of Brisbane. Approximately 10km north of the university is the site of the Bureau of Meteorology weather monitoring station. (Google, 2015)

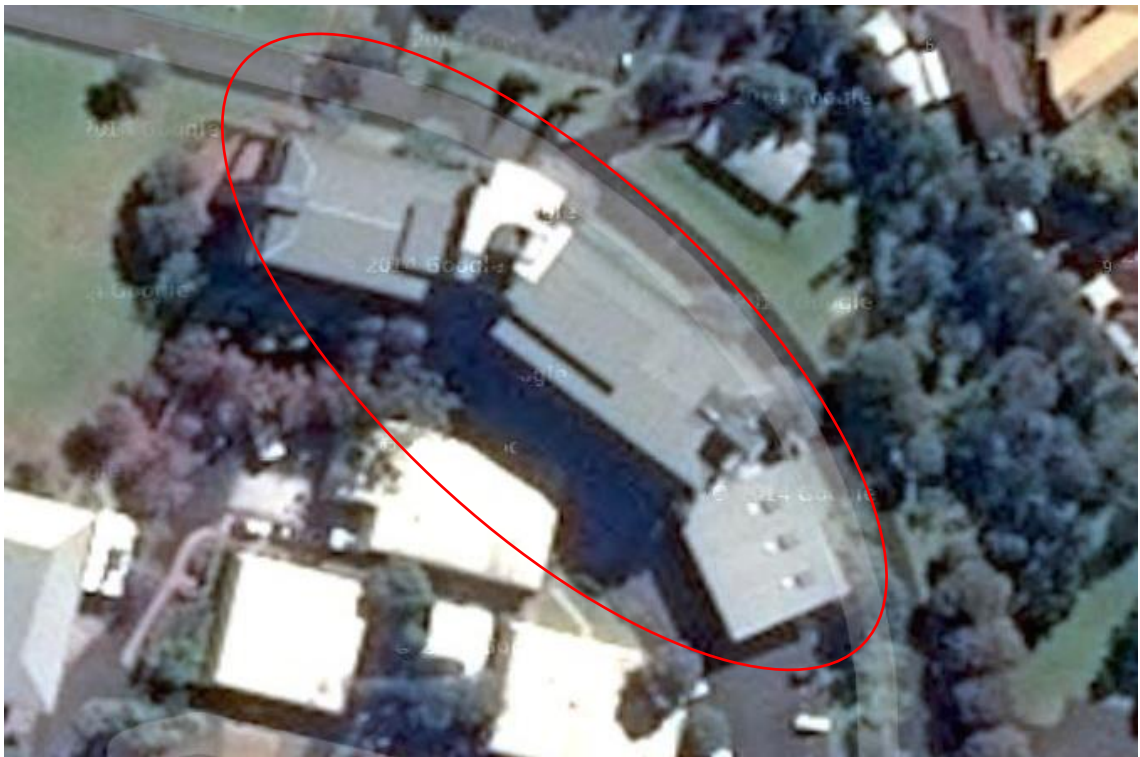


Figure 3.2 – Toowoomba site overview

Google, 2015

Building Azimuth 195° / 217° / 246°

3.2.6.c. Darwin, N.T.

Site: Darwin Airport.

Location: 12.42°S, 130.89°E (Commonwealth of Australia, 2015)

As the most northerly Australian major city, Darwin was selected as the northern modelling location. The Darwin airport terminal is located 12km by road from the city (Google, 2015), and within close proximity to the Bureau of Meteorology weather monitoring station. (Commonwealth of Australia, 2015)

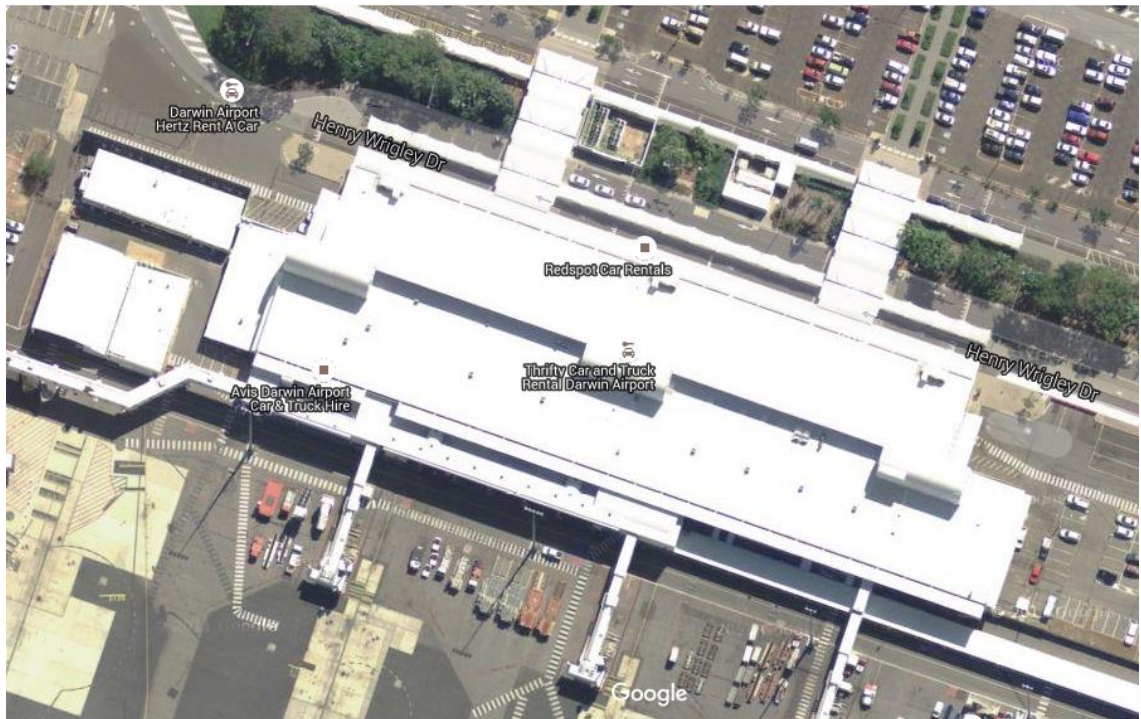


Figure 3.3 – Darwin site overview.

Google, 2015

Building Azimuth 199°

3.2.6.d. Hobart, Tas.

Site: Ellerslie Road, Battery Point.

Location: 42.89°S, 147.33°E (Commonwealth of Australia, 2015)

As the most southerly Australian major city, Hobart was selected as the southern modelling location. Ellerslie Road is located less than 2km by road from the city. (Google, 2015) The Bureau of Meteorology weather monitoring station is also located on Ellerslie road. (Commonwealth of Australia, 2015)



Figure 3.4 – Hobart site overview

Google, 2015

Building Azimuth 201°

3.2.7. Panel angle effect on cooling.

The effect panel tilt angle has on the convective cooling will be determined through experimentation.

1. The panel should remain open circuit throughout this experiment.
2. Ensure panel is sheltered from wind.
3. Align the panel to 0° relative to horizontal.
4. Record cell temperature using FLIR thermal camera
5. Repeat cell temperature measurement every 5 minutes until steady state is reached.
6. Align panel to an angle greater than 0° and repeat test steps 2 through 5

The global solar irradiance available from the USQ weather station, combined with the angle of the sun relative to the panel will be used to calculate the panel energy input.

The cell temperature rise values recorded using the FLIR camera will then be used to determine the cell temperature. Since cell temperature is a function of the irradiance, the resulting values can be scaled to reflect a solar irradiance value of $1000\text{W}/\text{m}^2$. ((Migan, 2013)A line of best fit will used to be approximate the angle versus temperature rise and related efficiency decrease, with the resulting efficiency changes factored into the Homer modelling outputs.

3.2.8. Development of installation guidelines.

The modelling process is expected to generate a large amount of energy output data. The data will need to be analysed to identify the parameters which provide the greatest energy yields, and will be used to form the basis for the recommended installation guidelines.

Parameters which will be included in the final recommendations are listed below.

- Preferred inverter configurations.
- This will detail the best inverter configuration which should be selected for a range of solar panel installation parameters.
- Maximum permissible angles between strings on the same maximum power point tracking circuit.
- This details the maximum installation azimuth and tilt angles which should be permitted if two strings are connected to a common maximum power point tracking circuit.
- Optimum tilt angles for the installation of solar panels.

The use of renewable energies, and reduction of fossil fuel generated power should could lead to a Greenhouse Installing solar panels at angles which provide the largest annual energy generation a greater annual generation The optimum angle for installation will be used to define the best panel tilt angle for a range of azimuth angles. , providing maximum power.

3.3. **Project timeline.**

Some of the major project milestones are listed below, and a detailed project timeline is located in appendix B.

- Completion of project allocation
- Completion of Project specification
- Selection of potential sites
- Completion of IV curve modelling
- Commencement of site modelling
- Submission of project preliminary report
- Project completion

3.4. **Assessment of consequential effects.**

The work health safety act require health and safety be maintained through the identification of safety hazards. If the elimination of a safety hazard is not possible, the risk must be reduced to as safe level as possible. (Safe work Australia, 2011) Used under a Creative Commons Attribution 3.0 (<http://creativecommons.org/licenses/by-nc/3.0/au/>).

Responsibility for the effective implementation of risk elimination and control is normally initiated by company management, although does extend to all persons on site. (Safe work Australia, 2011) Used under a Creative Commons Attribution 3.0 (<http://creativecommons.org/licenses/by-nc/3.0/au/>).

The risk management process consists of four steps.

- i. Identify any hazard associated with the project.
- ii. Assess the risk of all identified hazards, including details on seriousness of injury if an accident were to occur, and the chance of an accident occurring.
- iii. Determine the required measures to eliminate or reduce the severity of the risk, and implement the solution.
- iv. Review the risk management measures which have been implemented to ensure effectiveness of the solution, and new hazards have not been introduced.

(Safe work Australia, 2011) Used under a Creative Commons Attribution 3.0 (<http://creativecommons.org/licenses/by-nc/3.0/au/>).

During the risk management, the work health safety act also requires an appropriate level of consultation with any person who may be affected by the work carried out. (Safe work Australia, 2011) Used under a Creative Commons Attribution 3.0 (<http://creativecommons.org/licenses/by-nc/3.0/au/>)

3.4.1. Identification of hazards.

Identification of hazards is simply an analysis of a product, process or situation which has the potential to cause harm to any person. This may require an observation of a specific processes being conducted, consultation with workers regarding near misses or an assessment of a piece of equipment being commissioned. (Safe work Australia, 2011) Used under a Creative Commons Attribution 3.0 (<http://creativecommons.org/licenses/by-nc/3.0/au/>).

3.4.2. Risk assessment.

Following the identification of potential hazards, each hazard is then assessed for the potential to cause harm. The risk assessment may assist in determining the severity of a potential risk, effectiveness of current risk mitigation measures, what corrective action is most appropriate and urgency of the urgency of corrective action. (Safe work Australia, 2011) Used under a Creative Commons Attribution 3.0 (<http://creativecommons.org/licenses/by-nc/3.0/au/>).

Risk assessments should be conducted prior to the introduction of a new piece of equipment, modification to existing processes, when there is no information of the risk of a specific task or equipment, or how specific hazards will interact. (Safe work Australia, 2011) Used under a Creative Commons Attribution 3.0 (<http://creativecommons.org/licenses/by-nc/3.0/au/>).

3.4.3. Risk matrix scores.

The overall risk is then identified using a scoring system. Each hazard is assessed, and assigned an individual score for time of exposure to the hazard, chance of an accident occurring and the potential consequence if an accident were to occur. (University of Melbourne, 2004)

Tables relating to the risk assessment scores can be located in Appendix F.

3.4.4. Risk assessment outcomes.

Following the assignment of the risk scores, control measures need to be identified for each of the hazard. (University of Melbourne, 2004)

Control measures should be selected for each hazard in a hierarchical manner,

1. Elimination of the hazard
2. Substitution of the process with a reduced risk process.
3. Providing a barrier between the worker and the hazard in the form of guarding or fencing.
4. Engineering controls include the use of mechanical aids to reduce manual handling, or setting work output requirements to a level which is more suited to the task.
5. Administrative controls include the introduction of work processes designed to reduce the workers exposure to certain hazards, or informing workers of the potential hazard.
6. Requiring the use of personal protective equipment.

- Steps 5 & 6 should only be used when all other possible solutions have been exhausted, or as a short term control measure until more suitable measures can be introduced. (Safe work Australia, 2011) Used under a Creative Commons Attribution 3.0 (<http://creativecommons.org/licenses/by-nc/3.0/au/>).

3.4.5. Project hazard identification and risk assessment.

Hazard identification and risk assessments which have been conducted for this project are located in Appendix F.

4. Results

4.1. IV Curve modelling.

The photovoltaic panel specifications, and environmental input specifications used throughout the modelling were from the Hareon Solar model HR-250W, which has a maximum power output of 250W under standard test conditions. (Jiangyin Hareon Power Co Ltd, n.d.)

- Maximum power voltage 29.90V
- Open circuit voltage 37.10V
- Maximum power current 8.36A
- Short circuit current 8.81A
- Irradiance 1000W/m²
- Ambient temperature 25°C (Jiangyin Hareon Power Co Ltd, n.d.)
- No shading on the panel surface.

Full specifications are available in appendix G.

The above specification have been used throughout each modelling section, unless otherwise specified.

The modelling consisted of two photovoltaic panels connected in parallel, or in series and compared to the benchmark condition. Panel 1 was set at a fixed angle with a normal vector relative to the light source. Panel 2 was set with the normal facing the light source, and rotated through to 56° during the simulation. Each panel consisted of three modules with bypass diode, and the panel was fitted with a blocking diode.

This section is intended to compare the effect of differing panel angles on the maximum power generated. The benchmark for maximum power capability used throughout the modelling is the sum total of maximum power capabilities with the same installation parameters. This is to compare the effect of offset panel angles on the maximum power capability, irrespective of the installation or environmental conditions.

4.1.1. Differing panel angle.

The differing panel angle simulation is intended to assess the maximum power capability of a solar installation with panels installed at different angles relative to a light source. Figure 4.1a represents a parallel connected system with panel 1 at 0° and panel 2 rotated from 0° through to 56° , and figure 4.1b represents the series connected equivalent.

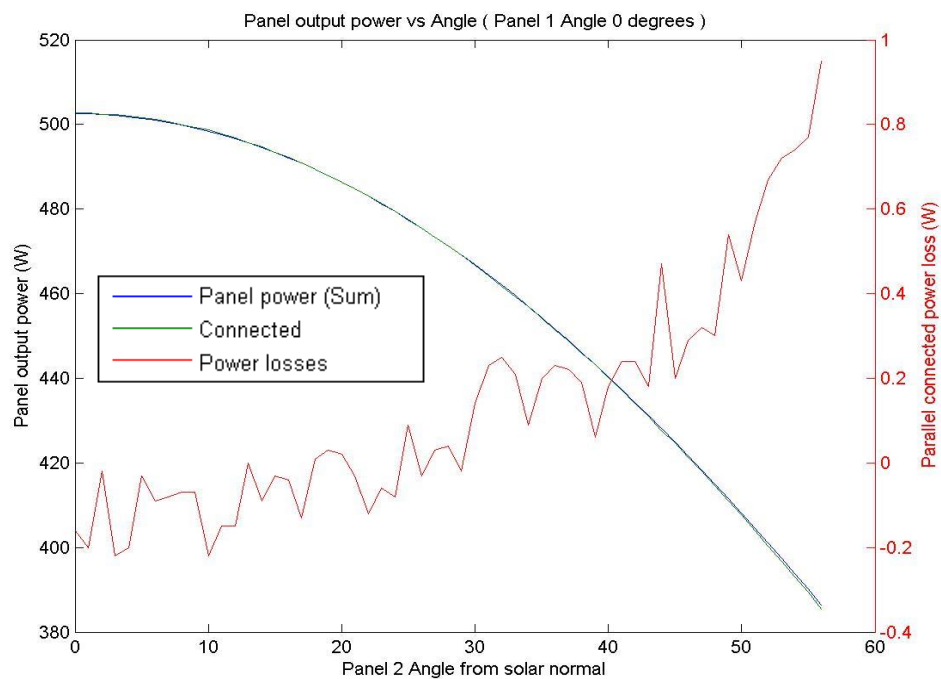


Figure 4.1a –Parallel MPPT: Panel 1: 0° , Panel 2: 0° - 56° .

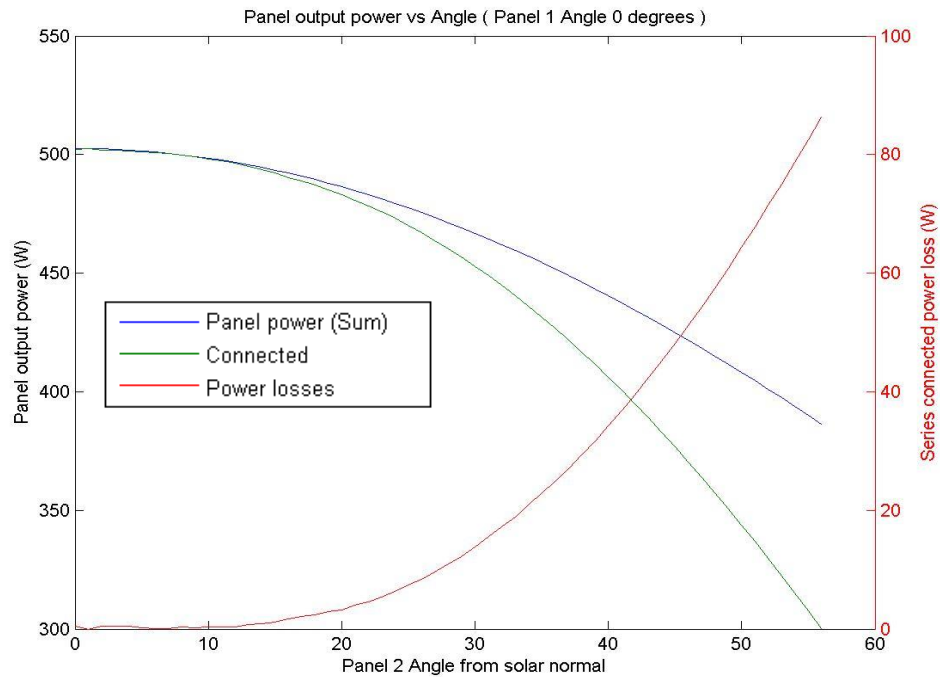


Figure 4.1b –Series MPPT: Panel 1: 0°, Panel 2: 0°-56°.

Panels connected in parallel displayed a minor reduction in the maximum power capability of the system compared to the benchmark. When panel 2 was angled to 56°, the benchmark maximum power was 385W. The reduction of 1W at this angle represented 0.26% of the benchmark output.

The maximum power capability of the series connected panels displayed a high level of immunity to the angle of panel 2 up to 10°. The benchmark maximum power was 495W, and the reduction was 1W or 0.2%. From 20° through to 56°, the maximum power reduction changed from approximately 5W to 85W. The reduction represented 22% of the benchmark value when panel 2 was angled to 56°.

4.1.2. Hard shading panels with varied panel angle.

The hard shading simulation is intended to assess the maximum power capability of a solar installation with offset panel angles, and a variety of shading patterns. Each module within the panel was considered to be fully illuminated, or fully shaded.

4.1.2.a. Equal shaded area.

When offset panels were subjected to an equal shading pattern, the resulting maximum power capability resembled the unshaded equivalent. The power generated by the shaded system was scaled by the percentage of panel exposed to the light source. Figure 4.2a shows the maximum power capability for a parallel connected system with both panels subjected to a 1/3 shading, and the series connected equivalent shown in figure 4.2b.

The maximum parallel system output was 335W, observed with both panels directly facing the light source. Rotating panel 2 to an angle of 56° from the light source resulted in a system output of 255W, 0.6W below the benchmark. This represented 0.24% of the system capability.

The series connected system with 1/3 shading demonstrated a similar level of immunity to the unshaded system. The maximum output of 335W occurred with both panels facing the light source. As panel 2 was rotated more than 20° from the light source, the maximum power capability decreased rapidly. With panel 2 facing 56° to the light source, the maximum power output was 200W, 21% below the benchmark value.

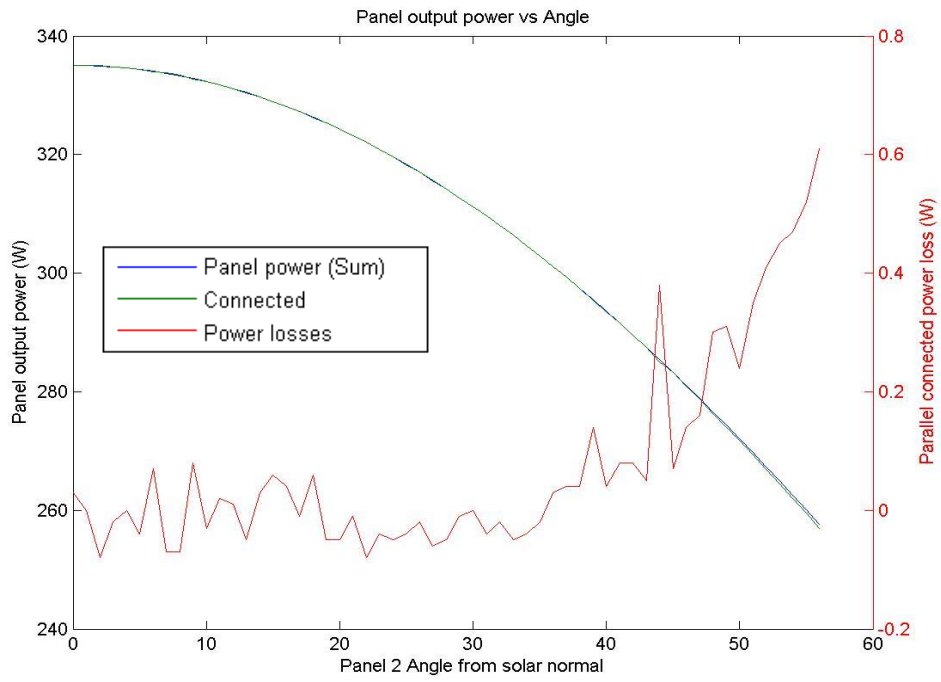


Figure 4.2a –Parallel MPPT: 1/3 panel shading.

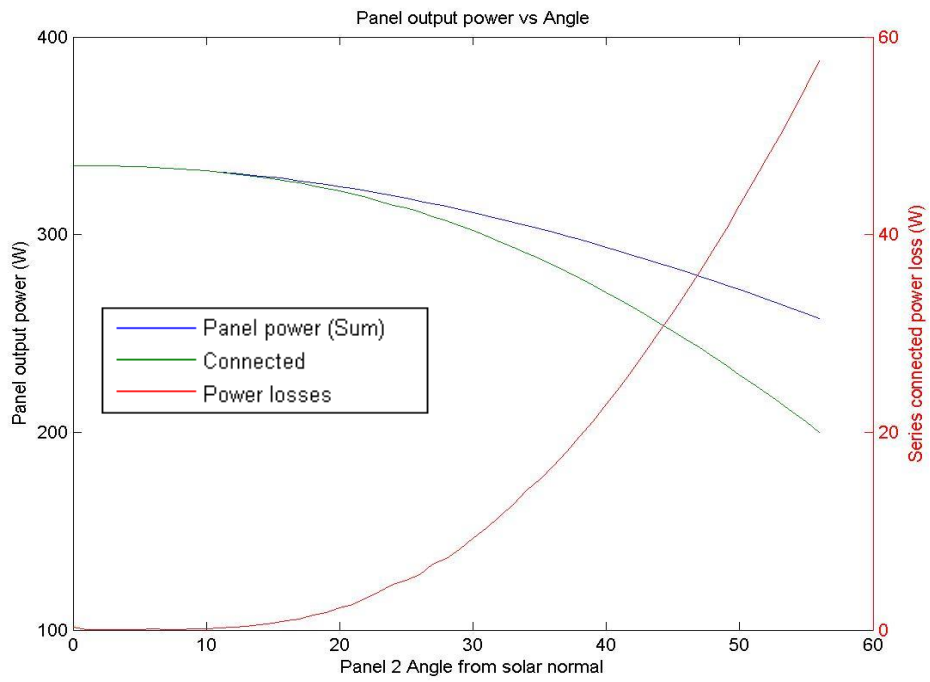


Figure 4.2b –Series MPPT: 1/3 panel shading.

4.1.2.b. Unequal shaded area: Parallel connected.

The maximum power capability of parallel connected panels subjected to an uneven area of shading is heavily reduced when compared to the individual capability of each panel. The difference in angle to the light source provided minimal effect on the maximum power. Shading a greater area on the panel angle closer to the light source caused a significant reduction in the maximum power capability of the system. Changes to the light incidence angle of the second panel resulted in negligible changes to the maximum power. Figure 4.3a shows the capability of a parallel connected system with 2/3 of panel 1 shaded, and panel 2 completely unshaded, and figure 4.3b shows the same system with 1/3 of panel 2 shaded.

The maximum power capability losses shown in figure 4.3b represent 33% of the system benchmark when the panels are both aligned to the sun, through to 48% with the second panel angled 56° from the light source.

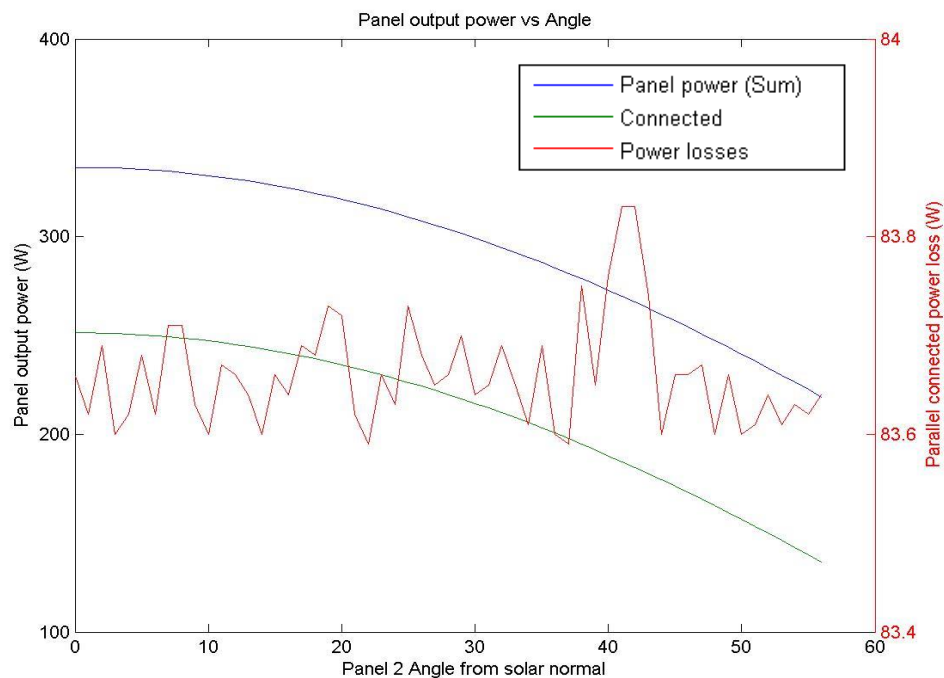


Figure 4.3a –Parallel MPPT: Panel 1 @ 2/3 & Panel 2 @ unshaded.

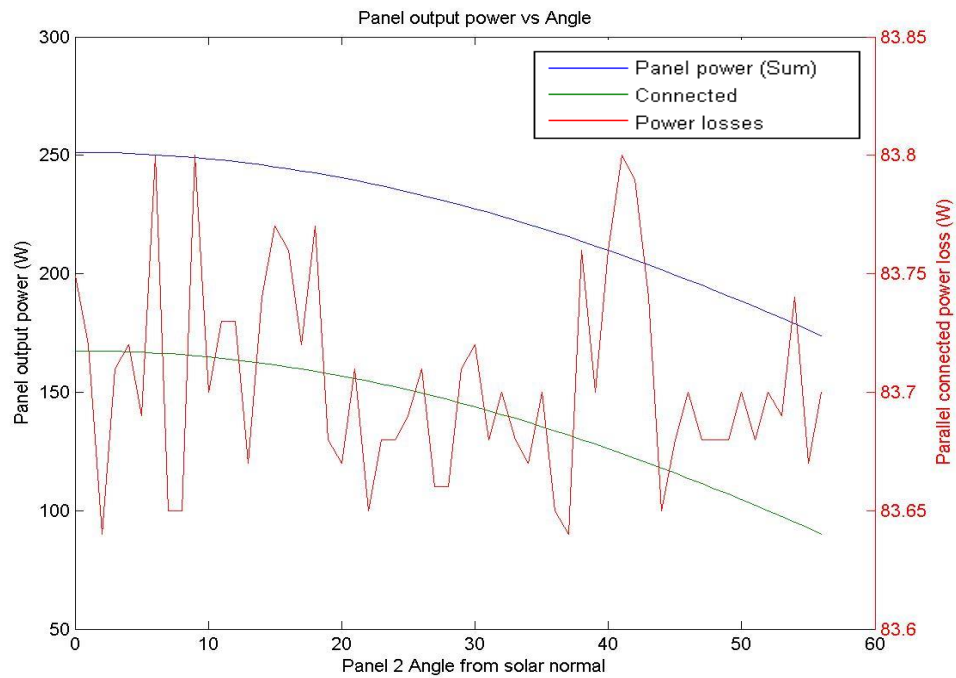


Figure 4.3b – Parallel MPPT: Panel 1 @ 2/3 & Panel 2 @ 1/3 shading.

Rotating the second panel away from the light source, presented a slightly larger effect to the maximum power capability of the system when the shading was changed to cover more area of the panel angled further from the light source. The maximum power capability of a system with 2/3 shading applied to panel 2 and no shading on panel 1 is shown in figure 4.4a, and the system which has 1/3 shading applied to panel 1 is shown in figure 4.4b.

The maximum power capability losses shown in figure 4.4a represent 46% of the system benchmark when the panels are both aligned to the sun, through to 53% with the second panel angled 56° from the light source.

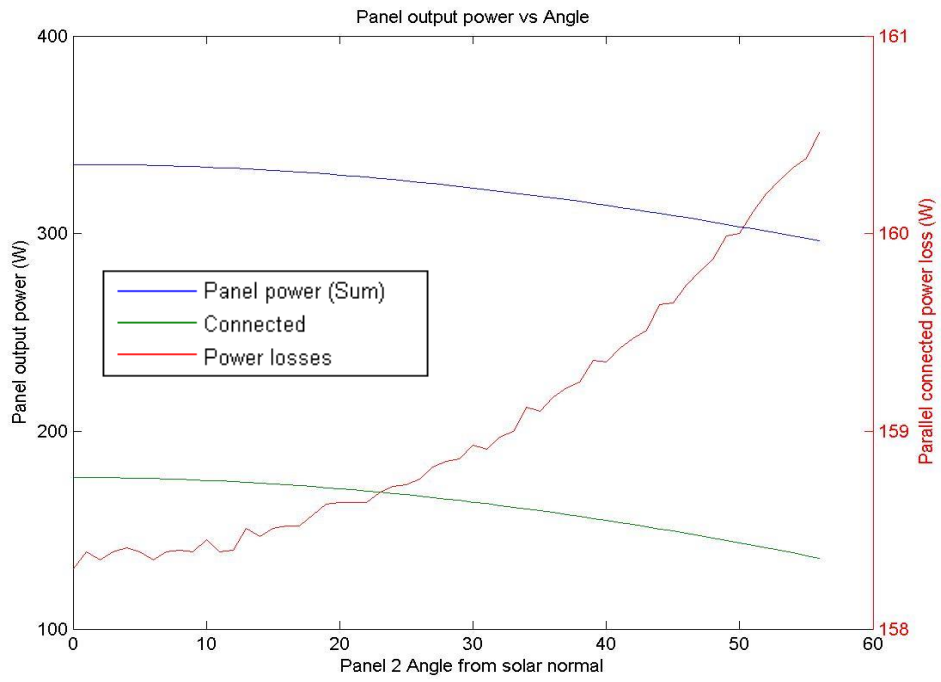


Figure 4.4a – Parallel MPPT: Panel 1 unshaded & Panel 2 @ 2/3 shading.

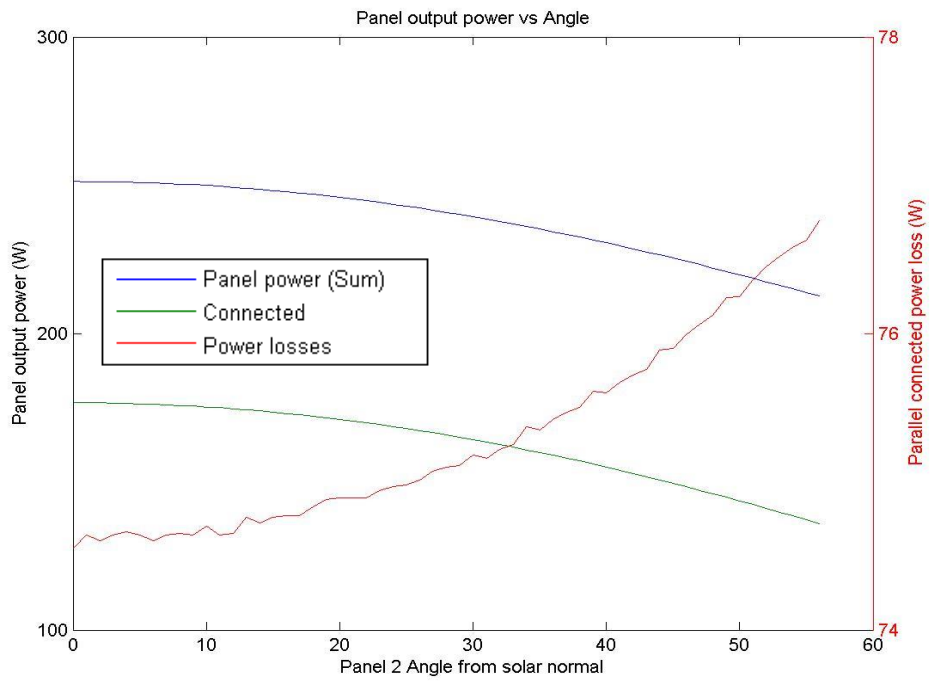


Figure 4.4b – Parallel MPPT: Panel 1 @ 1/3 & Panel 2 @ 2/3 shading.

4.1.2.c. Unequal shaded area: Series connected.

Series connected systems subjected to unequal shading performed better than the parallel equivalent when both panels were angled within approximately 30° difference to the light source. As the second panel was angled further from the light source, the maximum power capability declined rapidly. This resulted in the series connected system being less efficient than the parallel equivalent at high levels of angle offset. Shading a greater area of one panel changed only the magnitude for the losses. Rotating panel 2 away from the light source provided the same effect for both cases. The reduction of the maximum power capability ranged from 0% for aligned panels through to 27% for a system with 1/3 shading on panel 2 which is shown in figure 4.5a. The system with 2/3 shading on the second panel is shown in figure 4.5b.

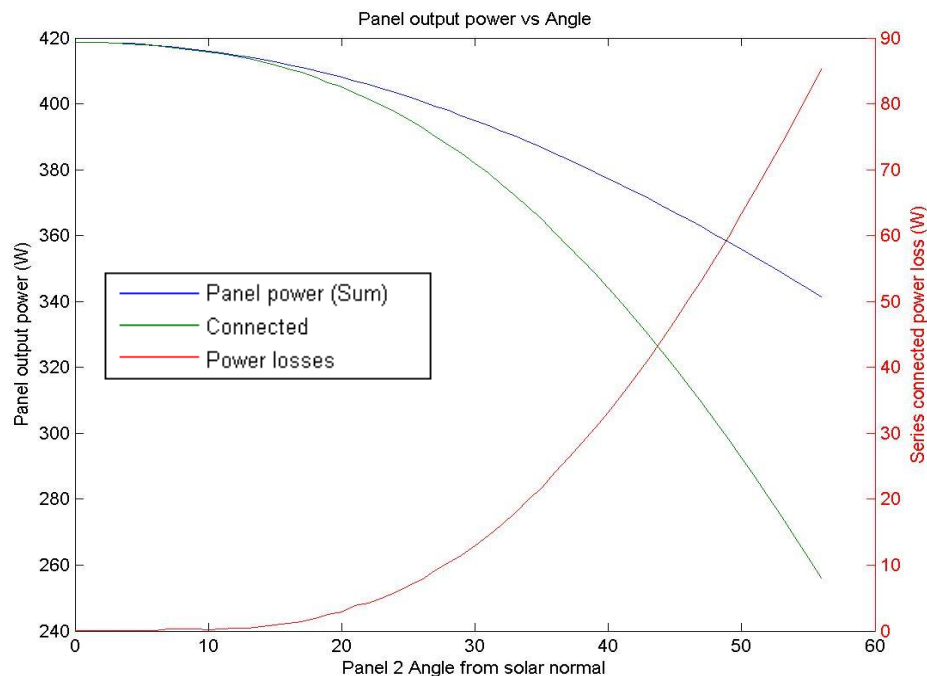


Figure 4.5a – Series MPPT: Panel 1 @ unshaded & Panel 2 @ 1/3 shading.

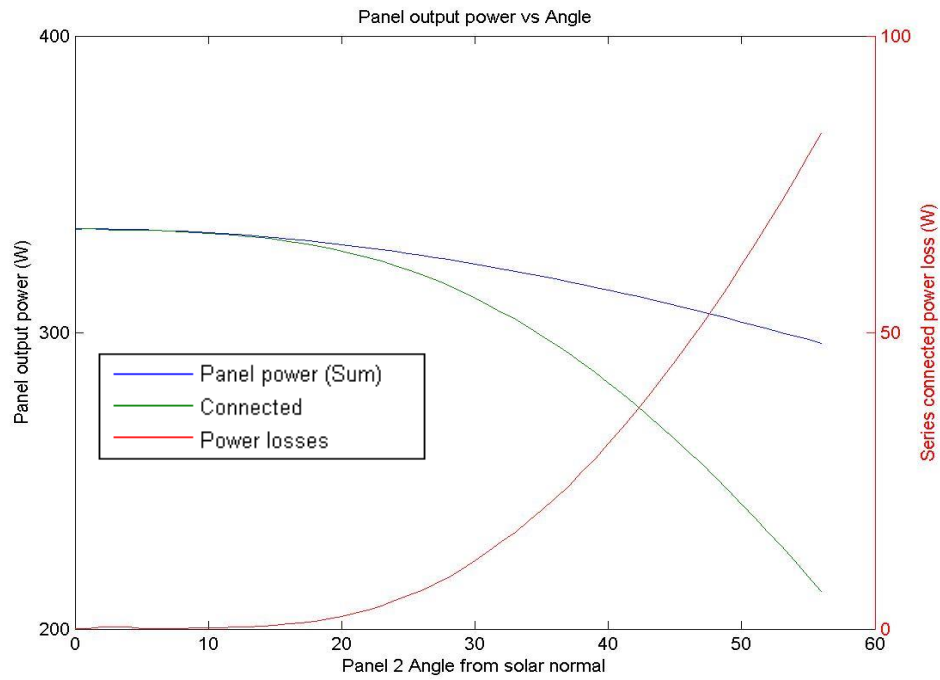


Figure 4.5b – Series MPPT: Panel 1 @ unshaded & Panel 2 @ 2/3 shading.

The reduction in the maximum power capability for the system with a greater area of shading fixed angle panel ranged from 0% for aligned panels through to 14% for a system with 2/3 shading on panel 1 which is shown in figure 4.6a. The system with 1/3 shading added to the second panel is shown in figure 4.6b.

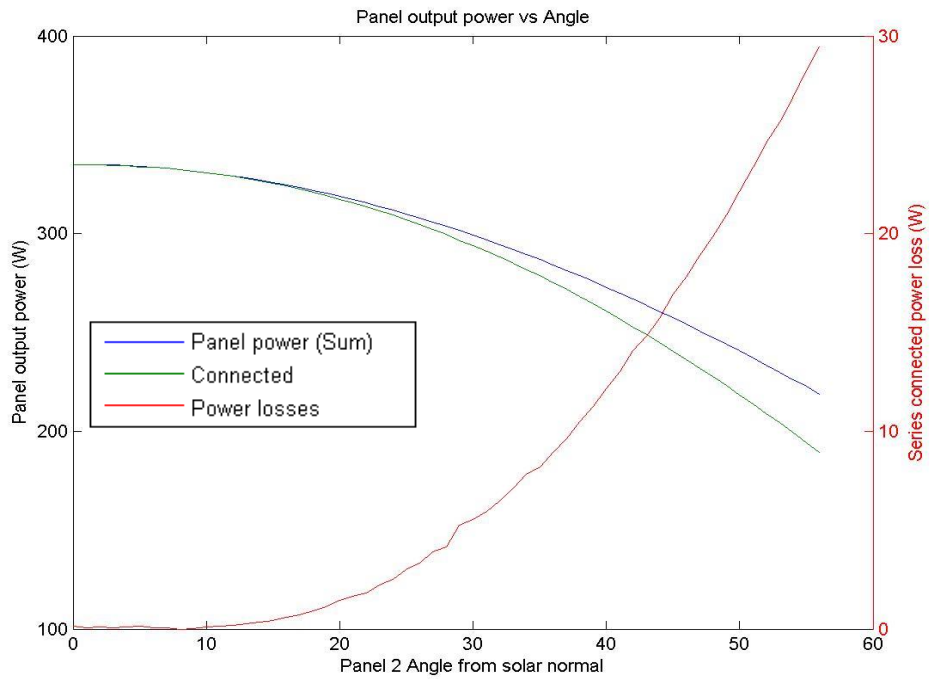


Figure 4.6a – Series MPPT: Panel 1 @ 2/3 shaded & Panel 2 @ unshaded.

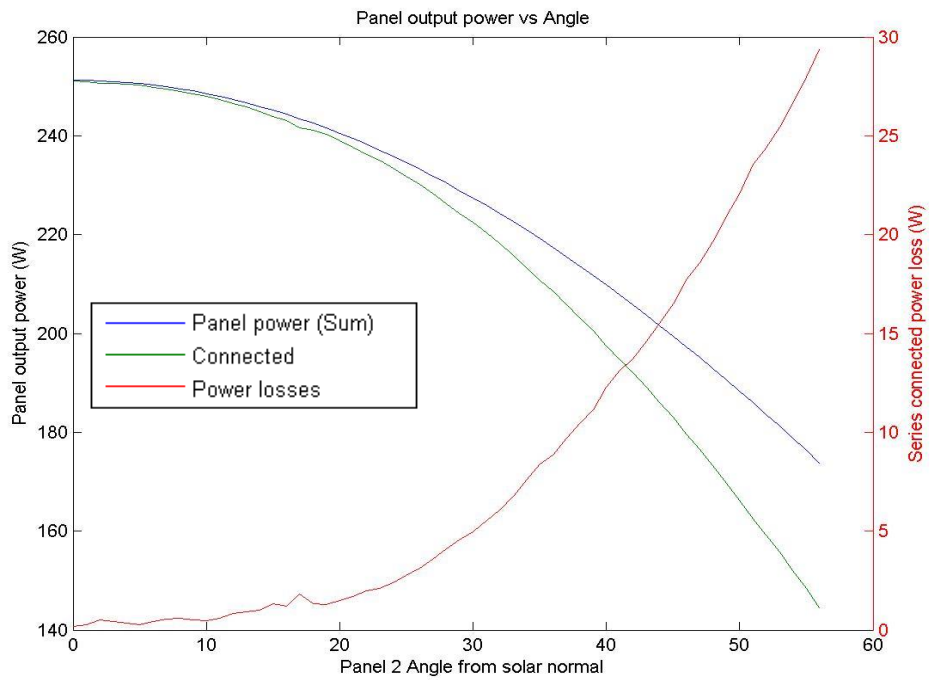


Figure 4.6b – Series MPPT: Panel 1 @ 2/3 shaded & Panel 2 @ 1/3 shading.

4.1.3. Mismatched panel specifications.

The connection of non-identical panels together may lead to mismatch losses. (Honsberg & Bowden, 2013k) This section will analyse the effect of connecting panels with different specifications in both series and parallel configurations. Voltage values used are based on the Hareon solar panel specifications $\pm 10\%$.

4.1.3.a. Mismatched voltage specifications: Parallel connection

The maximum power capability of a parallel connected system was showed only a minor reduction change as the second panel was rotated away from the light source when compared to the benchmark test. Orienting both panels to face the light source, the offset voltage characteristic caused a 0.6% reduction of the system maximum power capability.

Rotating the higher voltage specification panel away from the light source resulted in an improvement in the maximum power capability compared to the benchmark test. Figure 4.7a shows the maximum system power for a panel with the lower voltage specifications facing the light source, and the second panel with the higher voltage specifications rotated from 0° through 56° where the reduction of the maximum power was 0.1%. Figure 4.7b shows the same system with the voltage specifications switched. Rotating panel 2 increased the magnitude of maximum power reduction. At 56° the reduction was equal to 1.7%.

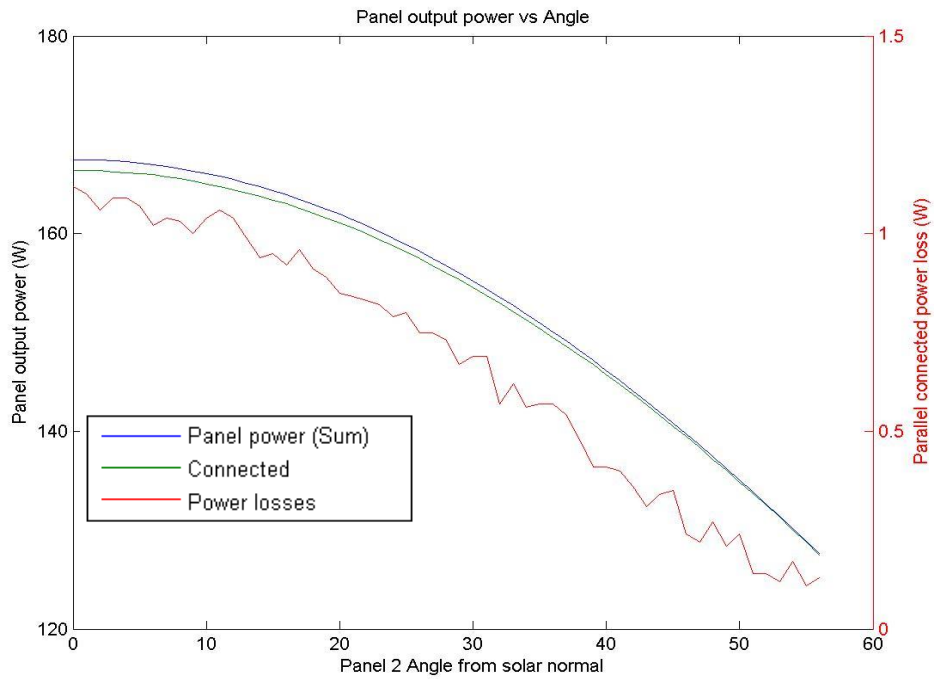


Figure 4.7a –Parallel MPPT: Voc @ 29.0V & 30.8V.

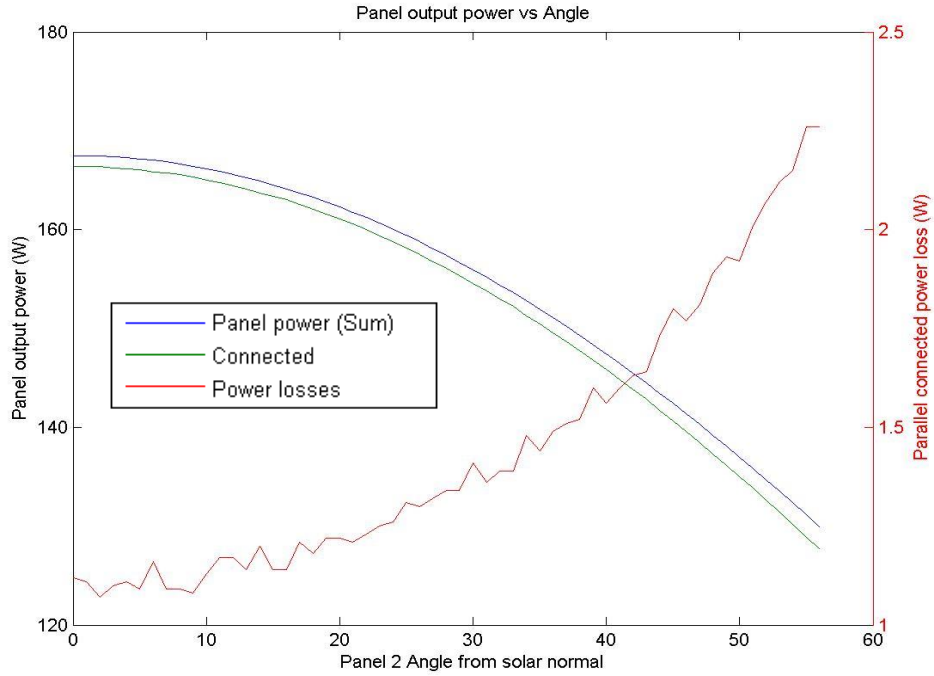
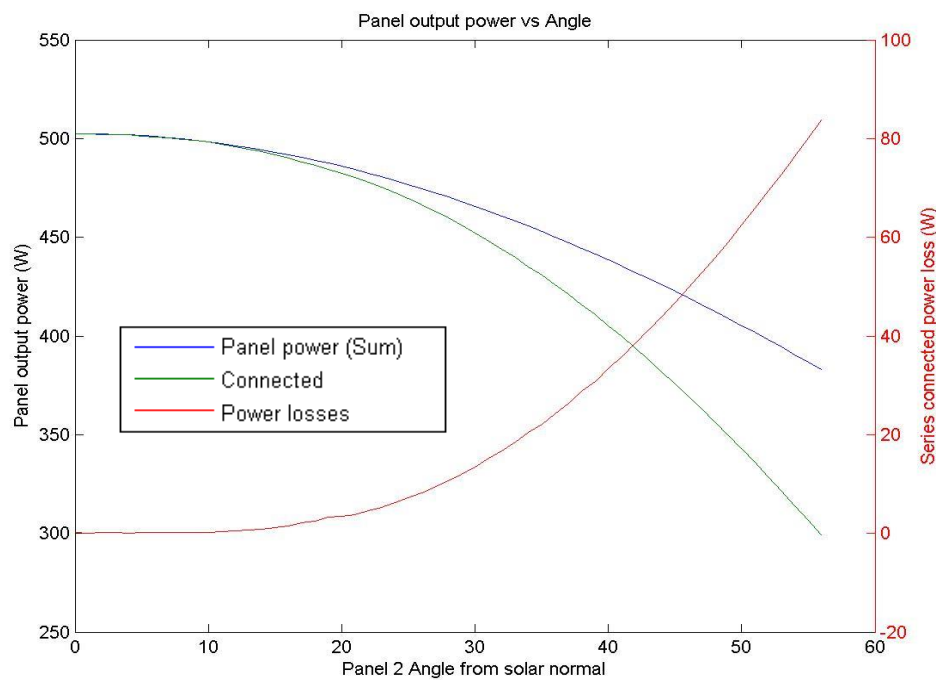


Figure 4.7b – Parallel MPPT: Voc @ 30.8V & 29.0V

4.1.3.b. Mismatched voltage specifications: Series connection

The connection of photovoltaic panels in series with mismatched voltage specifications showed little effect on the maximum power capability of the system. The effect of rotating one of the panels had limited effect on the system for differences in angle of 10° . The losses grew in magnitude as the angular difference was moved beyond 20° . Irrespective of which panel was specified with the higher voltage output, the reduction of the system capability increased to 22% of the benchmark value at 56° . Figure 4.8a shows the system having a panel with lower voltage specification facing the light source, and panel rotated from the light source through to 56° with the higher voltage specification. The system with switched voltage specifications is shown in figure 4.8b.



Figure

4.8a – Series MPPT: V_{oc} @ 29.0V & 30.8V.

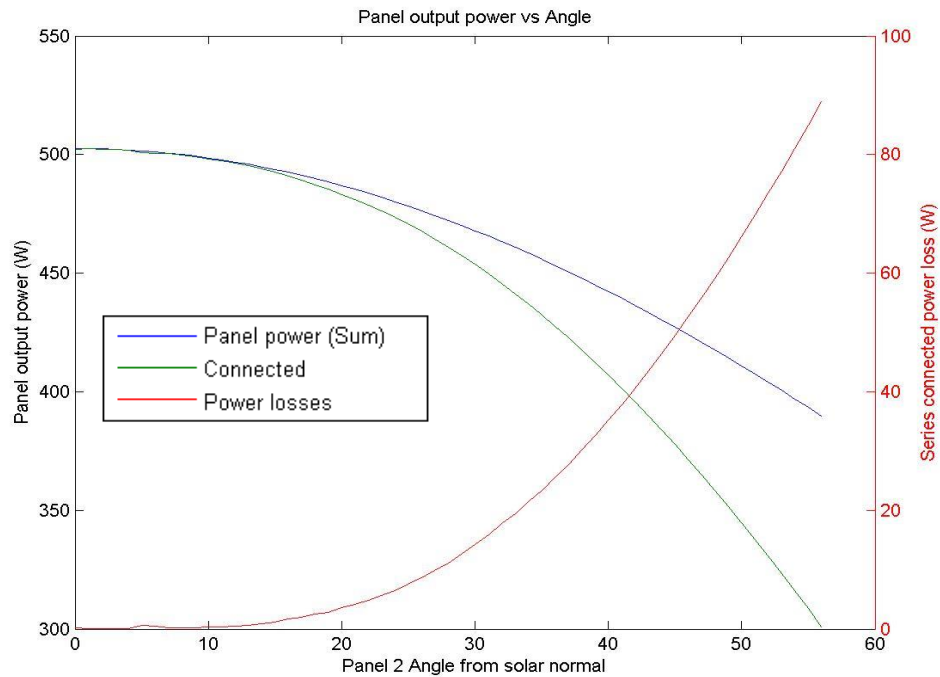


Figure 4.8b –Series MPPT: Voc @ 30.8V & 29.0V

4.1.3.c. Mismatched current specifications: Parallel connection.

The effect of mismatched current specifications on the maximum power of the system was minor as either panel is rotated from the light source to 56° and compared to the benchmark simulation. The mismatched current specifications caused a reduction of the maximum power capability of 0.4W with one panel rotated 56° from the light source, equalling 0.3% of the maximum system output.

Figure 4.9a shows the system having a panel with lower current specification facing the light source, and panel rotated from the light source through to 56° having a higher current specification. The system with switched current specifications is shown in figure 4.9b.

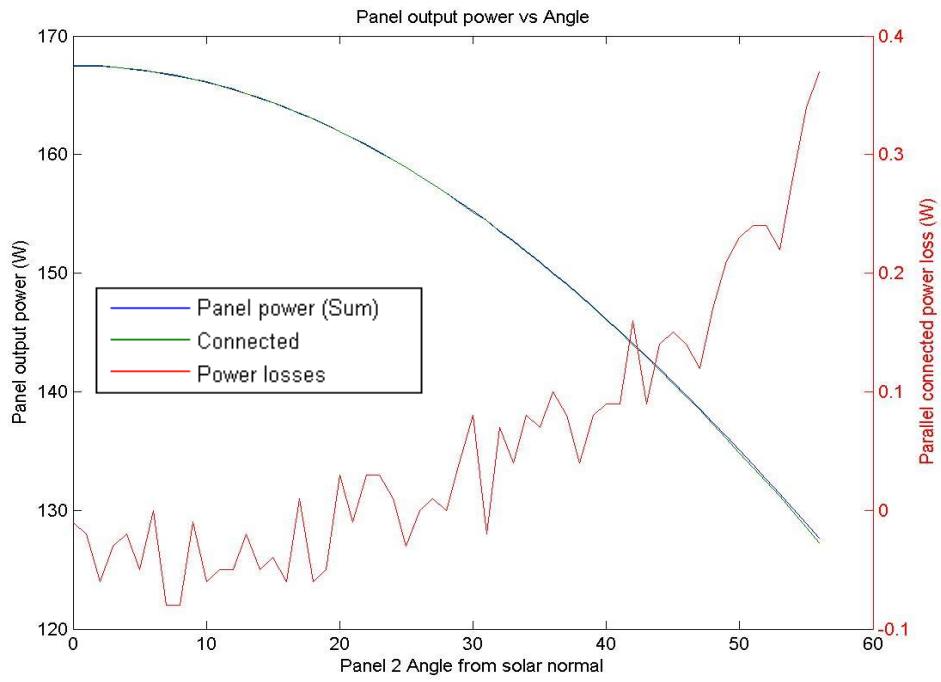


Figure 4.9a –Parallel MPPT: Isc @ 8.11A & 8.61A

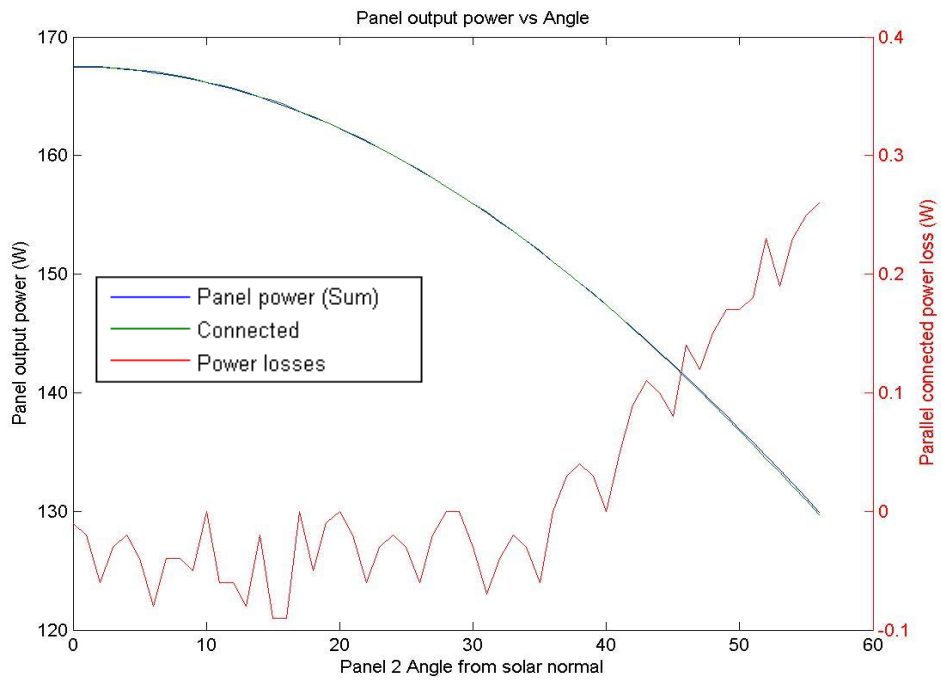


Figure 4.9b – Parallel MPPT: Isc @ 8.61A & 8.11A

4.1.3.d. Mismatched current specifications: Series connection.

The connection of photovoltaic panels in series with mismatched current specifications generated substantial losses, especially when the second panel was rotated beyond 30°. Figure 4.10a shows the effect of angling the lower rated panel to the light source, and rotating the panel with the higher current specification. The effect was an initial improvement compared to the benchmark simulation. The increased angle led to a reduction of the second panel output, eventually reaching a point where the maximum output was equal to the benchmark. Further rotation led to a reduction in the maximum capability of the system.

Figure 4.10b shows the effect of angling the higher rated panel to the light source, rotating the panel with the lower current specification. The effect on the maximum capability of the system was a loss of 1% for both panels aimed at the light source, increasing to 25% when the second panel is angled 56° from the light source.

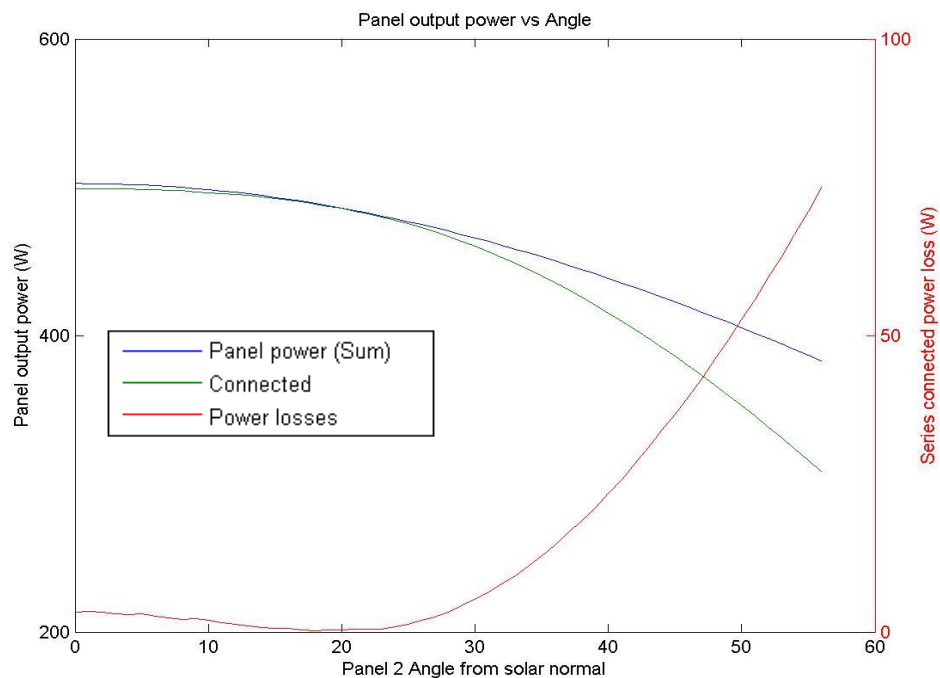


Figure 4.10a –Series MPPT: I_{SC} @ 8.11A & 8.61A

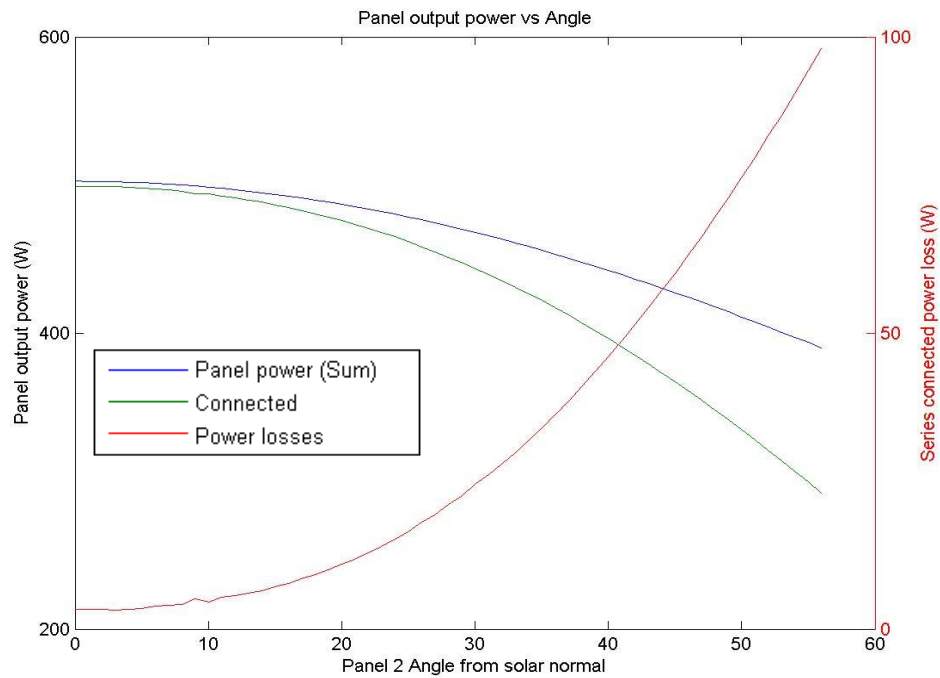


Figure 4.10b – Series MPPT: I_{SC} @ 8.61A & 8.11A

4.1.4. Varied temperature.

Analysis of the Bellini et.al. (n.d.) model that the panel voltage is affected by temperature at a rate determined by the characteristic of the panel. Temperature related changes in the current output of a panel also affected by the characteristic of the panels in addition being scaled by the ratio of irradiance to the test condition irradiance and the specified current parameter of the panel. (Bellini et. al, n.d.) Throughout the simulation, both panels are exposed to the same ambient temperature.

4.1.4.a. Varied temperature: Parallel connection

The parallel connected panels demonstrated a reasonable level of immunity to offset panel installation angles irrespective of the ambient temperature when compared to the benchmark model. Figure 4.11a, 4.11b and 4.11c represent a system installed with one panel angled to the light source, and a second rotated from the light source to 56° using ambient temperatures of 25°C, 15°C and 35°C respectively.

Changes to the maximum power point can be seen as the temperature is varied. The maximum power capability is reduced by 0.27% compared to the benchmark at a temperature of 25°C, increasing to 0.33% at 15°C and 0.32% at 35°C.

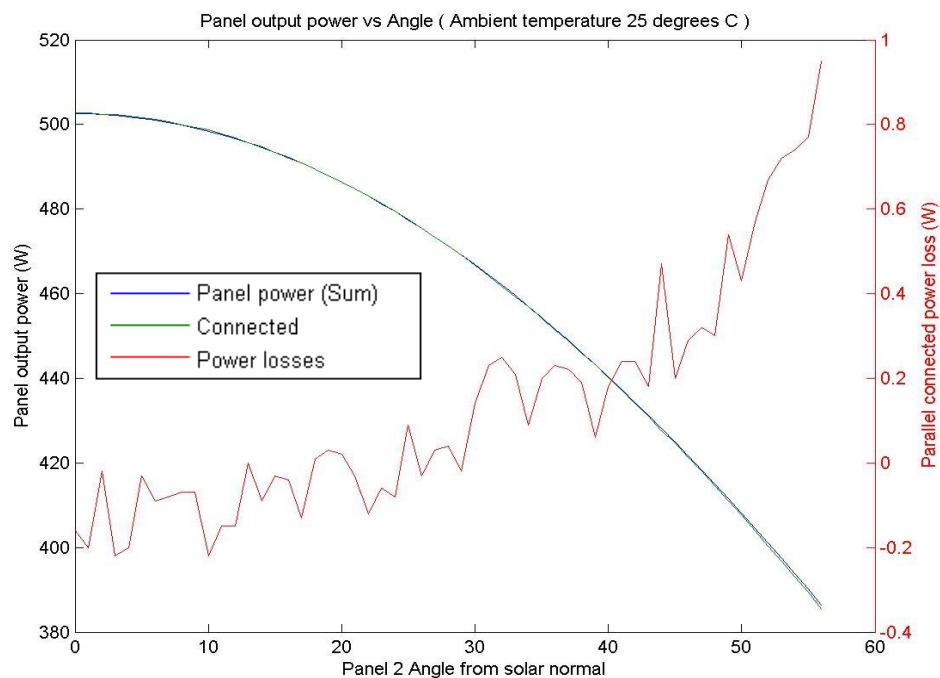


Figure 4.11a – Parallel MPPT: T @ 25°C

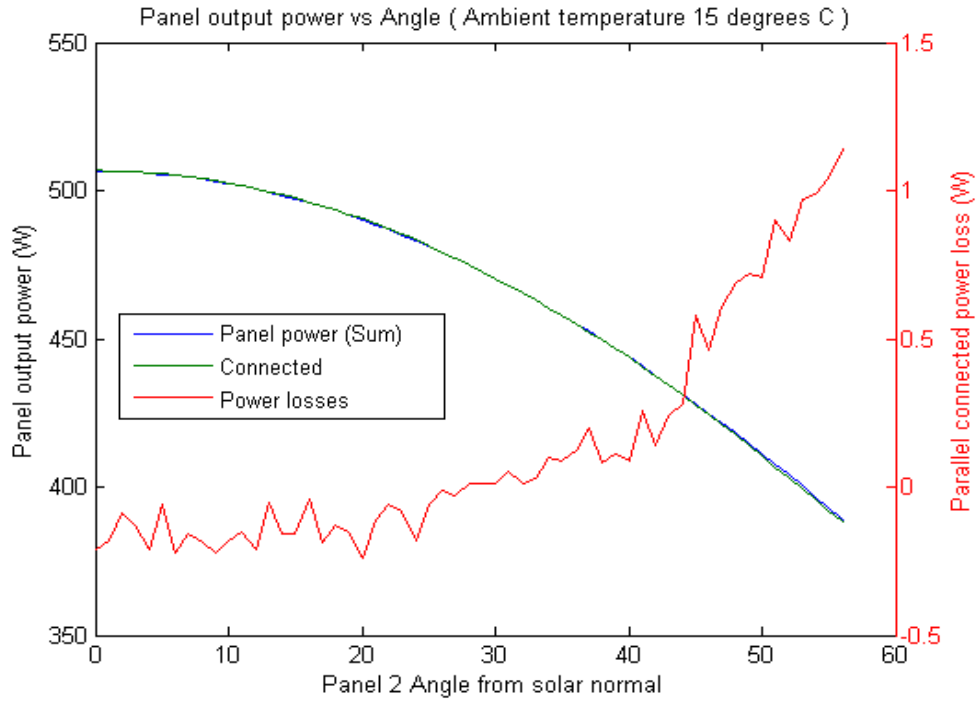


Figure 4.11b – Parallel MPPT: T @ 15°C

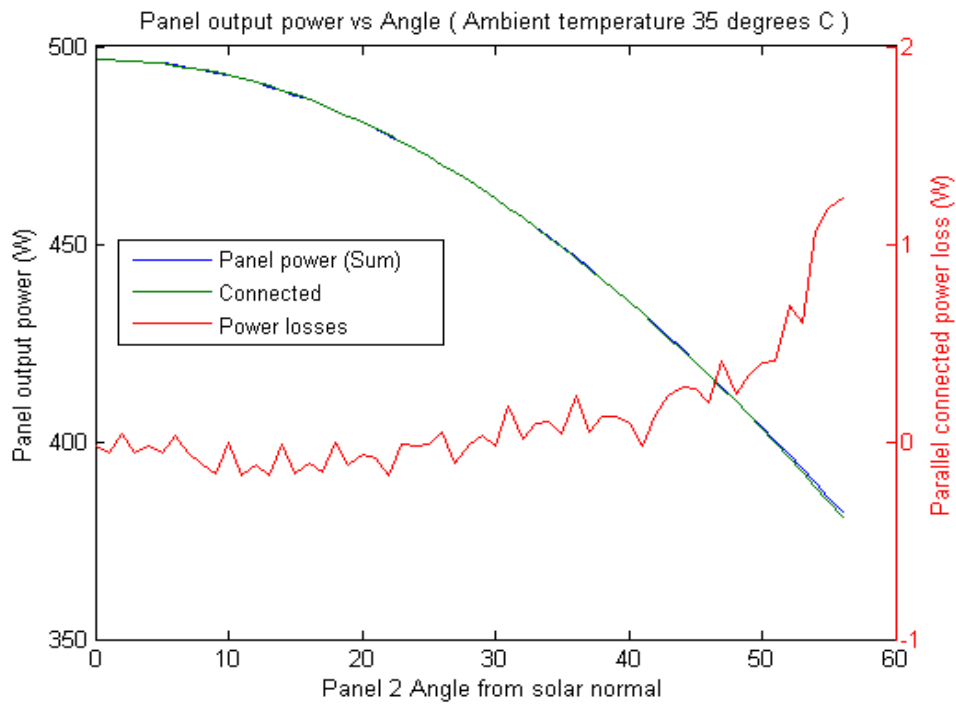


Figure 4.11c – Parallel MPPT: T @ 35°C

4.1.4.b. Varied temperature: Series connection

The maximum power capability of a series shows minimal effect due to temperature variations. One panel was aimed at the light source, and a second rotated from the light source through 56° . Figure 4.12a, 4.12b and 4.12c represent the system with ambient temperatures of 25°C , 15°C and 15°C respectively.

The largest reduction of the maximum power capability remained approximately 80W below the benchmark simulation regardless of the ambient temperature, occurring when the second panel was rotated to 56° . With panel 2 at 56° rotation, the losses compared to the benchmark were 22% of the system output at 25°C , 21% at 15° and 35° .

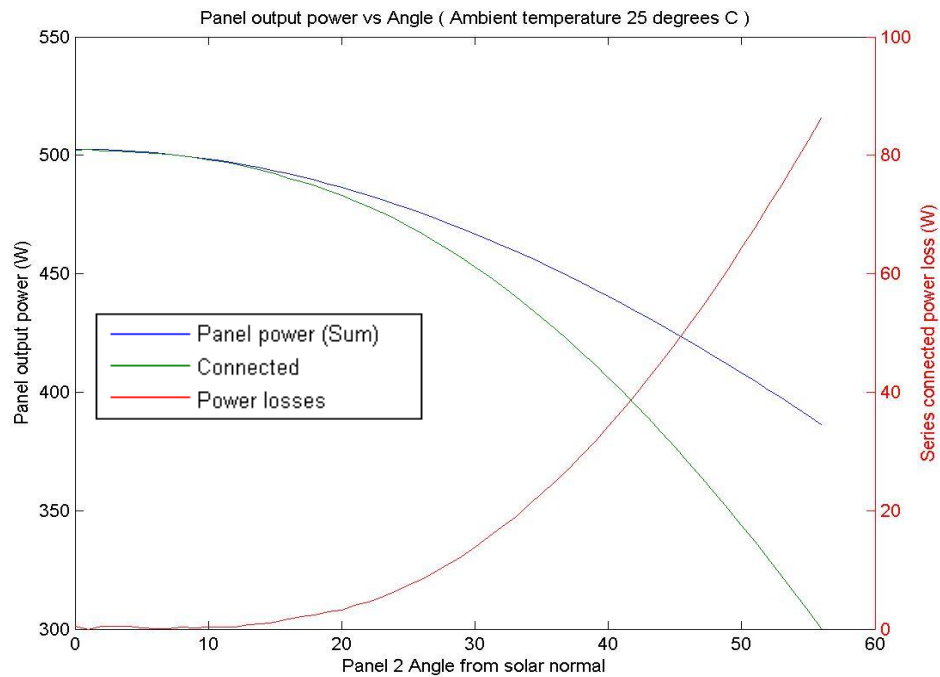


Figure 4.12a – Series MPPT: T @ 25°C

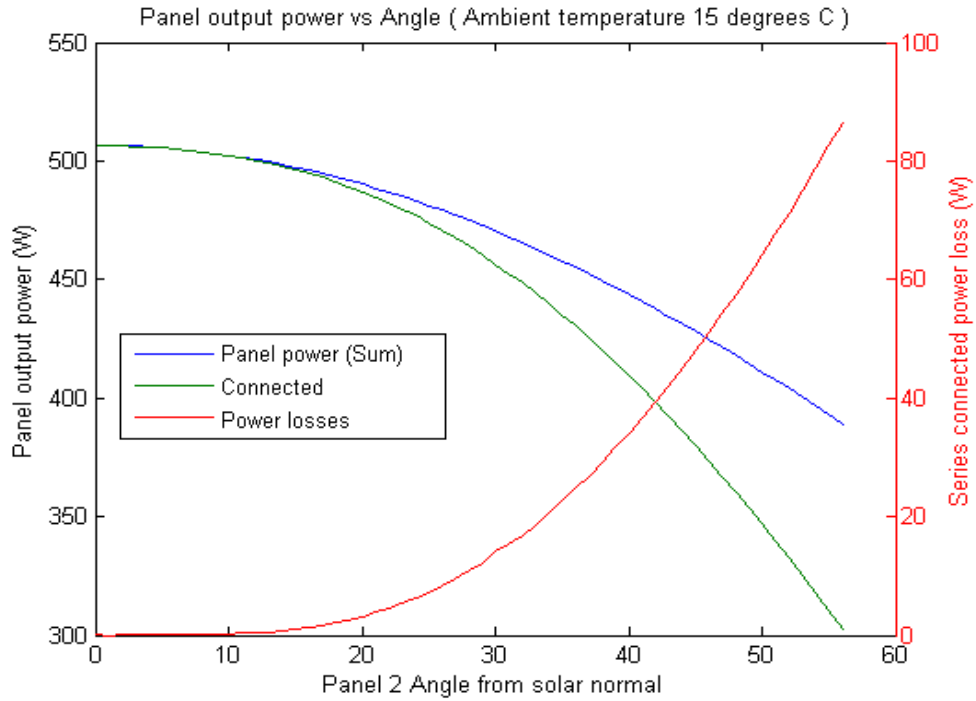


Figure 4.12b – Series MPPT: T @ 15°C

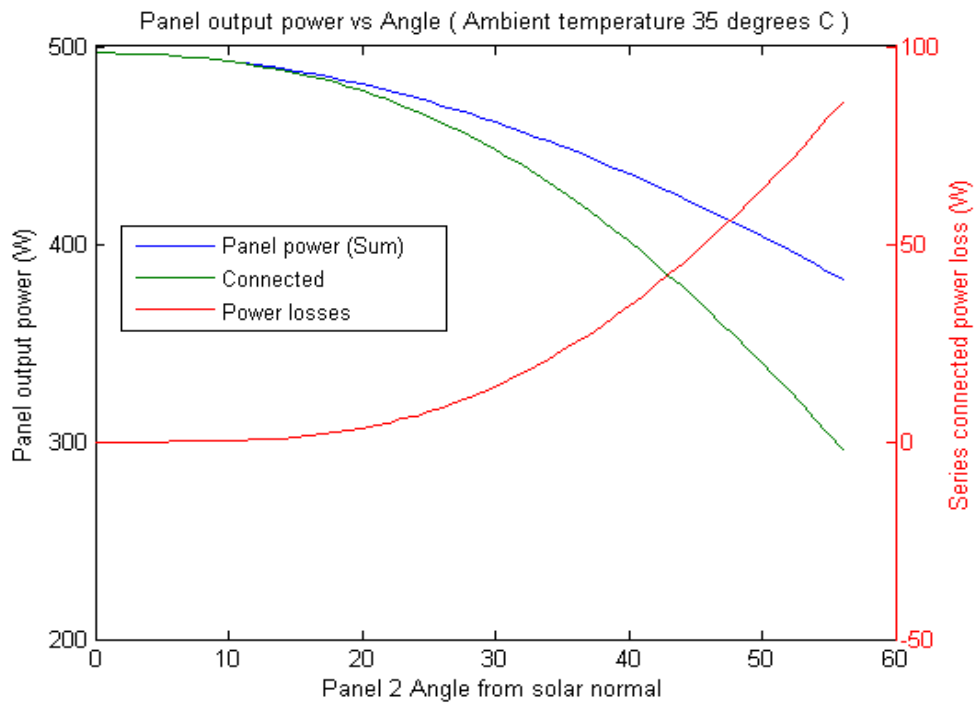


Figure 4.12c – Series MPPT: T @ 35°C

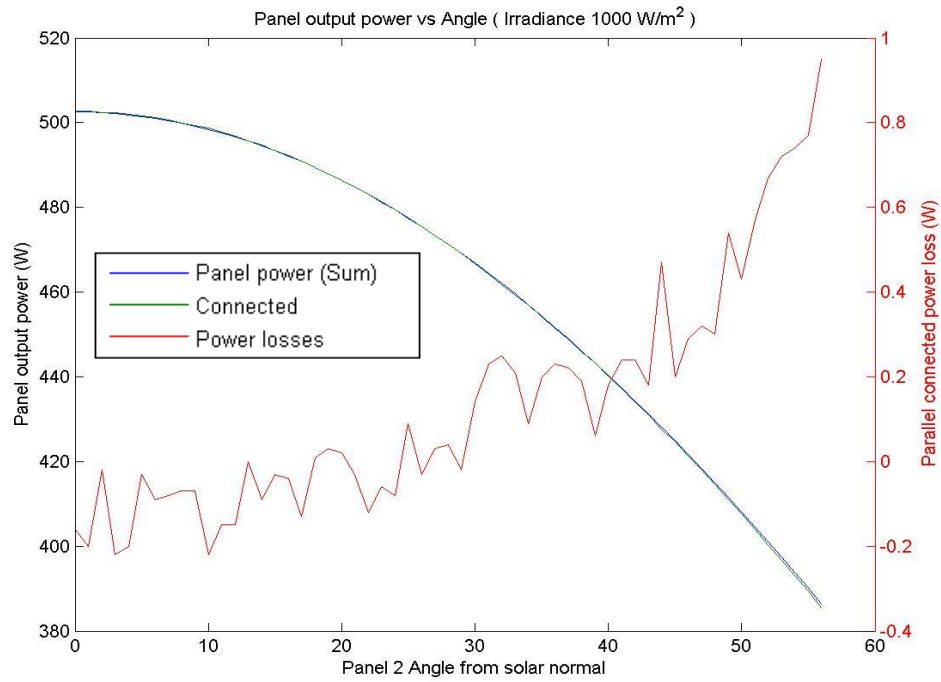
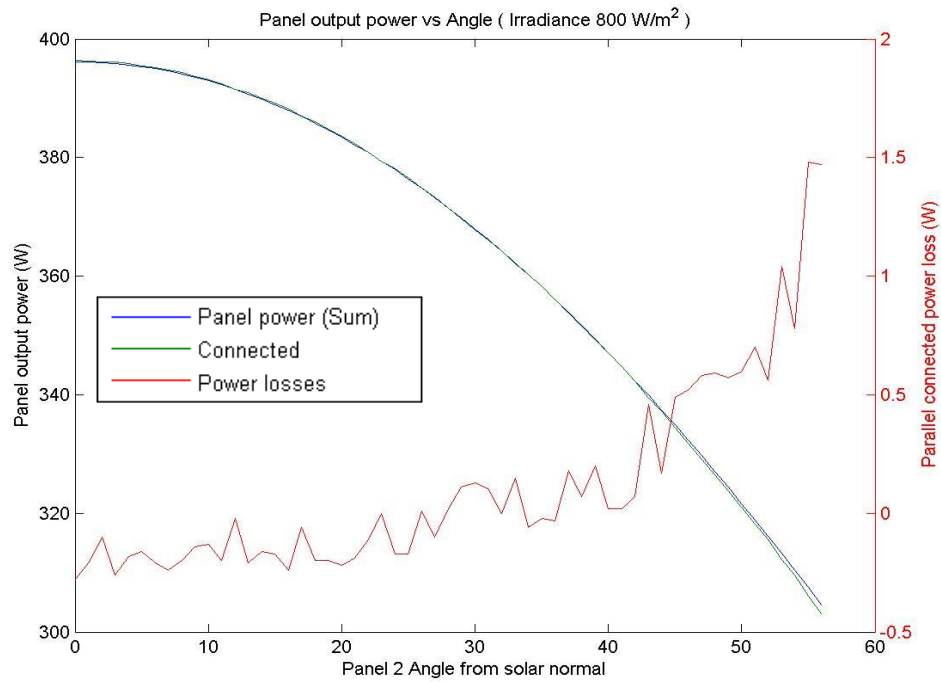
4.1.5. Varied irradiance.

Analysis of the Bellini et al. (n.d.) photovoltaic model indicate the panel current output is proportional to the irradiance input. The model also shows a minor change in output voltage with changes in the irradiance. (Bellini et. al, n.d.) The combined result of irradiance changes using this model is an approximately proportional change in power output as the irradiance changes.

4.1.5.a. Varied irradiance: Parallel connection

This section demonstrates the maximum power capability of a parallel connected system with irradiance variations, one fixed panel angled to the light source, and a second rotated from the light source through 56° . Figure 4.13a, 4.13b and 4.13c represent the system exposed to $1000\text{W}/\text{m}^2$, $800\text{W}/\text{m}^2$ and $400\text{W}/\text{m}^2$ respectively.

Comparison of each of the figures below, the proportional nature of the maximum power becomes evident. The reduction of the maximum power capability compared to the respective benchmark simulation indicate an increase on losses as the irradiance falls. The maximum reduction for the $1000\text{W}/\text{m}^2$ simulation was approximately 0.25% of the system output, and 1.25% for the $200\text{W}/\text{m}^2$ system.

Figure 4.13a – Parallel MPPT: G @ 1000 W/m^2 Figure 4.13b – Parallel MPPT: G @ 800 W/m^2

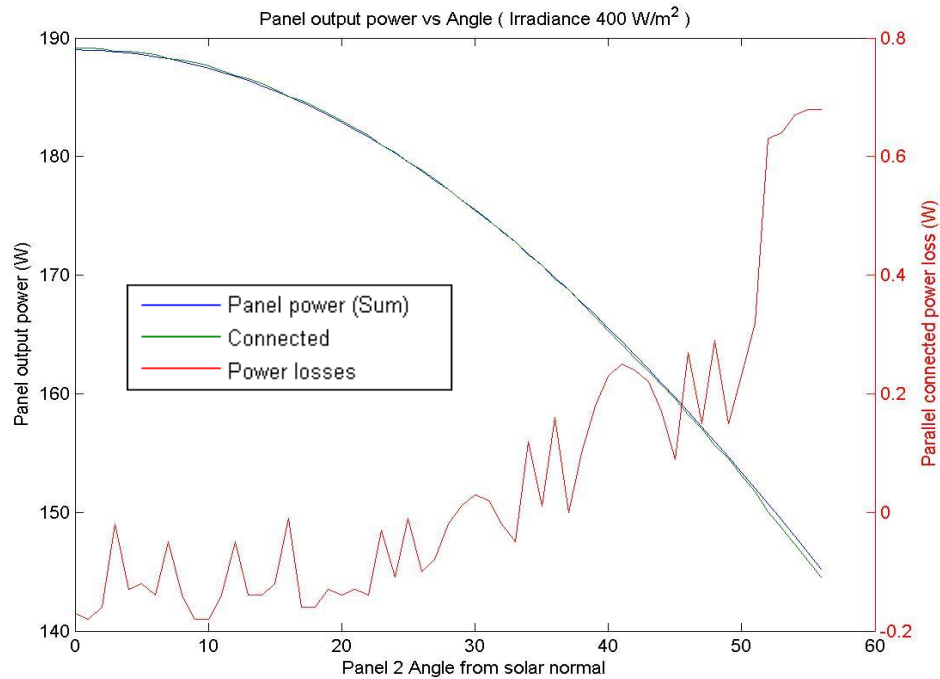


Figure 4.13c – Parallel MPPT: G @ 400W/m²

4.1.5.b. Varied irradiance: Series connection

The maximum power capability of a series connected system with irradiance variations, one fixed panel angled to the light source, and a second rotated from the light source through 56°. Figure 4.14a, 4.14b and 4.14c represent the system exposed to 1000W/m², 800W/m² and 400W/m² respectively.

Again the comparing each of the figures below indicates the proportional nature of the maximum power. The reduction of the maximum power capability increased as the irradiance increased, when compared to the respective benchmark simulation remained relatively stable. At an offset angle from through to approximately 10°, the reduction was close to zero, increasing to approximately 22% at 56°.

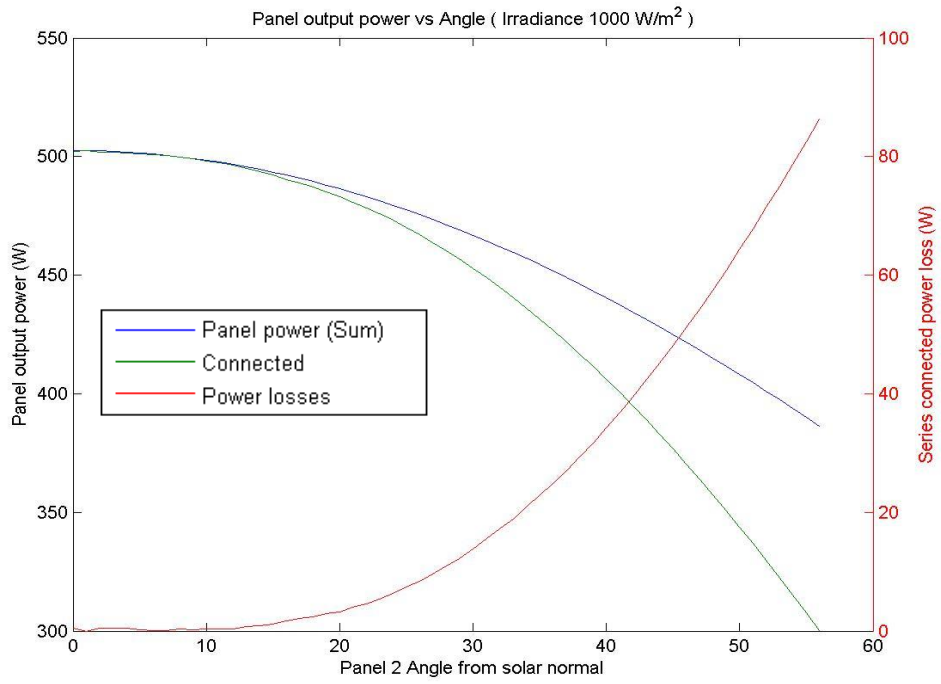


Figure 4.14a – Series MPPT: G @ 1000W/m²

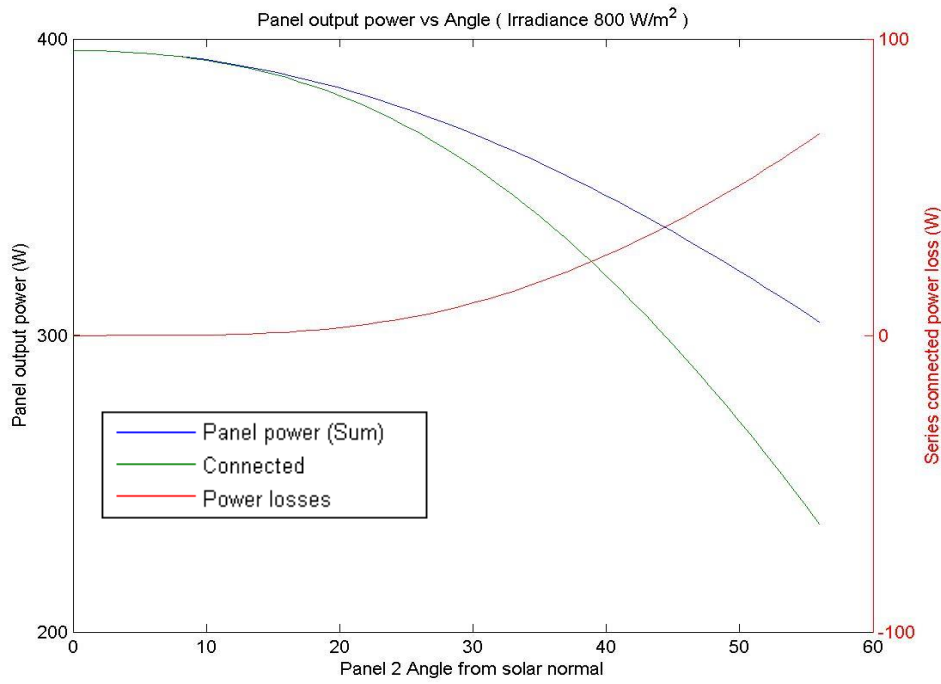


Figure 4.14b – Series MPPT: G @ 800W/m²

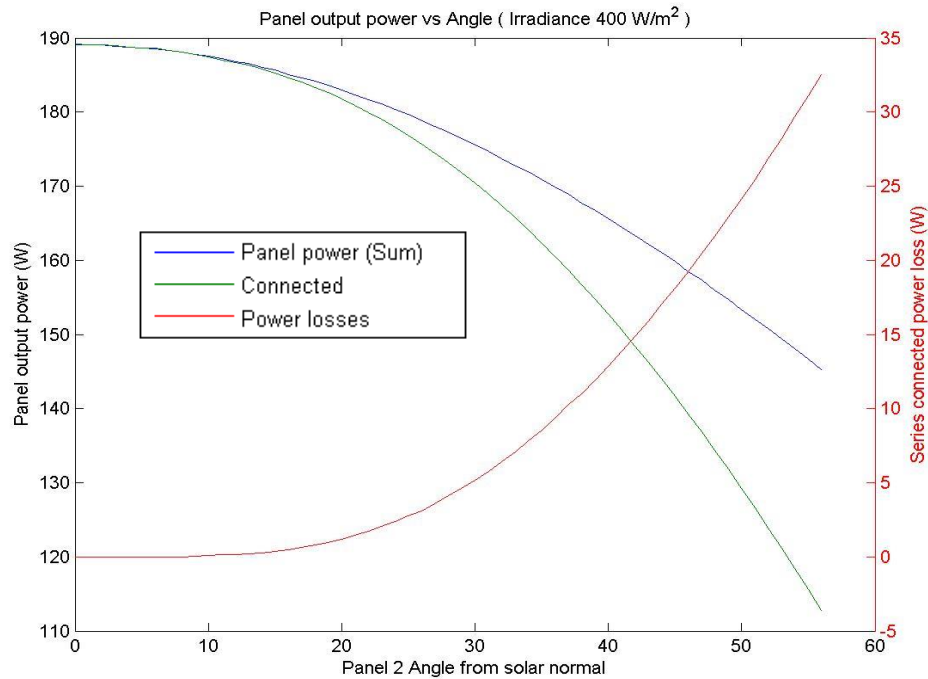


Figure 4.14c – Series MPPT: G @ 400W/m²

4.2. Thermal cooling experimentation.

Thermal measurements taken from an open circuit photovoltaic panel exposed to direct solar radiation indicated the installation tilt angle of a panel will affect the rate of cooling. Testing was conducted with the panel angled to the sun, and tilted to 0°, 14° and 24°. Temperature data obtained through the University of Southern Queensland, Faculty of Engineering and Surveying weather station, was interpolated to one minute intervals. Relative angle between the sun and panel was calculated using data obtained through the National Oceanic and Atmospheric Administration. (Cornwall, et. al, 2015) The calculated temperature rise values were scaled by the solar irradiance to provide cell temperature values normalised to 1000W/m², and results are shown in figure 4.15.

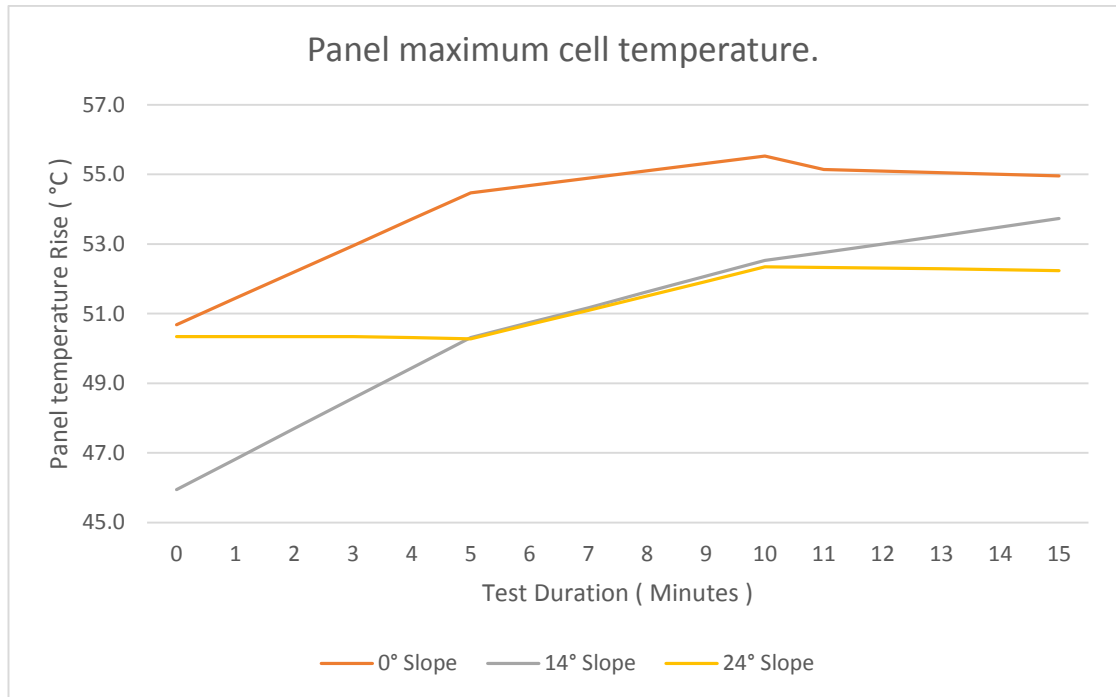


Figure 4.15 – Normalised cell temperature

The worst case cell temperatures for each angle were used to determine the efficiency of the cell. The cell characteristic is nominal temperature of 45°C and thermal power reduction of 0.44% per degree. Figure 4.16 shows the extrapolated efficiency values for panel tilt angles ranging from horizontal through to 45°. Increasing the panel tilt angle provided improved cell cooling and therefore higher energy outputs should occur. Panel efficiencies increased at a rate approximately 0.058% per degree of tilt increased from horizontal through to 24° tilt, starting at 95.37% when horizontal.

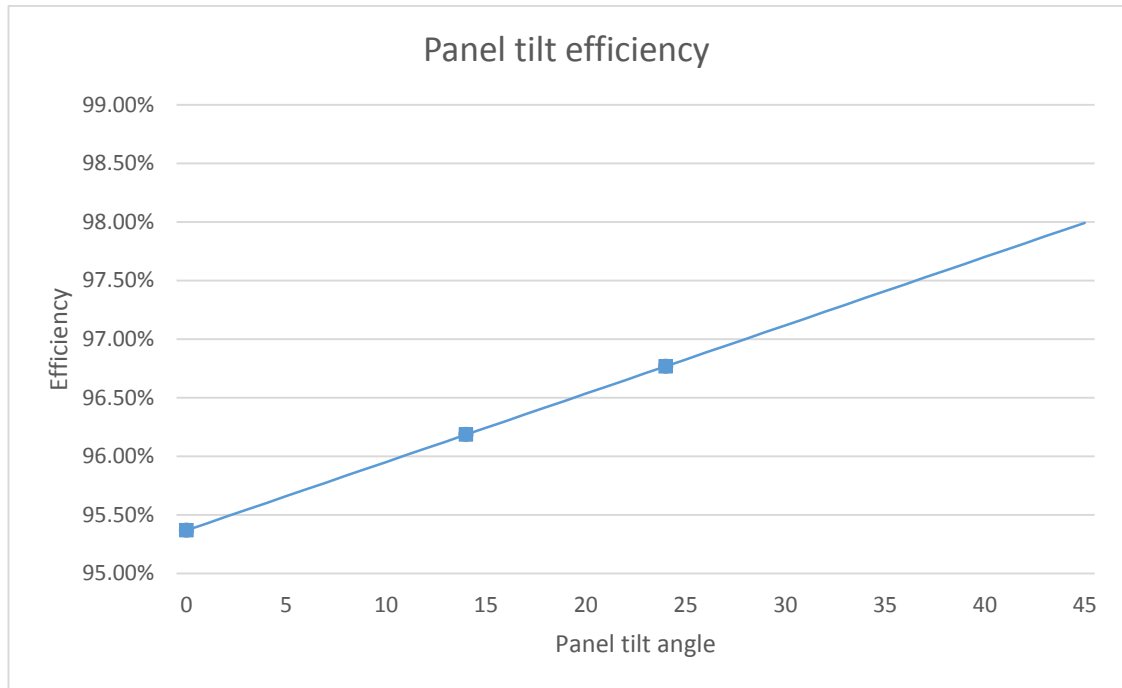


Figure 4.16 – Tilt angle efficiency

4.3. Homer energy modelling.

4.3.1. Single string

Simulations conducted at each of the selected sites were used to determine the optimum azimuth and tilt angles. Homer version 2.68 was used to simulate a 1kW photovoltaic system at each of the installation sites. The system modelled consisted of a four photovoltaic panels connected in series, connected to a single channel grid fed inverter. Annual power values results from Homer simulations have been scaled according to the panel cooling efficiency detailed in section 4.2. Optimum installation angles will be defined as those producing the greatest annual energy yield.

Inverter and panel specifications used for the simulations.

- Panel rating: 250W
- Module efficiency: 15.4%
- Nominal Temperature: 45°C (Jiangyin Hareon Power Co Ltd, n.d.)

- No of MPPT: 1
- Maximum Input Power: 1100W
- Maximum efficiency: 97% (Foshan ASEP Industrial Electronics Co, Ltd, 2015)

4.3.1.a. **Optimum installation angle: 15 degree resolution.**

Installing solar panels facing north provides the highest annual energy yield. Figure 4.17a shows the installation tilt angle relative to the installation azimuth for the Brooklyn Park site. As the installation azimuth angle is varied from the north, the maximum capability of the system is reduced. In order to maintain maximum power, the tilt angle must be reduced for azimuth angles other than the optimum. The maximum capability of panels installed at an azimuth 90° or more either direction from north occurs when the panels are parallel with the surface of the earth, occurring on all of the sites modelled. Graphs for each site can be located in appendix E.

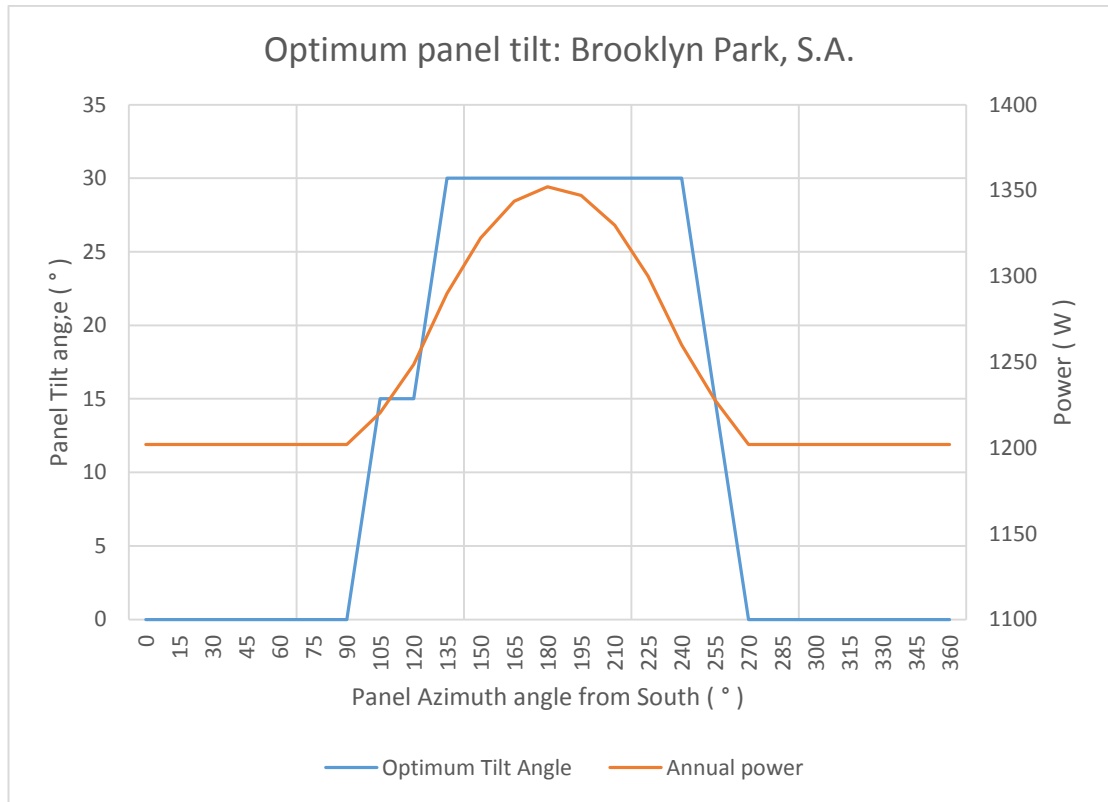


Figure 4.17a – Brooklyn Park optimum tilt angle and generated power.

4.3.1.b. Optimum installation angle: 1 degree resolution.

The identification of the optimum installation angles with an accuracy within one degree, was achieved by repeating the simulations using one degree changes of both azimuth and tilt angle. The range of azimuth and tilt angles covered were reduced to minimise the number of data points to be simulated.

Figure 4.17b shows the optimum panel tilt and azimuth angles for the Brooklyn Park site. The simulation was limited to an azimuth range of 90° through to 270° measured from due south and tilt angles ranging from flat to 35°, as the 15 degree modelling identified the optimum values for this site within this range. Table 4.1 shows the optimum installation angles for each site, and graphs for each location are located in appendix E.

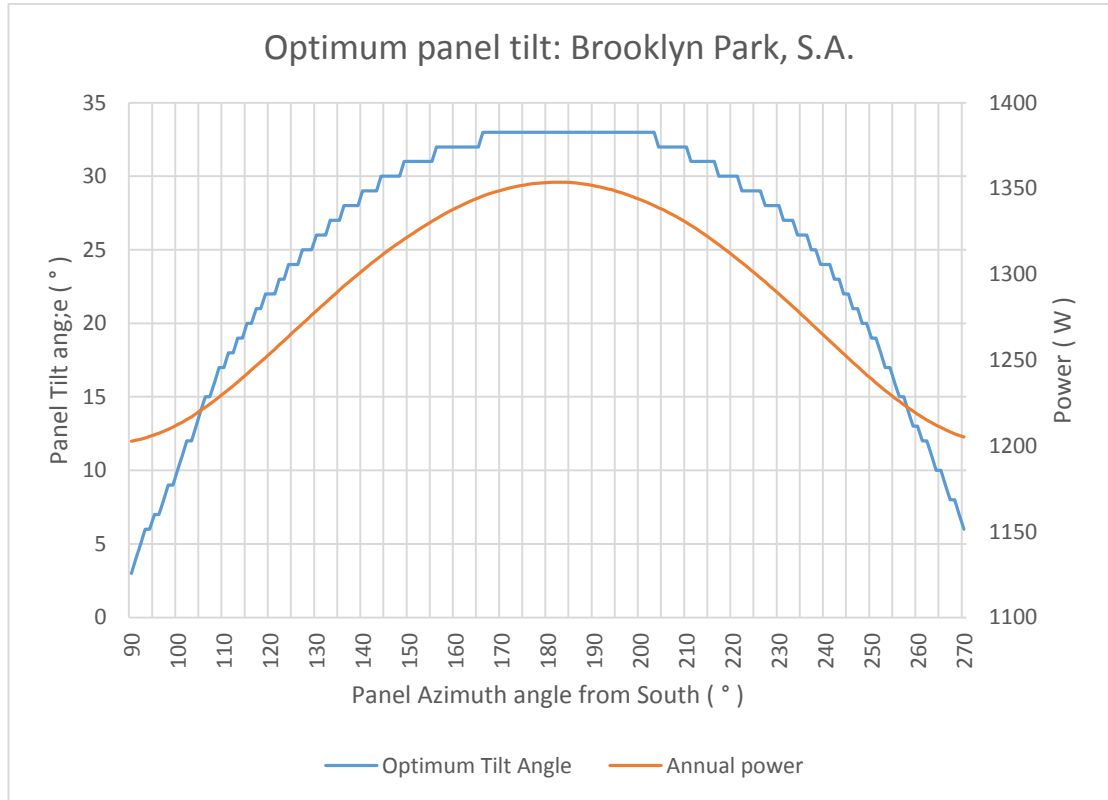


Figure 4.17b – Brooklyn Park optimum tilt angle and generated power.

Table 4.1 – Optimum installation angles and generated power.

| Location | Panel tilt angle (degrees) | Panel azimuth (degrees) | Annual power generated (kWh) |
|---------------|---------------------------------|---------------------------------|-----------------------------------|
| Brooklyn Park | 33 | 182 | 1353.7 |
| Toowoomba | 29 | 178 | 1538.3 |
| Darwin | 19 | 195 | 1649.2 |
| Hobart | 38 | 181 | 1136.2 |

4.3.1.c. **Site position effect on optimum installation angle.**

The effect of site location was investigated by repeating the simulation for each of the four sites to the north, south, east and west. Temperature data remained unchanged, however the solar radiation was updated to reflect the modified location.

The installation angles providing the greatest annual energy yield were affected by a change to the geographic location of the site, with results shown in table 4.2. Minimal effect was observed on the optimum azimuth angle with changes to the latitude, similarly the effect of the tilt angle was minor for changes to the site longitude. The change in optimum azimuth angle for Darwin was vastly different to the remaining sites, therefore omitted from the average difference. This may be due to the close proximity to the equator and will need further investigation.

Changes in site latitude presented a noticeable effect to the tilt angle, while changes in the longitude showed similar results for changes to the longitude. Simulations indicated a change to the optimum tilt angle of 0.85° per degree of latitude, while results for the azimuth indicated a change of 0.9° per degree of longitude. With the other angle set to the optimum position. These results were averaged across all four simulated sites.

Increasing the site latitude required an increased angle of tilt to maintain optimum power generation while moving the site to an increased longitude (east) required a decrease of the installation azimuth.

Table 4.2 – Optimum installation at varied site location.

| Location | | Brooklyn Park | Toowoomba | Darwin | Hobart |
|---------------------|-----------------------------|---------------|-----------|--------|--------|
| Original Simulation | Azimuth | 182 | 178 | 195 | 181 |
| | Tilt | 33 | 29 | 19 | 38 |
| Northern Simulation | Azimuth | 182 | 177 | 213 | 182 |
| | Change per degree latitude | 0 | -0.2 | 3.6 | 0.2 |
| | Tilt | 30 | 24 | 12 | 36 |
| | Change per degree latitude | -0.6 | -1 | -1.4 | -0.4 |
| Southern Simulation | Azimuth | 182 | 179 | 192 | 181 |
| | Change per degree latitude | 0 | 0.2 | -0.6 | 0 |
| | Tilt | 37 | 32 | 22 | 39 |
| | Change per degree latitude | 0.8 | 0.6 | 0.6 | 0.2 |
| North – South | Tilt | 0.7 | 0.8 | 1 | 0.3 |
| | Change per degree latitude | | | | |
| Eastern Simulation | Azimuth | 179 | 173 | 188 | 178 |
| | Change per degree longitude | -0.6 | -1 | -1.4 | -0.6 |
| | Tilt | 33 | 28 | 17 | 39 |
| | Change per degree longitude | 0 | -0.2 | -0.4 | 0.2 |
| Western Simulation | Azimuth | 186 | 182 | 202 | 184 |
| | Change per degree longitude | 0.8 | 0.8 | 1.4 | 0.6 |
| | Tilt | 34 | 29 | 18 | 38 |
| | Change per degree longitude | 0.2 | 0 | -0.2 | 0 |
| East – West | Azimuth | 0.7 | 0.9 | 1.4 | 0.6 |
| | Change per degree longitude | | | | |

4.3.1.d. Site position effect on optimum tilt without optimum azimuth.

The data generated through the simulations at locations surrounding each of the sites indicated change in panel tilt was relatively constant, irrespective of the panel installation azimuth. Figure 4.18 shows the change in panel tilt per degree of latitude for azimuth angles 60 degrees either side of the optimum value.

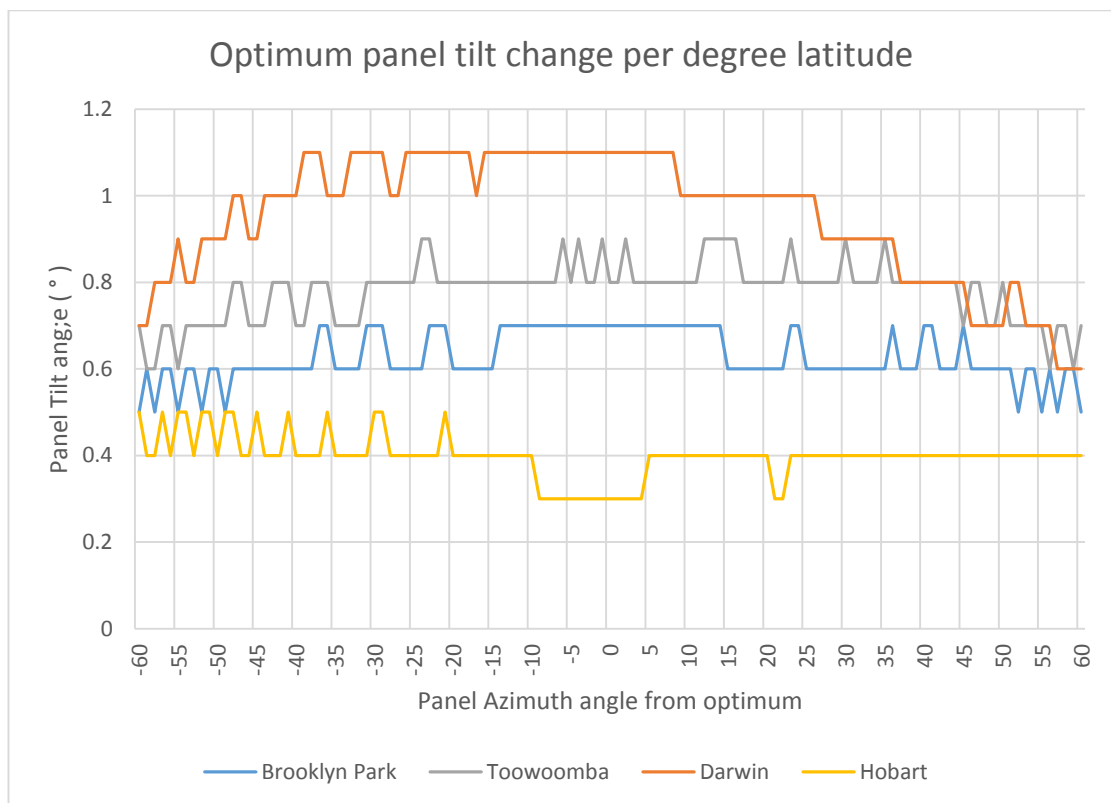


Figure 4.18 – Optimum tilt angle change per° of latitude versus panel azimuth.

4.3.1.e. Model for determination of optimum tilt and azimuth.

The location of an installation site affected both the optimum azimuth angle and the optimum tilt angle for the panels. Changes in latitude affected the tilt angle, while changes in longitude affected the optimum azimuth angle. Equation 4.1a and 4.1b can be used to approximate values of optimum azimuth and optimum panel tilt angle. Equation 4.1c is

provided to compensate for the effect of installation azimuth angles other than the optimum, valid for any value producing a non-negative result.

$$A(P_{Lo}) = 19500.882191 - 402.912829 \times P_{Lo} + 2.800723 \times P_{Lo}^2 - 0.006489 \times P_{Lo}^3 \quad (4.1a)$$

$$T(P_{LA}) = (5.288730 + 1.418184 \times P_{LA} - 0.029227 \times P_{LA}^2 + 0.000325 \times P_{LA}^3) \times C \quad (4.1b)$$

$$C(A_{Er}) = \{1 + 0.002381 \times |A_{Er}| - 0.000132 \times |A_{Er}|^2 \quad | -90 \leq A_{Er} \leq 90 \quad (4.1c)$$

$P_{Longitude}$ and $P_{Latitude}$ are geographic location coordinates for the installation site, and AZ_{Err}° is the difference between optimum and actual installation azimuth angle.

The optimum results calculated using equations 4.1a to 4.1c are close to the values identified for the majority of simulations conducted. Figure 4.19 shows error in calculated optimum azimuth for each site, including the 5° offset sites. The average error was slightly under 3°, with Darwin being the most inaccurate at 18°.

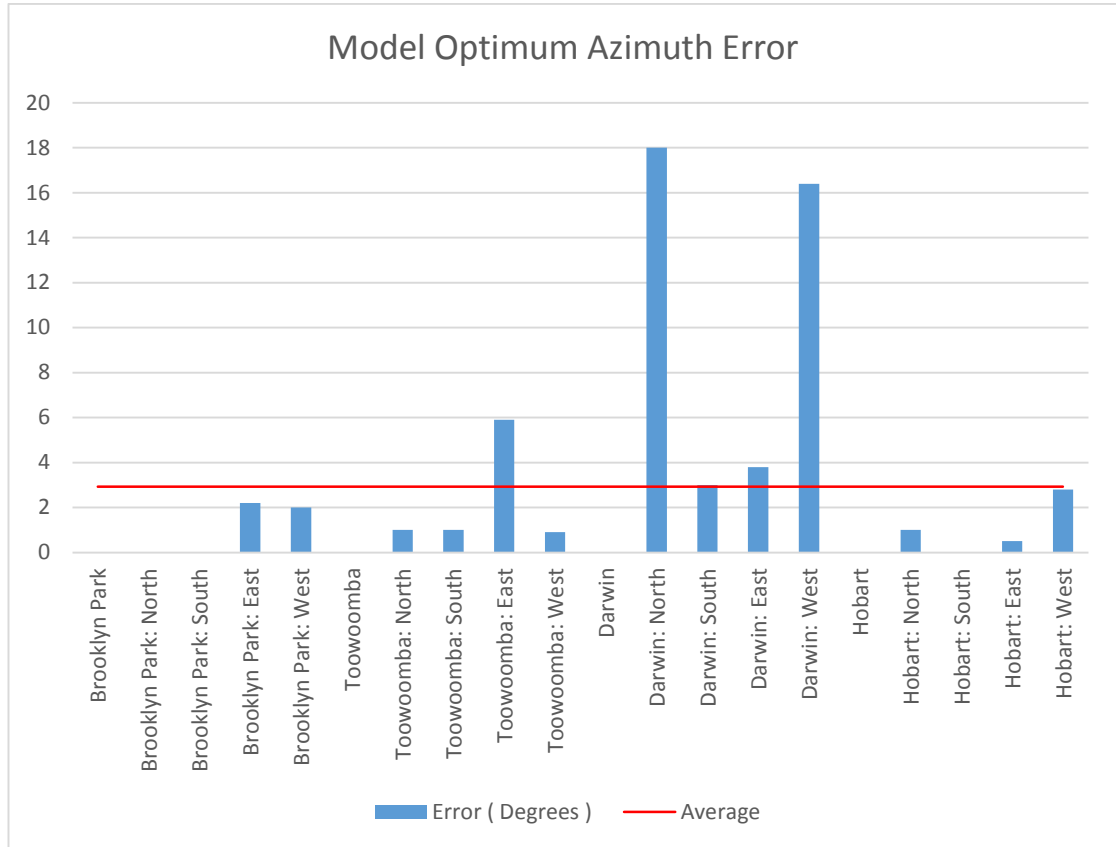


Figure 4.19 – Optimum azimuth calculated model error.

Figure 4.20 shows error in calculated optimum tilt for each site at optimum azimuth. The average error was 1° compared to the simulations, and only 2 locations exceeding 2° error.

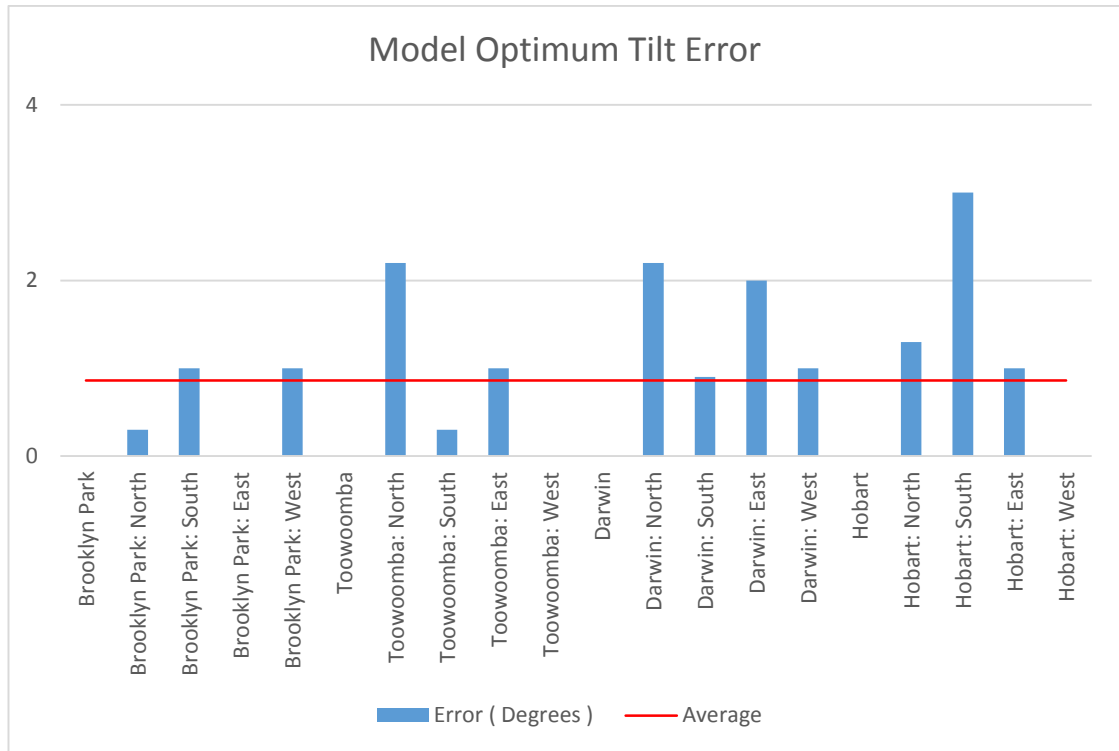


Figure 4.20 – Optimum tilt calculated model error.

4.3.1.f. Single panel model using calculated tilt installation angles.

Table 4.3 lists each potentially suitable installation surface identified from aerial images. The listed azimuth values relate to the direction of the most northern face of each building, as a clockwise rotation from south. Tilt is the angle of the panel relative to horizontal toward the selected azimuth. The annual power generation was determined for a generic 1kW single direction using Homer Energy 2.68. Resulting annual power generated was compared to an equivalent system with optimum installation orientation

Table 4.3 – Calculated optimum installation angles.

| | Surface azimuth (degrees) | Absolute Azimuth error (degrees) | Calculated Panel tilt angle (degrees) | Annual power generated (kWh) | Percentage of optimum installation |
|---------------|---------------------------|----------------------------------|---------------------------------------|--------------------------------|------------------------------------|
| Brooklyn Park | 177 | 5 | 33 | 1352.8 | 99.94 |
| | 267 | 85 | 8 | 1208.2 | 89.25 |
| | 357 | 175 | 0 | 1201.9 | 88.79 |
| | 87 | 95 | 0 | 1201.9 | 88.78 |
| Toowoomba | 195 | 17 | 29 | 1530.2 | 99.48 |
| | 217 | 39 | 26 | 1497.8 | 97.37 |
| | 246 | 68 | 16 | 1437.4 | 93.45 |
| | 66 | 112 | 0 | 1404.2 | 91.29 |
| | 37 | 141 | 0 | 1404.2 | 91.29 |
| | 15 | 163 | 0 | 1404.2 | 91.29 |
| Darwin | 199 | 4 | 19 | 1648.9 | 99.98 |
| | 19 | 176 | 0 | 1586.0 | 96.17 |
| Hobart | 201 | 20 | 38 | 1123.0 | 98.83 |
| | 21 | 160 | 0 | 971.1 | 85.46 |

4.3.2. Dual string modelling.

The optimum installation angle results from simulations with two independent photovoltaic strings resembled the results of the equivalent single string installation, while confirming the results of the IV curve simulations for panels at different angles. Maximum power generation occurred when both strings installed at the single string optimum installation angles. Figure 4.21 shows the annual energy generated with 2 strings, each installed at 177° from south. The reduction of generated power occurs when the tilt angle of either of the strings is varied from the optimum, and also occurs with changes to the azimuth. The further the installation angle is from the optimum installation, the greater the magnitude of the reduction in power generation.

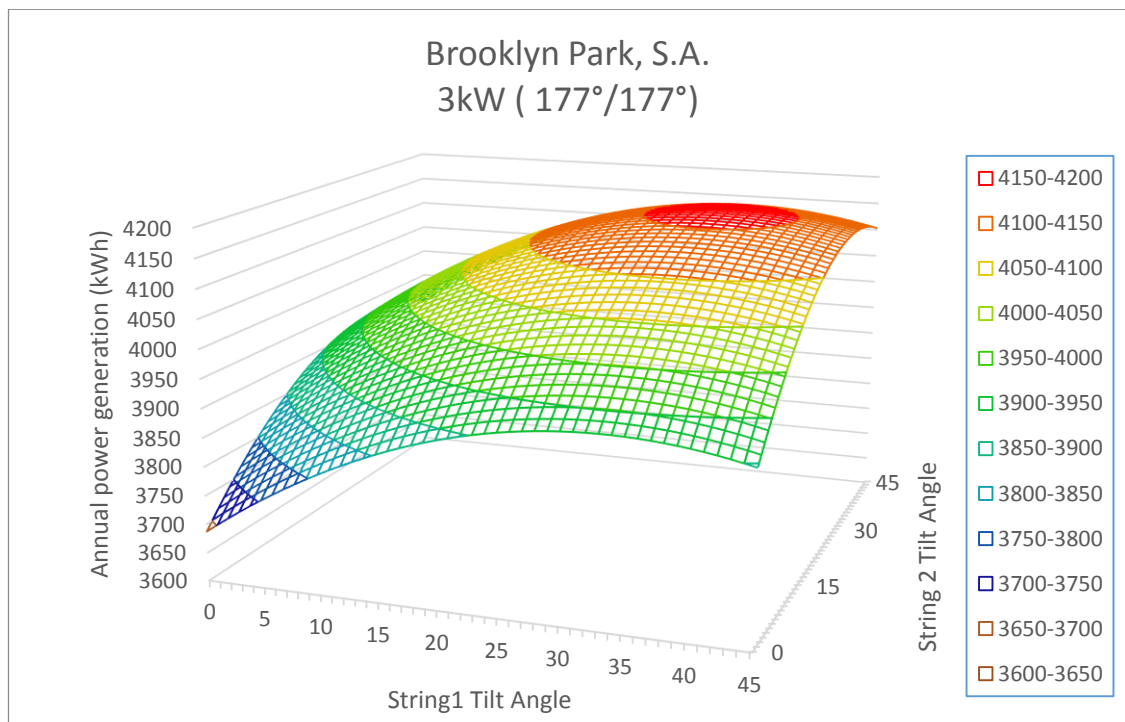


Figure 4.21 – Generated power: 2 string 3kW at Azimuth 177.

5. Conclusion

There are many factors identified throughout this dissertation which affect the volume of energy generated by a photovoltaic installation. The design of such systems can be used to accommodate some of these factors including but not limited to, panel angle, panel efficiency and inverter configuration. Factors such as temperature and solar irradiance are beyond our control.

The connection of a number of solar panels together will lead to an increase in the system output. Differences from one panel to the next combined with unequal energy input and variations in installation conditions. The effect parallel and series connected panels installed at two separate angles leads to energy losses within the system, and generally increases as the difference in angle is increased. Under most conditions, the magnitude of these losses remained constant while the difference in angle was less than 10° .

Panels which have been installed within 15 degrees from north should generate more energy over a year than other azimuth ranges. Therefore installation should be prioritised to the roof surface facing nearest to north, and the tilt angle should be set relative to the actual installation azimuth. Equations 4.1a, 4.1b and 4.1c can assist in the determination of the optimum angles for installation.

Wherever possible, the installation of solar panels in locations which are subjected to a large amount of shading should be avoided. Where there is no possibility of installing the system in a location completely free of shade, the D.C. connection between must not be connected in parallel as this will lead to substantial energy losses.

The selection of the inverter is an equally important factor in the design of a solar energy system. The system designer must take care to ensure the maximum voltage generated within each string does not exceed the maximum input of the inverter, at the same time maximising the time where the string voltage will exceed the minimum voltage required to drive the circuitry of the inverter. The maximum power capable of being delivered to the input of the inverter should remain within a range 30 - 100% of the rating of the input. Operating outside of this range will lead to a decreased efficiency of the system Inverters with dual maximum power point tracking provided the lowest efficiency losses for two

string systems. The use of two inverters, or a single channel power point tracking inverters were able to demonstrate similar efficiency values, generally only when all panels were installed on common orientation.

5.1. Further work.

Information identified throughout the course of this research has provided opportunity for further work into the optimisation of solar power systems.

Modelling which was conducted within Matlab was limited to two separate panels connected in either series or parallel. Shading was modelled by reducing the panel output relative to the shaded area. The model could be revised to include the effect of partial shading over the panel. Modelling the IV curve of each cell separately using a common voltage vector could assist in the analysis of more complex shading patterns, and the effect of a combination of connection methods.

The intention of the energy optimisation model was to maximise the power generated using photovoltaic solar power systems, although this approach may not provide maximum benefit for all circumstances. The model could be revised to include a profile of electrical demand to identify, allowing customisation of the model to a consumers requirements.

The geographic locations used for the optimisation simulations covered a wide range of latitudes, ranging from the far north through to the south. The locations were limited in longitude covering a range from central Australia through to the east coast. The model could be extended to include locations across to the west coast.

6. References

Ahfock, A 2011, *ELE3805 Power electronics principles and communications: Study book 1*, University of Southern Queensland, Toowoomba.

Bellini, A, Bifaretti, S, Iacovone, V, Cornaro, C n.d. '*Simplified Model of a Photovoltaic Module*', viewed 2 May 2015, <http://www.google.com.au/url?sa=t&rct=j&q=&esrc=s&source=web&cd=13&cad=rja&uact=8&ved=0CGEQFjAM&url=http%3A%2F%2Fwww.researchgate.net%2Fprofile%2FCristina_Cornaro%2Fpublication%2F224605112_Simplified_model_of_a_photovoltaic_module%2Flinks%2F0c960527a618b46d97000000.pdf&ei=yq9EVYzjJKHGmQX_-IG4Ag&usq=AFQjCNGwdKwEr3DKEbDpo_2B-ryaRMoPYg&bvm=bv.92291466,d.dGY>

Commonwealth of Australia 2015, '*Climate Data Online*', Bureau of Meteorology, viewed 18 March 2015, <<http://www.bom.gov.au/climate/data/>>

Cornwall, C, Horiuchi, A & Lehman, C, 2015. '*Solar Position Calculator*', viewed 29 September 2015, <<http://www.esrl.noaa.gov/gmd/grad/solcalc/azel.html>>

Encyclopædia Britannica, Inc. 2015a, *Brewsters Law*, viewed 8 June 2015, <<http://www.britannica.com/EBchecked/topic/79080/Brewsters-law>>

Encyclopædia Britannica, Inc. 2015b, *Refractive index*, viewed 8 June 2015, <<http://www.britannica.com/EBchecked/topic/495677/refractive-index>>

ENG4111 Research project part 1: *Project reference book 2014*, University of Southern Queensland, Toowoomba.

European Agency for Safety and Health at Work, n.d. *HAZARD IDENTIFICATION CHECKLIST: OSH RISKS ASSOCIATED WITH SMALL-SCALE SOLAR ENERGY APPLICATIONS*, viewed 20 May 2015, <[https://www.google.com.au/url?sa=t&rct=j&q=&esrc=s&frm=1&source=web&cd=1&cad=rja&uact=8&ved=0CDkQFjAA&url=https%3A%2F%2Fosha.europa.eu%2Fen%](https://www.google.com.au/url?sa=t&rct=j&q=&esrc=s&frm=1&source=web&cd=1&cad=rja&uact=8&ved=0CDkQFjAA&url=https%3A%2F%2Fosha.europa.eu%2Fen%2F)>

2Fpublications%2Fe-facts%2Fe-fact-69-hazard-identification-checklist-osh-risks-associated-with-small-scale-solar-energy-applications&ei=a3ZcVc6hB4bNmWXPYDoAg&usg=AFQjCNEML9PgSjaT3bGcvw2S9gVIzfeNwQ&bvm=bv.93756505,d.dGY>.

Folsom Labs, 2014, *Inverter Modelling*, viewed 25 September 2015, <<https://www.folsomlabs.com/modeling/system/inverter>>

Foshan ASEP Industrial Electronics Co, Ltd. 2014, *Single Channel Grid-Tie Inverter*, viewed 15 May 2015, <<http://www.asepups.com/single-channel-grid-tie-inverter1.html>>

Google, 2015, *Google Maps*, viewed May 2015, <<https://www.google.com.au/maps>>

Green Rhino Energy Ltd. 2013, *Solar power: Radiation*, viewed 25 April 2015, <<http://www.greenrhinoenergy.com/solar/radiation/characteristics.php>>

Homer Energy 2015, *The HOMER® Microgrid Software*, viewed 21 October 2015, <<http://www.homerenergy.com/software.html>>

Honsberg, C & Bowden, S 2013a, *Air Mass*, viewed 29 March 2015, <<http://pveducation.org/pvcdrom/properties-of-sunlight/air-mass>>

Honsberg, C & Bowden, S 2013b, *Anti-Reflection Coatings*, viewed 29 March 2015, <<http://pveducation.org/pvcdrom/design/anti-reflection-coatings>>

Honsberg, C & Bowden, S 2013c, *Bypass Diodes*, viewed 29 March 2015, <<http://pveducation.org/pvcdrom/modules/bypass-diodes>>

Honsberg, C & Bowden, S 2013d, *Characteristic Resistance*, viewed 29 March 2015, <<http://pveducation.org/pvcdrom/solar-cell-operation/charecteristic-resistance>>

Honsberg, C & Bowden, S 2013e, *Effect of parasitic Resistances*, viewed 29 March 2015, <<http://pveducation.org/pvcdrom/solar-cell-operation/effect-of-parasitic-resistances>>

Honsberg, C & Bowden, S 2013f, *Effect of Temperature*, viewed 29 March 2015, <<http://pveducation.org/pvcdrom/solar-cell-operation/effect-of-temperature>>

Honsberg, C & Bowden, S 2013g, *Efficiency*, viewed 29 March 2015, <<http://pveducation.org/pvcdrom/solar-cell-operation/efficiency>>

Honsberg, C & Bowden, S 2013h, *Energy of Photon*, viewed 29 March 2015, <<http://pveducation.org/pvcdrom/properties-of-sunlight/energy-of-photon>>

Honsberg, C & Bowden, S 2013i, *Heat Generation in PV Modules*, viewed 29 March 2015, <<http://pveducation.org/pvcdrom/modules/heat-generation-in-pv-modules>>

Honsberg, C & Bowden, S 2013j, *Hot Spot Heating*, viewed 29 March 2015, <<http://pveducation.org/pvcdrom/modules/hot-spot-heating>>

Honsberg, C & Bowden, S 2013k, *Mismatch Effects*, viewed 29 March 2015, <<http://pveducation.org/pvcdrom/modules/mismatch-effects>>

Honsberg, C & Bowden, S 2013m, *Optical Losses*, viewed 29 March 2015, <<http://pveducation.org/pvcdrom/design/optical-losses>>

Honsberg, C & Bowden, S 2013n, *Photon Flux*, viewed 29 March 2015, <<http://pveducation.org/pvcdrom/properties-of-sunlight/photon-flux>>

Honsberg, C & Bowden, S 2013o, *Properties of Light*, viewed 29 March 2015, <<http://pveducation.org/pvcdrom/properties-of-sunlight/properties-of-light>>

Honsberg, C & Bowden, S 2013p, *Radiant Power Density*, viewed 29 March 2015, <<http://pveducation.org/pvcdrom/properties-of-sunlight/radiant-power-density>>

Honsberg, C & Bowden, S 2013q, *Series Resistance*, viewed 29 March 2015, <<http://pveducation.org/pvcdrom/solar-cell-operation/series-resistance>>

Honsberg, C & Bowden, S 2013r, *Shunt Resistance*, viewed 29 March 2015, <<http://pveducation.org/pvcdrom/solar-cell-operation/shunt-resistance>>

Honsberg, C & Bowden, S 2013s, *Solar Radiation on a Tilted Surface*, viewed 29 March 2015, <<http://pveducation.org/pvcdrom/properties-of-sunlight/solar-radiation-on-tilted-surface>>

Honsberg, C & Bowden, S 2013t, *Surface Texturing*, viewed 29 March 2015, <<http://pveducation.org/pvcdrom/design/surface-texturing>>

Honsberg, C & Bowden, S 2013u, *Heat Loss in PV Modules*, viewed 29 March 2015, <<http://pveducation.org/pvcdrom/modules/heat-loss-in-pv-modules>>

Howell, J, Menguc, P & Siegel, R 2010, *Thermal Radiation Heat Transfer*, CRC Press.

Jiangyin Hareon Power Co Ltd, n.d, *Solar Module*.

Jordan, D & Kurtz, S , *Photovoltaic Degradation Rates — An Analytical Review*, *Photovoltaics: Research and Applications*, viewed 18 March 2015, <<http://www.nrel.gov/docs/fy12osti/51664.pdf>>

Larson, R & Falvo, D 2009, *Elementary linear algebra*, Horton Mifflin Harcourt Publishing Company, Boston.

Migan, G, 2013 *Study of the operating temperature of a PV module*, <http://www.google.com.au/url?sa=t&rct=j&q=&esrc=s&frm=1&source=web&cd=14&cad=rja&uact=8&ved=0CCsQFjADOApqFQoTCK6joqnZkcgCFYgolAod6aEEpA&url=http%3A%2F%2Fwww.ht.energy.lth.se%2Ffileadmin%2Fht%2FKurser%2FMVK160%2F2012%2FGail-Angee_Migan.pdf&usq=AFQjCNFsSU9gLkEQiPY1kRGXcdphRu5Csg&bvm=bv.103627116,d.dGo>

MPPT Solar n.d a, *Connecting solar panels in parallel*, viewed 8 June 2015, <<http://www.mpptsolar.com/en/solar-panels-in-parallel.html>>

MPPT Solar n.d b, *Connecting solar panels in series*, viewed 8 June 2015, <<http://www.mpptsolar.com/en/solar-panels-in-series.html>>

National Instruments, 2009a 'Part I – *Photovoltaic Cell Overview*', National Instruments, Austin, Texas, USA, viewed 29 March 2015, <<http://www.ni.com/white-paper/7229/en/>>

National Instruments, 2009b 'Part II – *Photovoltaic Cell I-V Characterization Theory and LabVIEW Analysis Code*', National Instruments, Austin, Texas, USA, viewed 29 March 2015, <<http://www.ni.com/white-paper/7230/en/>>

National Instruments, 2009c '*Maximum Power Point Tracking*', National Instruments, Austin, Texas, USA, viewed 29 March 2015, <<http://www.ni.com/white-paper/8106/en/>>

Palm, W 2009, *Introduction to MATLAB for engineers*, McGraw Hill, New York.

Pandit, PK & Chaurasia, PBL 2014 'Experimental Study of Shading Effect on PV Module and Improvement in Power Using Diode on Series & Parallel PV Module', International Journal of Science and Research (IJSR), vol. 3, issue. 6, viewed 8 April 2015, <<http://ijsr.net/archive/v3i6/MDIwMTQ1MjE%3D.pdf>>

Perlin, J n.d, *A History of Photovoltaic*, viewed 12 March 2015, <<http://www.usc.edu/org/edisonchallenge/2008/ws1/A%20History%20of%20Photovoltaics.pdf>>

Renew Economy, 2015, *Australia reaches 4GW of rooftop solar PV*, viewed 25 July 2015, <<http://reneweconomy.com.au/2014/australia-reaches-4gw-rooftop-solar-pv-44719>>

Rosenblatt, L 2015 '*A GRID TIE INVERTER FOR SOLAR SYSTEMS*', viewed 19 April 2015, <<http://solar.smeps.us/grid-tie-inverter-schematic.html>>

Safe work Australia, 2011 '*HOW TO MANAGE WORK HEALTH AND SAFETY RISKS*' *Code of Practice*.

Sargosis Solar & Electric 2014a, *Calculating the IV and PV curves for a Solar Module*, viewed 7 April 2015, <<http://sargosis.com/articles/science/how-pv-modules-work/calculating-the-iv-and-pv-curves-for-a-solar-module/>>

Sargosis Solar & Electric 2014b, *How Shade Affects a Solar Array*, viewed 20 June 2015, <<http://sargosis.com/articles/science/how-shade-affects-a-solar-array/>>

Solar edge 2010, *Technical Note Bypass Diode Effects in Shaded Conditions*, viewed 20 June 2015, <<http://resources.solmetric.com/get/Guide%20to%20Interpreting%20I-V%20Curves.pdf>>

Tayyan, Dr A 2006, *An empirical model for Generating the IV characteristics for a Photovoltaic system*, viewed 2 May 2015, <http://www.alaqsa.edu.ps/site_resources/aqsa_magazine/files/225.pdf>

The Florida Solar Energy Center , 2014a '*Cells, Modules and arrays*', University of Central Florida, Cocoa, Florida, USA, viewed 18 March 2015, <http://www.fsec.ucf.edu/en/consumer/solar_electricity/basics/cells_modules_arrays.htm>

The Florida Solar Energy Center , 2014b, '*How PV cells are made*', University of Central Florida, Cocoa, Florida, USA, viewed 18 March 2015, <http://www.fsec.ucf.edu/en/consumer/solar_electricity/basics/how_cells_made.htm>

The Florida Solar Energy Center , 2014c '*How PV cells work + more*', University of Central Florida, Cocoa, Florida, USA, viewed 18 March 2015, <http://www.fsec.ucf.edu/en/consumer/solar_electricity/basics/how_pv_cells_work.htm>

Tindo Solar, 2015, *Data Sheet Karra Model*, Mawson Lakes.

University of Melbourne, 2004. *RISK ASSESSMENT 3D Model*, viewed 22 May 2015, <<http://www.google.com.au/url?sa=t&rct=j&q=&esrc=s&frm=1&source=web&cd=1&ved=0CCQQFjAA&url=http%3A%2F%2Fwww.cab.unimelb.edu.au%2Fpdf%2Fehs3d.doc&ei=KglfVdzjMYXn8AWrlIGIAw&usg=AFQjCNGEoDvOKSB2qVqDoz0xgkqg5kHy7A&bvm=bv.93990622,d.dGc>>.

Xue, Y, Chang, L, Bækthøj Kjær, S, Bordonau, J & Shimizu, T 2004 '*Topologies of Single-Phase Inverters for Small distributed power generators: An Overview*', IEEE

TRANSACTIONS ON POWER ELECTRONICS, vol. 19, no. 5, viewed 12 February 2015,

<<http://ieeexplore.ieee.org.ezproxy.usq.edu.au/stamp/stamp.jsp?tp=&arnumber=1331492>>

Yakoob, J & Abbas, E. 2014 '*Experimental investigation of convection heat transfer for laminar flow in an inclined annulus*', International Journal of Mechanical Engineering and Technology (IJMET), vol. 5, issue. 4, viewed 28 September 2015, <<http://www.iaeme.com/MasterAdmin/UploadFolder/30120140504020/30120140504020.pdf>>

Appendix A. Project Specification

UNIVERSITY OF SOUTHERN QUEENSLAND

ENG4111 & ENG4112 Engineering research project 2015

PROJECT SPECIFICATION

Issue C,

03 April 2015

Student: Christopher KIRBY

Topic: Comparison of PV maximum power point.

Topic Author: Andreas HELWIG

Supervisor: Catherine HILLS

Enrolment: ENG4111 Semester 1, 2015

ENG4112 Semester 2, 2015

Project Aim: The final goal of this project is to provide guidelines for the installation of photovoltaic (solar) systems within Australia. These guides will assist in maximising the efficiency of such systems.

Programme:

- Provide a basic introduction to photovoltaic (PV) panels.
- Research factors affecting the efficiency of PV systems.
- Research and define maximum power point tracking (MPPT).

- Research various inverter configurations for a 2 different direction string system.
- Generate Matlab models for each configuration, accounting for the characteristics of the inverter, panels and string design.
- Based on the results obtained from the modelling, produce a set of guidelines to optimise system output for PV systems throughout Australia.
- Using Homer Energy software, model different sized PV array in differing climate locations throughout Australia for the selected inverter configurations in order to quantify the financial and economic benefits of system optimisation.

As time permits:

- Calculate financial savings and environmental benefits from improving efficiency of existing installations throughout Australia.
- Conduct a basic feasibility into reworking existing installations to improve efficiency.

Agreed:

Christopher J Kirby (Student) _____ (Supervisor)

04 / 04 / 2015 ____ / ____ / _____

Appendix B. Project timeline

Table B.1 – Project timeline

| | Date | | |
|---|----------|----------|----------|
| | Target | Start | Complete |
| Project allocation | 11/03/15 | 25/09/14 | 11/03/15 |
| Project specification | 18/03/15 | 12/03/15 | 03/04/15 |
| Search and identify suitable literature | 05/04/15 | 25/09/14 | 05/04/15 |
| Conduct literature review | 13/05/15 | 25/09/14 | 14/05/15 |
| Project writing: Literature review | 20/05/15 | 10/04/15 | 26/05/15 |
| Project writing: Background information | 03/06/15 | 10/04/15 | 05/06/15 |
| Preliminary report - Submit to supervisor | 27/05/15 | -- | 31/05/15 |
| Submission of project preliminary report | 03/06/15 | -- | 03/06/15 |
| IV curve modelling | 15/07/15 | 10/06/15 | 13/06/15 |
| Project writing: IV curve modelling | 29/07/15 | 13/06/15 | 31/07/15 |
| Site installation modelling: Single panel | 26/08/15 | 05/08/15 | 26/08/15 |
| Site installation modelling: Dual String | 31/08/15 | 25/08/15 | 19/09/15 |
| Project writing: Site modelling information | 23/09/15 | 20/09/15 | 11/10/15 |
| Project writing: Abstract | 01/10/15 | 14/10/15 | 18/10/15 |
| Project writing: Disclaimer page | 01/10/15 | 19/10/15 | 19/10/15 |
| Project writing: Certification page | 01/10/15 | 19/10/15 | 19/10/15 |
| Project writing: Acknowledgements | 01/10/15 | 19/10/15 | 21/10/15 |
| Project writing: Results | 01/10/15 | 16/06/15 | 11/10/15 |
| Project writing: Conclusion | 01/10/15 | 11/10/15 | 12/10/15 |
| Partial draft submission | 16/09/15 | -- | 16/09/15 |
| Project completion and submission | 29/10/15 | | 28/10/15 |

Appendix C. Derivation of formulas

C.1. Current voltage relationship: IV curve

C.1.1. Solar panel model

Generalised procedure of the solar panel model developed by Bellini et al. (n.d.)

1. The function of panel current is defined as,

$$I_p = I_{SC} \left[1 - C_1 \left(e^{\left(\frac{V_p}{C_2 \times V_{OC}} \right)} - 1 \right) \right] \quad (C.1a)$$

$$V_p = C_2 \times V_{OC} \times \ln \left(1 + \frac{\left(1 - \frac{I_p}{I_{SC}} \right)}{C_1} \right) \quad (C.1b)$$

2. Determine the panel voltage and current specifications for the given temperature and irradiance.

$$I_{SC}(G, T) = I_{SCS} \frac{G}{G_s} [1 + \alpha (T - T_s)] \quad (C.2)$$

$$V_{OC}(T) = V_{OCS} + \beta (T - T_s) \quad (C.3)$$

$$I_{MPP}(G, T) = I_{MPPS} \frac{G}{G_s} [1 + \alpha (T - T_s)] \quad (C.4)$$

$$V_{MPP}(T) = V_{MPPS} + \beta (T - T_s) \quad (C.5)$$

3. Determine the values of coefficients C_1 and C_2 .

$$C_2 = \frac{\left(\frac{V_{MPP}}{V_{OC}} - 1 \right)}{\ln \left(1 - \frac{I_{MPP}}{I_{SC}} \right)} \quad (C.6)$$

$$C_1 = \left(1 - \frac{I_{MPP}}{I_{SC}}\right) e^{\left(\frac{-V_{MPP}}{C_2 \times V_{OC}}\right)} \quad (C.7)$$

4. Determine the open circuit voltage value at the irradiance value, and voltage correction value.

$$V_{OCM} = C_2 \times V_{OCS} \times \ln\left(1 + \frac{\left(1 - \frac{G}{G_S}\right)}{C_1}\right) \quad (C.8a)$$

$$\Delta V(G) = V_{OCS} - V_{OCM} \quad (C.9)$$

5. Revise equations C.3 and C.5 to include the voltage correction value.

$$V_{OC}(G, T) = V_{OCS} + \beta(T - T_s) - \Delta V(G) \quad (C.3a)$$

$$V_{MPP}(G, T) = V_{MPPS} + \beta(T - T_s) - \Delta V(G) \quad (C.5a)$$

C.1.2. Solar panel model error

The IV curves generated using the procedure described by Bellini et al. shown in figure C.1a and C.1b for varied irradiance and temperature levels respectively were significantly different to figures C.2a and C.2b listed within the paper. The input specified by Bellini et al. (n.d.) are listed in table C.1.

Table C.1 – IV curve input parameters.

| Parameter | Value | Unit |
|-----------|-------|------------------|
| I_{SC} | 5.30 | A |
| V_{OC} | 44.60 | V |
| V_{MPP} | 35.40 | V |
| I_{MPP} | 4.95 | A |
| α | 1.46 | mA/ °C |
| β | -158 | mV / °C |
| T_s | 25 | °C |
| G_s | 1000 | W/m ² |

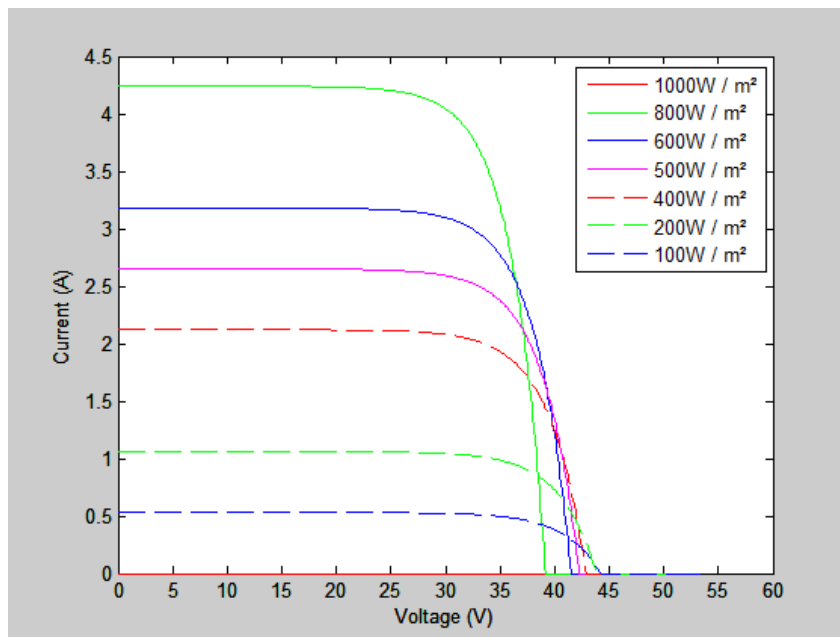


Figure C.1a – Varied irradiance model.

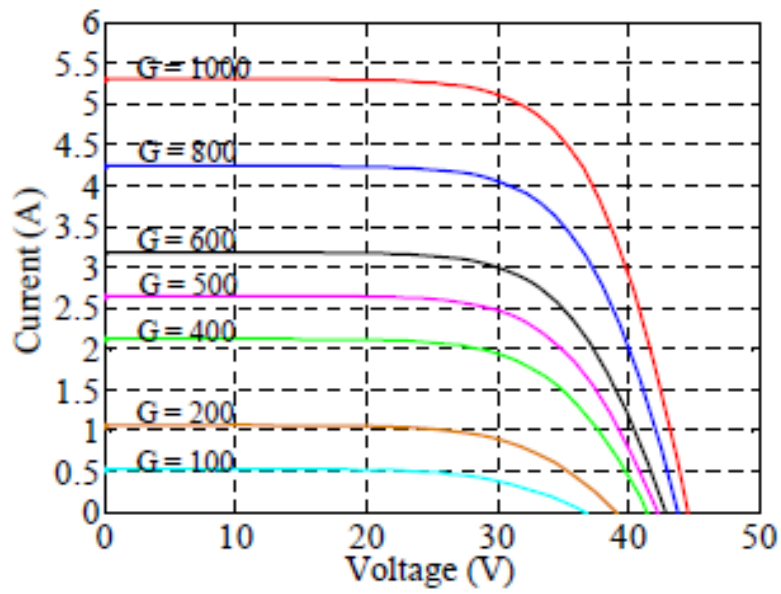


Figure C.1b – Bellini et al. Varied irradiance.

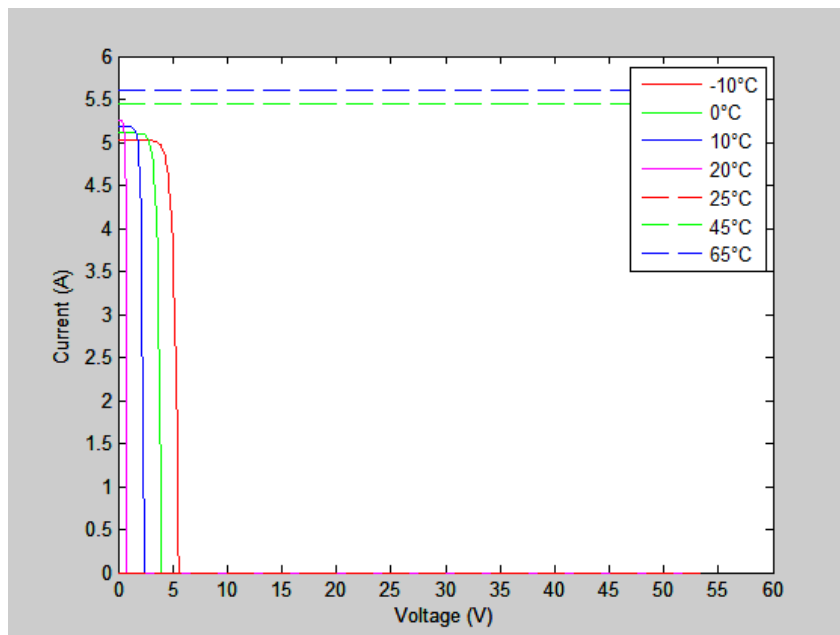


Figure C.2a – Varied temperature model.

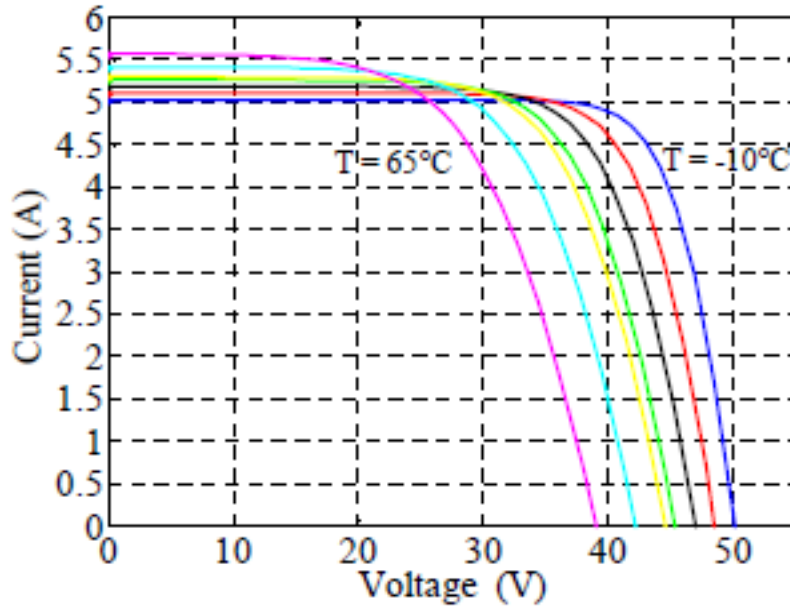


Figure C.2b – Bellini et al. Varied temperature.

Analysis of the model using varying levels of irradiation identified equation C.8 as the source of the error. This equation represents the open circuit voltage at irradiance levels other than the standard test conditions. (Bellini et al, n.d.) Figure C.3a details the open circuit voltage versus irradiance for the uncorrected model using equation C.8a, and figure C.3b for the corrected model using equation C.8b.

$$V_{OCM} = C_2 \times V_{OCS} \times \ln \left(1 + \frac{\left(\frac{G}{G_S} \right)}{c_1} \right) \quad (\text{C.8b})$$

The IV curves which have been generated using the method detailed by Bellini et al. (n.d.) and the corrected equation C.8b are shown in figure C.4a for varied irradiance and figure C.4b for varied temperature.

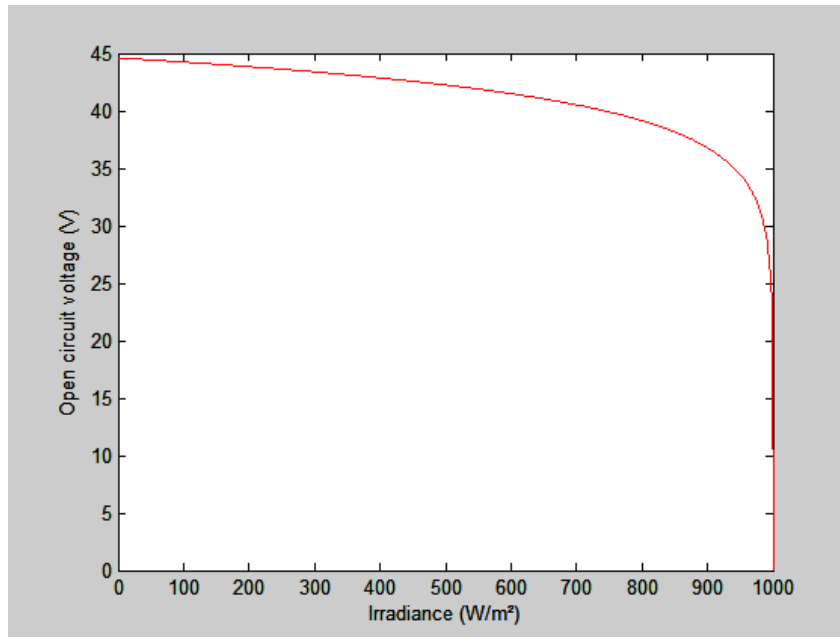


Figure C.3a – Model V_{OCM} vs irradiance.

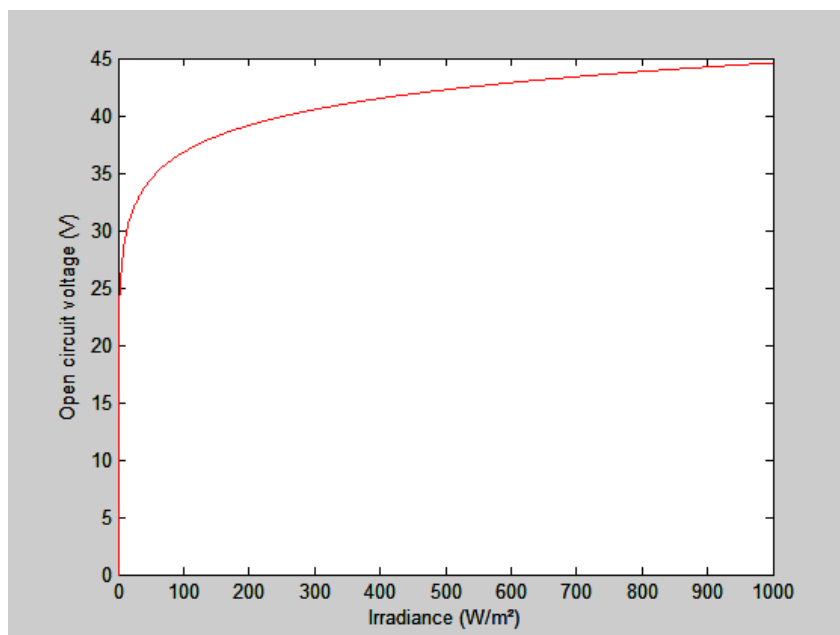


Figure C.3b – Corrected V_{OCM} vs irradiance

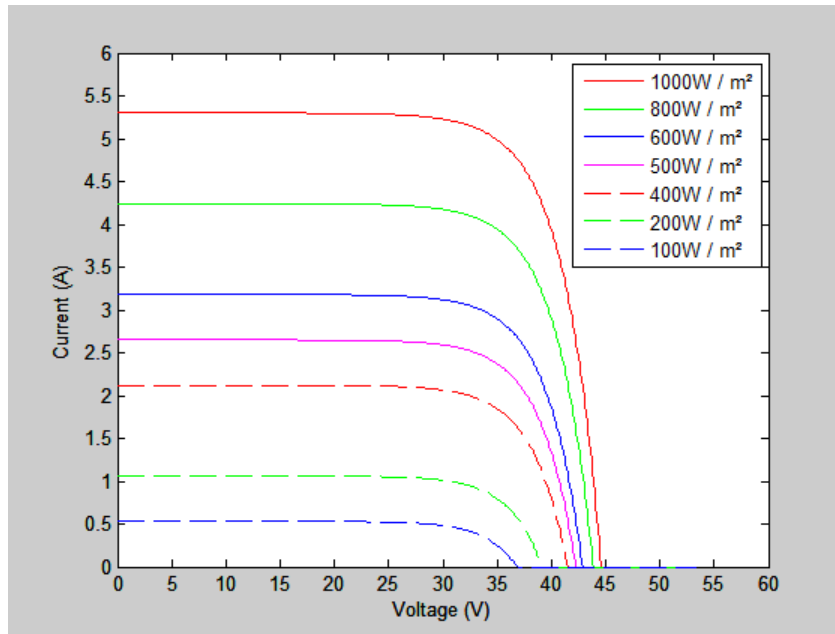


Figure C.4a – Varied irradiance corrected.

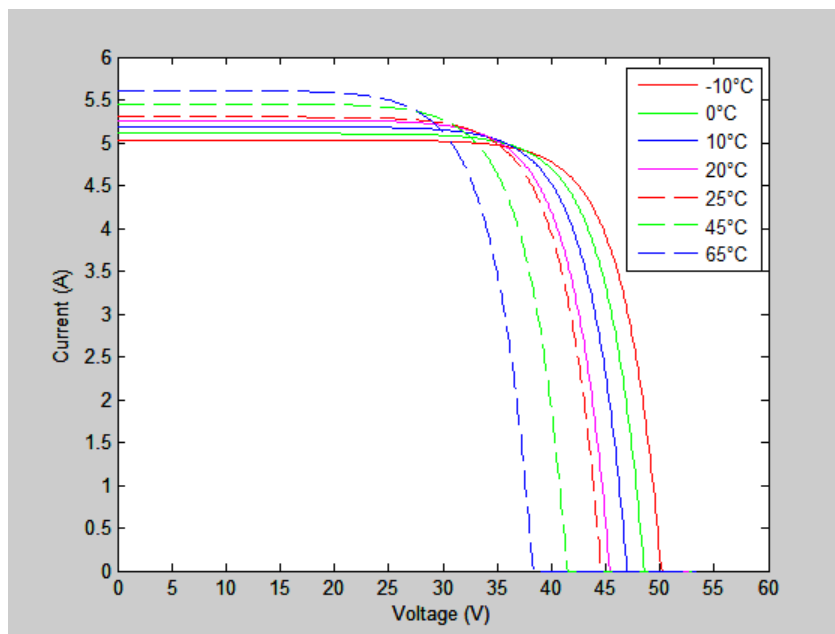


Figure C.4b – Varied temperature corrected.

C.1.3. Optimum azimuth

The function used to describe the optimum installation azimuth was defined using a polynomial curve fit based on the four locations which were simulated in Homer.

Using the generic equation

$$a_0 + a_1x + a_2x^2 + a_3x^3 = y_0 \quad (\text{C.10})$$

Converting to augmented matrix form,

$$\left[\begin{array}{cccc|c} 1 & P_{Lo1} & P_{Lo1}^2 & P_{Lo1}^3 & Az(P_{Lo1}) \\ 1 & P_{Lo2} & P_{Lo2}^2 & P_{Lo2}^3 & Az(P_{Lo2}) \\ 1 & P_{Lo3} & P_{Lo3}^2 & P_{Lo3}^3 & Az(P_{Lo3}) \\ 1 & P_{Lo4} & P_{Lo4}^2 & P_{Lo4}^3 & Az(P_{Lo4}) \end{array} \right]$$

Let,

$$P_{Lo1} = 138.55$$

$$P_{Lo2} = 151.93$$

$$P_{Lo3} = 130.89$$

$$P_{Lo4} = 147.33$$

$$Az(P_{Lo1}) = 182$$

$$Az(P_{Lo2}) = 178$$

$$Az(P_{Lo3}) = 195$$

$$Az(P_{Lo4}) = 181$$

$$\left[\begin{array}{cccc|c} 1 & 138.55 & 19196.10 & 2659620.00 & 182 \\ 1 & 151.93 & 23082.72 & 3506958.39 & 178 \\ 1 & 130.89 & 17132.19 & 2242432.62 & 195 \\ 1 & 147.33 & 21706.13 & 3197963.97 & 181 \end{array} \right]$$

$$\left[\begin{array}{cccc|c} 1 & 138.55 & 19196.10 & 2659620.00 & 182 \\ 0 & 1 & 290.48 & 63328.73 & -0.298954 \\ 1 & 130.89 & 17132.19 & 2242432.62 & 195 \\ 1 & 147.33 & 21706.13 & 3197963.97 & 181 \end{array} \right]$$

$$R_2 \rightarrow \frac{(R_2 - R_1)}{13.38}$$

$$\left[\begin{array}{cccc|c} 1 & 138.55 & 19196.10 & 2659620.00 & 182 \\ 0 & 1 & 290.48 & 63328.73 & -0.298954 \\ 0 & 0 & 1 & 421.37 & 0.066453 \\ 1 & 147.33 & 21706.13 & 3197963.97 & 181 \end{array} \right]$$

$$R_3 \rightarrow \frac{(R_3 - R_1 + 7.66R_2)}{161.1664}$$

$$\left[\begin{array}{cccc|c} 1 & 138.55 & 19196.10 & 2659620.00 & 182 \\ 0 & 1 & 290.48 & 63328.73 & -0.298954 \\ 0 & 0 & 1 & 421.37 & 0.066453 \\ 0 & 0 & 0 & 1 & -0.006489 \end{array} \right]$$

$$R_4 \rightarrow \frac{-(R_4 - R_1 - 8.78R_2 + 40.388R_3)}{663.979}$$

$$\left[\begin{array}{cccc|c} 1 & 138.55 & 19196.10 & 2659620.00 & 182 \\ 0 & 1 & 290.48 & 63328.73 & -0.298954 \\ 0 & 0 & 1 & 0 & 2.800723 \\ 0 & 0 & 0 & 1 & -0.006489 \end{array} \right]$$

$$R_3 \rightarrow R_3 - 421.37R_4$$

$$\left[\begin{array}{cccc|c} 1 & 138.55 & 19196.10 & 2659620.00 & 182 \\ 0 & 1 & 0 & 0 & -402.912829 \\ 0 & 0 & 1 & 0 & 2.800723 \\ 0 & 0 & 0 & 1 & -0.006489 \end{array} \right]$$

$$R_2 \rightarrow R_2 - 290.48R_3 - 63328.73R_4$$

$$\left[\begin{array}{cccc|c} 1 & 0 & 0 & 0 & 19500.882191 \\ 0 & 1 & 0 & 0 & -402.912829 \\ 0 & 0 & 1 & 0 & 2.800723 \\ 0 & 0 & 0 & 1 & -0.006489 \end{array} \right]$$

$$R_1 \rightarrow R_1 - 138.55R_2 - 19196.10R_3 - 2659620.00R_4$$

$$a_0 = 19500.882191$$

$$a_1 = -402.912829$$

$$a_2 = 2.800273$$

$$a_3 = -0.006489$$

Therefore,

$$Az(P_{Lo}) = 19500.882191 - 402.912829 \times P_{Lo} + 2.800273 \times P_{Lo}^2 - 0.006489 \times P_{Lo}^3 \quad (\text{C.11})$$

C.1.4. Optimum tilt

The function used to describe the optimum installation tilt was defined using a polynomial curve fit based on the four locations which were simulated in Homer. The variable C is included as a tilt angle reduction factor for installation at non optimum azimuth.

Using the generic equation

$$a_0 + a_1x + a_2x^2 + a_3x^3 = y_0 \quad (C.10)$$

Converting to augmented matrix form,

$$\left[\begin{array}{cccc|c} 1 & P_{LA1} & P_{LA1}^2 & P_{LA1}^3 & Ti(P_{LA1}) \\ 1 & P_{LA2} & P_{LA2}^2 & P_{LA2}^3 & Ti(P_{LA2}) \\ 1 & P_{LA3} & P_{LA3}^2 & P_{LA3}^3 & Ti(P_{LA3}) \\ 1 & P_{LA4} & P_{LA4}^2 & P_{LA4}^3 & Ti(P_{LA4}) \end{array} \right]$$

Let,

$$P_{LA1} = 34.93$$

$$P_{LA2} = 27.60$$

$$P_{LA3} = 12.42$$

$$P_{LA4} = 42.88$$

$$Ti(P_{LA1}) = 33$$

$$Ti(P_{LA2}) = 29$$

$$Ti(P_{LA3}) = 19$$

$$Ti(P_{LA4}) = 38$$

$$\left[\begin{array}{cccc|c} 1 & 34.93 & 1220.11 & 42618.26 & 33 \\ 1 & 27.60 & 761.76 & 21024.58 & 29 \\ 1 & 12.42 & 154.26 & 1915.86 & 19 \\ 1 & 42.88 & 1838.69 & 78843.22 & 38 \end{array} \right]$$

$$\left[\begin{array}{cccc|c} 1 & 34.93 & 1220.11 & 42618.26 & 33 \\ 0 & 1 & 62.53 & 2945.93 & 0.545703 \\ 1 & 12.42 & 154.26 & 1915.86 & 19 \\ 1 & 42.88 & 1838.69 & 78843.22 & 38 \end{array} \right]$$

$$R_2 \rightarrow \frac{-(R_2 - R_1)}{7.33}$$

$$\left[\begin{array}{cccc|c} 1 & 34.93 & 1220.11 & 42618.26 & 33 \\ 0 & 1 & 62.53 & 2945.93 & 0.545703 \\ 0 & 0 & 1 & 74.95 & -0.005023 \\ 1 & 42.88 & 1838.69 & 78843.22 & 38 \end{array} \right]$$

$$R_3 \rightarrow \frac{(R_3 - R_1 + 22.51R_2)}{341.70}$$

$$\left[\begin{array}{cccc|c} 1 & 34.93 & 1220.11 & 42618.26 & 33 \\ 0 & 1 & 62.53 & 2945.93 & 0.545703 \\ 0 & 0 & 1 & 74.95 & -0.005023 \\ 0 & 0 & 0 & 1 & 0.000344 \end{array} \right]$$

$$R_4 \rightarrow \frac{(R_4 - R_1 - 7.95R_2 - 121.476R_3)}{3700.16}$$

$$\left[\begin{array}{cccc|c} 1 & 34.93 & 1220.11 & 42618.26 & 33 \\ 0 & 1 & 62.53 & 2945.93 & 0.545703 \\ 0 & 0 & 1 & 0 & -0.030806 \\ 0 & 0 & 0 & 1 & 0.000344 \end{array} \right]$$

$$R_3 \rightarrow R_3 - 74.95R_4$$

$$\left[\begin{array}{cccc|c} 1 & 34.93 & 1220.11 & 42618.26 & 33 \\ 0 & 1 & 0 & 0 & 1.458601 \\ 0 & 0 & 1 & 0 & -0.030806 \\ 0 & 0 & 0 & 1 & 0.000344 \end{array} \right]$$

$$R_2 \rightarrow R_2 - 62.53R_3 - 2945.93R_4$$

$$\left[\begin{array}{cccc|c} 1 & 0 & 0 & 0 & 4.976936 \\ 0 & 1 & 0 & 0 & 1.458601 \\ 0 & 0 & 1 & 0 & -0.030806 \\ 0 & 0 & 0 & 1 & 0.000344 \end{array} \right]$$

$$R_1 \rightarrow R_1 - 34.93R_2 - 1220.10R_3 - 42618.24R_4$$

$$a_0 = 4.976936$$

$$a_1 = 1.458601$$

$$a_2 = -0.030806$$

$$a_3 = 0.000344$$

Therefore,

$$Ti(P_{LA}) = 4.976936 - 1.458601 \times P_{LA} - 0.030806 \times P_{LA}^2 + 0.000344 \times P_{LA}^3 \quad (\text{C.12a})$$

C.1.5. Optimum tilt correction factor (C)

Table C.2 – Non optimum tilt angle scaling relative to optimum tilt.

| Location | Azimuth Error (Degrees) | | | | |
|-------------------|---------------------------|----------|----------|----------|----------|
| | 0 | -90 | 90 | -45 | 45 |
| Brooklyn Park | 1 | 0.151515 | 0.151515 | 0.848485 | 0.848485 |
| Toowoomba | 1 | 0.137931 | 0.137931 | 0.827586 | 0.827586 |
| Darwin | 1 | 0.263158 | 0.105263 | 0.789474 | 0.789474 |
| Hobart | 1 | 0.131579 | 0.131579 | 0.868421 | 0.868421 |
| Magnitude Average | 1 | 0.151309 | | 0.833492 | |

The correction factor function is used to account for changes to the optimum tilt angle for a variety of azimuth values. A_{Er} is magnitude of the error in degrees between actual and optimum azimuth, while C is the decimal fraction of the tilt value relative to the optimum azimuth tilt value.

Using the generic equation

$$a_0 + a_1x + a_2x^2 + a_3x^3 = y_0 \quad (\text{C.10})$$

Converting to augmented matrix form,

$$\left[\begin{array}{ccc|c} 1 & Er_{90} & Er_{90}^2 & C(A_{Er90}) \\ 1 & Er_{45} & Er_{45}^2 & C(A_{Er45}) \\ 1 & Er_0 & Er_0^2 & C(A_{Er0}) \end{array} \right]$$

Let,

$$Er_0 = 0$$

$$Er_{45} = 45$$

$$Er_{90} = 90$$

$$C(A_{Er0}) = 1$$

$$C(A_{Er45}) = 0.833492$$

$$C(A_{Er90}) = 0.151309$$

$$\left[\begin{array}{ccc|c} 1 & 90 & 8100 & 0.151309 \\ 1 & 45 & 2025 & 0.833492 \\ 1 & 0 & 0 & 1 \end{array} \right]$$

$$\left[\begin{array}{ccc|c} 0 & 0 & 1 & -0.000127 \\ 1 & 45 & 2025 & 0.833492 \\ 1 & 0 & 0 & 1 \end{array} \right]$$

$$\left[\begin{array}{ccc|c} 0 & 0 & 1 & -0.000127 \\ 0 & 1 & 0 & 0.002030 \\ 1 & 0 & 0 & 1 \end{array} \right]$$

$$R_1 \rightarrow \frac{R_1 - 2R_2 + R_3}{4050}$$

$$R_2 \rightarrow \frac{R_2 - R_3 - 2025R_1}{45}$$

$$a_0 = 1$$

$$a_1 = 0.002030$$

$$a_2 = -0.000127$$

Therefore,

$$C(A_{Er}) = 1 + 0.002030 \times |A_{Er}| - 0.000127 \times |A_{Er}|^2$$

(C.13)

Therefore equation C.11 could be redefined, allowing for non-optimum azimuth installations.

$$Ti(P_{LA}) = (4.976936 - 1.458601 \times P_{LA} - 0.030806 \times P_{LA}^2 + 0.000344 \times P_{LA}^3) \times C(A_{Er}) \quad (\text{C.12b})$$

Appendix D. Matlab code

D.1. Function: Solar_Panel_Model_Par

```

function                                [V,I,P]                                =
Solar_panel_model_Par(V_Step,G,T,Vmps,Vocs,Imps,Iscs, Shaded_dec)
%Function file   IV_PV_CURVE_MODEL.m
%Name           Christopher Kirby
%Student No     0050093295
%Subject        ENG4111
%Assignment     Engineering research project: Part 1
%Last Revised   11/06/2015 22:00
%
%Inputs
%   G           Solar irradiation W/m^2
%   T           Temperature Deg C
%   Vmps        Specified MPPT voltage
%   Vocs        Specified open circuit voltage
%   Imps        Specified MPPT current
%   Iscs        Specified short circuit current
%
%Outputs
%   V           Vector: Terminal voltage
%   I           Vector: Output current A
%   P           Vector: Output power W
%
%Constant
%   Gs          STC Solar irradiation W/m^2
%   Ts          STC Temperature Deg C
%   TCp_Voc     Voc Thermal coefficient percent
%   TCp_Isc     Isc Thermal coefficient percent
%
%Variable
%   Temp_Voc    Voc Thermal coefficient mV/DegC
%   Temp_Isc    Isc Thermal coefficient mA/DegC
%   Vmp         MPPT Voltage at tempeature
%   Voc         Open circuit Voltage at tempeature
%   Imp         MPPT current at temperature and irradiance
%   Isc         Short circuit current at temperature and irradiance
%   C1          Panel IV coefficient
%   C2          Panel IV coefficient

%Assign values to constant
Gs = 1000;
Ts = 25;
TCp_Voc = -0.32;
TCp_Isc = 0.055;

Vocs = (1 - Shaded_dec ) * Vocs;
Vmps = (1 - Shaded_dec ) * Vmps;

% Determine Voltage and Current coefficients
Temp_Voc = Vocs * TCp_Voc / 100;
Temp_Isc = Iscs * TCp_Isc / 100;

% Determine panel voltage and temperature characteristics
Isc = Iscs * G / Gs * (1 + Temp_Isc * (T - Ts));
Imp = Imps * G / Gs * (1 + Temp_Isc * (T - Ts));
Voc = Vocs + Temp_Voc * (T - Ts);
Vmp = Vmps + Temp_Voc * (T - Ts);

```

```

%Determine coefficient C2 & C1
C2 = (Vmp / Voc - 1) / (reallog(1 - Imp/Isc));
%Determine coefficient C1
C1 = (1 - Imp / Isc) * exp((-Vmp) / (C2 * Voc));

Vocm = C2 * Vocs * reallog(1+(G/Gs)/C1);
deltaV = Vocs-Vocm;

%Modify Voc & Vmp to allow for irradiance
Voc = Vocs + Temp_Voc * (T - Ts) - deltaV;
Vmp = Vmps + Temp_Voc * (T - Ts) - deltaV;

%Determine voltage vector
V = 0:V_Step:Voc;

%Calculate current and power as a function of voltage
I = Isc * (1-C1*(exp(V ./ (C2*Voc))-1));
P = I .* V;

```

D.2. Function: Solar_Panel_Model_Ser

```

function [V,I,P]
Solar_panel_model_Ser(I_Step,G,T,Vmps,Vocs,Imps,IsCs, Shaded_dec) =
%Function file IV_PV_CURVE_MODEL.m
%Name Christopher Kirby
%Student No 0050093295
%Subject ENG4111
%Assignment Engineering research project: Part 1
%Last Revised 11/06/2015 22:00
%
%Inputs
% G Solar irradiation W/m^2
% T Temperature Deg C
% Vmps Specified MPPT voltage
% Vocs Specified open circuit voltage
% Imps Specified MPPT current
% IsCs Specified short circuit current
%
%Outputs
% V Vector: Terminal voltage
% I Vector: Output current A
% P Vector: Output power W
%
%Constant
% Gs STC Solar irradiation W/m^2
% Ts STC Temperature Deg C
% TCp_Voc Voc Thermal coefficient percent
% TCp_IsC IsC Thermal coefficient percent
%
%Variable
% Temp_Voc Voc Thermal coefficient mV/DegC
% Temp_IsC IsC Thermal coefficient mA/DegC
% Vmp MPPT Voltage at temperature
% Voc Open circuit Voltage at temperature
% Imp MPPT current at temperature and irradiance
% IsC Short circuit current at temperature and irradiance
% C1 Panel IV coefficient

```

```

% C2          Panel IV coefficient

%Assign values to constant
Gs = 1000;
Ts = 25;
TCp_Voc = -0.32;
TCp_Isc = 0.055;

Vocs = (1 - Shaded_dec ) * Voc;
Vmpps = (1 - Shaded_dec ) * Vmpps;

% Determine Voltage and Current coefficients
Temp_Voc = Voc * TCp_Voc / 100;
Temp_Isc = Isc * TCp_Isc / 100;

% Determine panel voltage and temperature characteristics
Isc = Iscs * G / Gs * (1 + Temp_Isc * (T - Ts));
Imp = Impps * G / Gs * (1 + Temp_Isc * (T - Ts));
Voc = Vocs + Temp_Voc * (T - Ts);
Vmp = Vmpps + Temp_Voc * (T - Ts);

%Round Isc & Imp to 2 decimal places
Isc = round(Isc*100)/100;

%Determine coefficient C2 & C1
C2 = (Vmp / Voc - 1 ) / ( reallog(1 - Imp/Isc));
%Determine coefficient C1
C1 = ( 1- Imp / Isc ) * exp((-Vmp ) / (C2 * Voc));

Vocm = C2 * Vocs * reallog(1+(G/Gs)/C1);
deltaV = Vocs-Vocm;

%Modify Voc & Vmp to allow for irradiance
Voc = Vocs + Temp_Voc * (T - Ts) - deltaV;
Vmp = Vmpps + Temp_Voc * (T - Ts) - deltaV;

%Determine current vector - Extending 20% past STC Isc
%I = I_Step:I_Step:Isc;
I = 0:I_Step:Isc;
%Calculate Voltage and power as a function of Current
V = C2 * Voc * reallog(1+(1-I/Isc)/C1);

%I = [0, I]
%V = [0, V]

P = I .* V;

```

D.3. Script: Efficiency_calculator_Par

```

%Script file  Efficiency_calculator_Par.m
%Name        Christopher Kirby
%Student No   0050093295
%Subject      ENG4111
%Assignment   Engineering research project
%Last Revised 11/06/2015 22:00
%
%
%
%%%%%%%%%%%%%%%%%%%%%%%%%%%%%%%%%%%%%%%%%%%%%%%%%%%%%%%%%%%%%%%%%%%%%%%%
%clear all variables
%%%%%%%%%%%%%%%%%%%%%%%%%%%%%%%%%%%%%%%%%%%%%%%%%%%%%%%%%%%%%%%%%%%%%%%%
clear all

%%%%%%%%%%%%%%%%%%%%%%%%%%%%%%%%%%%%%%%%%%%%%%%%%%%%%%%%%%%%%%%%%%%%%%%%
%define and calculate fixed variables
%%%%%%%%%%%%%%%%%%%%%%%%%%%%%%%%%%%%%%%%%%%%%%%%%%%%%%%%%%%%%%%%%%%%%%%%
P1_Angle = input('Enter Panel 1 angle: ')           %Panel
angles to light source
P2_Angle = 0;

P1_Modules = 3;                                     %Number
of modules within panel
P2_Modules = 3;

P1_Shaded_Modules = input('Enter Panel 1 number of shaded modules: ')
%Number of hard shaded panels
P2_Shaded_Modules = input('Enter Panel 2 number of shaded modules: ')

P1_Shaded_dec = ( P1_Shaded_Modules / P1_Modules );
%Calculate percent of shaded modules as a decimal value
P2_Shaded_dec = ( P2_Shaded_Modules / P2_Modules );

G = input('Enter simulated irradiance value: ')
%Simulation irradiance
T = input('Enter simulated temperature: ')
%Simulation temperature

Vmgs1 = input('Enter panel 1 MP Voltage: ');        %Panel
1 specifications
Vocs1 = input('Enter panel 1 OC Voltage: ');
Imgs1 = input('Enter panel 1 MP Current: ');
Iocs1 = input('Enter panel 1 SC Current: ');
Vmgs2 = input('Enter panel 2 MP Voltage: ');        %Panel
2 specifications
Vocs2 = input('Enter panel 2 OC Voltage: ');
Imgs2 = input('Enter panel 2 MP Current: ');
Iocs2 = input('Enter panel 2 SC Current: ');

K = P1_Angle;                                       %Plot
index constant

Brewster_angle = 56.6;                             %Limiting

```

```

angle - Brewster angle
P2_Angle_Vector = []; %Rotated
panel vector
V_Step = 0.1; %Voltage
vector step

MP_Sep_Vector = []; %Non
connected panel MP vector
MP_Par_Vector = []; %Series
connected panel MP vector

%%%%%%%%%%%%%%%%%%%%%%%%%%%%%%%%%%%%%%%%%%%%%%%%%%%%%%%%%%%%%%%%%%%%%%%%
%%%%
%Model panel output
%%%%%%%%%%%%%%%%%%%%%%%%%%%%%%%%%%%%%%%%%%%%%%%%%%%%%%%%%%%%%%%%%%%%%%%%
%%%%
while P2_Angle <= Brewster_angle; %Program
loop for angles below limit
G1 = G * cos( P1_Angle *pi / 180 );
%Equivalent irradiance due to angle
G2 = G * cos( P2_Angle *pi / 180 );

%Model Panel 1: Solar panel model_Par
[V1,I1,P1] =
Solar_panel_model_Par(V_Step,G1,T,Vmps1,Vocs1,Imps1,Isocs1,P1_Shaded_de
c);
V1 = round(V1*100)/100;
I1 = round(I1*100)/100;
P1 = round(P1*100)/100;
I1(I1<0)=0;
P1(P1<0)=0;

%Locate actual MPPT using incremental

%method starting from panel spec MPPT
P1_Pmp = 0;
if max(V1) > Vmps1;
index = find( V1( : ) == Vmps1 );
else
index = length(V1) - 1;
end
while P1_Pmp == 0;

if (P1(index-1)<=P1(index) & P1(index)>=P1(index+1));
P1_Pmp = P1(index);
elseif (P1(index-1)>=P1(index) & P1(index)>=P1(index+1) );
index = index - 1;
elseif (P1(index-1)<=P1(index) & P1(index)<=P1(index+1));
index = index + 1;
elseif (P1(index-1)>=P1(index) & P1(index)<=P1(index+1));
index = index + 1;
else
P1(index) = 0;
index = index - 1;
end
end

%Model Panel 2: Solar panel model_Ser
[V2,I2,P2] =
Solar_panel_model_Par(V_Step,G2,T,Vmps2,Vocs2,Imps2,Isocs2,P2_Shaded_de

```

```

c);
V2 = round(V2*100)/100;
I2 = round(I2*100)/100;
P2 = round(P2*100)/100;
I2(I2<0)=0;
P2(P2<0)=0;

%Locate actual MPPT using incremental

%method starting from panel spec MPPT
P2_Pmp = 0;
if max(V2) > Vmps2;
    index = find( V2( : ) == Vmps2 );
else
    index = length(V2) - 1;
end
while P2_Pmp == 0;
    if (P2(index-1)<=P2(index) & P2(index)>=P2(index+1));
        P2_Pmp = P2(index);
    elseif (P2(index-1)>=P2(index) & P2(index)>=P2(index+1));
        index = index - 1;
    elseif (P2(index-1)<=P2(index) & P2(index)<=P2(index+1));
        index = index + 1;
    elseif (P2(index-1)>=P2(index) & P2(index)<=P2(index+1));
        index = index + 1;
    else
        P2(index) = 0;
        index = index - 1;
    end
end

difference = abs(length (V1) - length (V2));
%Standardise vector lengths
zero_vector = zeros(1,difference);
if length (V1) < length (V2);
V1 = V2;
I1 = [I1,zero_vector];
P1 = [P1,zero_vector];
end
if length (V1) > length (V2);
V2 = V1;
I2 = [I2,zero_vector];
P2 = [P2,zero_vector];
end

%%%%%%%%%%%%%%%%%%%%%%%%%%%%%%%%%%%%%%%%%%%%%%%%%%%%%%%%%%%%%%%%%%%%%%%%
%MODEL PARALLEL COMBINATION
%%%%%%%%%%%%%%%%%%%%%%%%%%%%%%%%%%%%%%%%%%%%%%%%%%%%%%%%%%%%%%%%%%%%%%%%

Vparallel = V1;
Iparallel = I1 + I2;
Pparallel = Vparallel .* Iparallel;
Vparallel = round(Vparallel*100)/100;
Iparallel = round(Iparallel*100)/100;
Pparallel = round(Pparallel*100)/100;

Parallel_Pmp = 0;
while Parallel_Pmp == 0;
    if (Pparallel(index-1)<=Pparallel(index)
&

```

```

Pparallel(index)>=Pparallel(index+1));
    Parallel_Pmp = Pparallel(index);
    elseif (Pparallel(index-1)>=Pparallel(index) &
Pparallel(index)>=Pparallel(index+1));
        index = index - 1;
    elseif (Pparallel(index-1)<=Pparallel(index) &
Pparallel(index)<=Pparallel(index+1));
        index = index + 1;
    elseif (Pparallel(index-1)>=Pparallel(index) &
Pparallel(index)<=Pparallel(index+1));
        index = index + 1;
    else
        Pparallel(index) = 0;
        index = index - 1;
    end
end

%%%%%%%%%%%%%%%%%%%%%%%%%%%%%%%%%%%%%%%%%%%%%%%%%%%%%%%%%%%%%%%%%%%%%%%%%%%%%%
%%%%%%%%%%%%%%%%%%%%%%%%%%%%%%%%%%%%%%%%%%%%%%%%%%%%%%%%%%%%%%%%%%%%%%%%%%%%%%
%PLOT RESULTING IV / PV curves for P1, P2 & Parallel COMBINATION
%%%%%%%%%%%%%%%%%%%%%%%%%%%%%%%%%%%%%%%%%%%%%%%%%%%%%%%%%%%%%%%%%%%%%%%%%%%%%%
%%%%%%%%%%%%%%%%%%%%%%%%%%%%%%%%%%%%%%%%%%%%%%%%%%%%%%%%%%%%%%%%%%%%%%%%%%%%%%
subplot(2,11,1:4);
plt = plotyy (V1,I1,V1,P1);
title('Panel 1: IV & PV');
xlabel('Voltage (V)');
ylabel(plt(1), 'Current (A)');
ylabel(plt(2), 'Power (W)');

subplot(2,11,8:11);
plt = plotyy (V2,I2,V2,P2);
title('Panel 2: IV & PV');
xlabel('Voltage (V)');
ylabel(plt(1), 'Current (A)');
ylabel(plt(2), 'Power (W)');

subplot(2,11,12:22);
plt = plotyy (Vparallel,Iparallel,Vparallel,Pparallel);
title('Parallel: IV & PV');
xlabel('Voltage (V)');
ylabel(plt(1), 'Current (A)');
ylabel(plt(2), 'Power (W)');

%%%%%%%%%%%%%%%%%%%%%%%%%%%%%%%%%%%%%%%%%%%%%%%%%%%%%%%%%%%%%%%%%%%%%%%%%%%%%%
%%%%%%%%%%%%%%%%%%%%%%%%%%%%%%%%%%%%%%%%%%%%%%%%%%%%%%%%%%%%%%%%%%%%%%%%%%%%%%
%SAVE PLOT IMAGE at 10 degree INCREMENTS
%%%%%%%%%%%%%%%%%%%%%%%%%%%%%%%%%%%%%%%%%%%%%%%%%%%%%%%%%%%%%%%%%%%%%%%%%%%%%%
%%%%%%%%%%%%%%%%%%%%%%%%%%%%%%%%%%%%%%%%%%%%%%%%%%%%%%%%%%%%%%%%%%%%%%%%%%%%%%
if P2_Angle == 0;
K=K+1;
print('-djpeg',sprintf('IV_PAR%d',K));
end;

if P2_Angle == 10;
K=K+1;
print('-djpeg',sprintf('IV_PAR%d',K));
end;

if P2_Angle == 20;
K=K+1;
print('-djpeg',sprintf('IV_PAR%d',K));

```

```

end;

if P2_Angle == 30;
K=K+1;
print('-djpeg',sprintf('IV_PAR%d',K));
end;

if P2_Angle == 40;
K=K+1;
print('-djpeg',sprintf('IV_PAR%d',K));
end;

if P2_Angle == 50;
K=K+1;
print('-djpeg',sprintf('IV_PAR%d',K));
end;

if P2_Angle == 56;
K=K+1;
print('-djpeg',sprintf('IV_PAR%d',K));
end;

%%%%%%%%%%%%%%%%%%%%%%%%%%%%%%%%%%%%%%%%%%%%%%%%%%%%%%%%%%%%%%%%%%%%%%%%
%%%%%%%%
%CALCULATE MAX POWER AND EFFICIENCY VECTORS
%%%%%%%%%%%%%%%%%%%%%%%%%%%%%%%%%%%%%%%%%%%%%%%%%%%%%%%%%%%%%%%%%%%%%%%%
%%%%%%%%
MP_Seperate = P1_Pmp + P2_Pmp; %Non
connected panel MP
MP_Parallel = Parallel_Pmp; %Parallel
connected panel MP
%

%Efficiency vector
Percent_Eff_to_Seperate(P2_Angle+1) = Parallel_Pmp / (P1_Pmp + P2_Pmp)
* 100;
%

P2_Angle_Vector = [P2_Angle_Vector,P2_Angle]; %Panel
angle vector
P2_Angle = P2_Angle + 1; %Increment
panel 2 angle

MP_Sep_Vector = [MP_Sep_Vector , MP_Seperate]; %Non
connected panel MP vector
MP_Par_Vector = [MP_Par_Vector , MP_Parallel];
%Series connected panel MP vector
%
end

%%%%%%%%%%%%%%%%%%%%%%%%%%%%%%%%%%%%%%%%%%%%%%%%%%%%%%%%%%%%%%%%%%%%%%%%
%%%%%%%%
%PLOT MAX POWER Versus ANGLE
%%%%%%%%%%%%%%%%%%%%%%%%%%%%%%%%%%%%%%%%%%%%%%%%%%%%%%%%%%%%%%%%%%%%%%%%
%%%%%%%%
%
clf %Clear
plot Window
plt = plotyy ( P2_Angle_Vector, [MP_Sep_Vector.'
MP_Par_Vector.'],P2_Angle_Vector,MP_Sep_Vector- MP_Par_Vector);

```

```

title(sprintf('Panel output power vs Angle ( Panel 1 Angle %d degrees
)', P1_Angle));
%title(sprintf('Panel output power vs Angle ( Ambient temperature %d
degrees C )', T));
%title(sprintf('Panel output power vs Angle ( Irradiance %d W/m^2 )',
G));
%title(sprintf('Panel output power vs Angle'));

xlabel('Panel 2 Angle from solar normal');
ylabel(plt(1), 'Panel output power (W)');
ylabel(plt(2), 'Parallel connected power loss (W)');

K=K+1;
print('-djpeg', sprintf('IV_PAR%d',K));
%Save Angle versus MP plot

```

D.4. Script: Efficiency_calculator_Ser

```

%Script file  Efficiency_calculator_Ser.m
%Name        Christopher Kirby
%Student No   0050093295
%Subject      ENG4111
%Assignment   Engineering research project
%Last Revised 11/06/2015 22:00
%
%
%
%%%%%%%%%%%%%%%%%%%%%%%%%%%%%%%%%%%%%%%%%%%%%%%%%%%%%%%%%%%%%%%%%%%%%%%%
%
%clear all variables
%%%%%%%%%%%%%%%%%%%%%%%%%%%%%%%%%%%%%%%%%%%%%%%%%%%%%%%%%%%%%%%%%%%%%%%%
%
clear all

%%%%%%%%%%%%%%%%%%%%%%%%%%%%%%%%%%%%%%%%%%%%%%%%%%%%%%%%%%%%%%%%%%%%%%%%
%
%define and calculate fixed variables
%%%%%%%%%%%%%%%%%%%%%%%%%%%%%%%%%%%%%%%%%%%%%%%%%%%%%%%%%%%%%%%%%%%%%%%%
%
P1_Angle = input('Enter Panel 1 angle: ')           %Panel
angles to light source
P2_Angle = 0;

P1_Modules = 3;                                     %Number
of modules within panel
P2_Modules = 3;

P1_Shaded_Modules = input('Enter Panel 1 number of shaded modules: ')
%Number of hard shaded panels
P2_Shaded_Modules = input('Enter Panel 2 number of shaded modules: ')

P1_Shaded_dec    = ( P1_Shaded_Modules / P1_Modules );
%Calculate percent of shaded modules as a decimal value
P2_Shaded_dec    = ( P2_Shaded_Modules / P2_Modules );

```

```

G      =      input('Enter      simulated      irradiance      value:      ')
%Simulation irradiance
T      =      input('Enter      simulated      temperature:      ')
%Simulation temperature

Vmgs1 = input('Enter panel 1 MP Voltage: ');           %Panel
1 specifications
Vocs1 = input('Enter panel 1 OC Voltage: ');
Imgs1 = input('Enter panel 1 MP Current: ');
Iscs1 = input('Enter panel 1 SC Current: ');
Vmgs2 = input('Enter panel 2 MP Voltage: ');           %Panel
2 specifications
Vocs2 = input('Enter panel 2 OC Voltage: ');
Imgs2 = input('Enter panel 2 MP Current: ');
Iscs2 = input('Enter panel 2 SC Current: ');

K = P1_Angle;                                         %Plot
index constant

Brewster_angle = 56.6;                               %Limiting
angle - Brewster angle
P2_Angle_Vector = [];                                %Rotated
panel vector
I_Step = 0.01;                                       %Current
vector step

MP_Sep_Vector = [];                                  %Non
connected panel MP vector
MP_Ser_Vector = [];                                  %Series
connected panel MP vector

%%%%%%%%%%%%%%%%%%%%%%%%%%%%%%%%%%%%%%%%%%%%%%%%%%%%%%%%%%%%%%%%%%%%%%%%
%%%%%%%%%%%%%%%%%%%%%%%%%%%%%%%%%%%%%%%%%%%%%%%%%%%%%%%%%%%%%%%%%%%%%%%%
%Model panel output
%%%%%%%%%%%%%%%%%%%%%%%%%%%%%%%%%%%%%%%%%%%%%%%%%%%%%%%%%%%%%%%%%%%%%%%%
%%%%%%%%%%%%%%%%%%%%%%%%%%%%%%%%%%%%%%%%%%%%%%%%%%%%%%%%%%%%%%%%%%%%%%%%
while P2_Angle <= Brewster_angle;                    %Program
loop for angles below limit
G1      =      G      *      cos(      P1_Angle      *pi      /      180      );
%Equivalent irradiance due to angle
G2 = G * cos( P2_Angle *pi / 180 );

%Model Panel 1: Solar panel model_Ser
[V1,I1,P1] =
Solar_panel_model_Ser(I_Step,G1,T,Vmgs1,Vocs1,Imgs1,Iscs1,P1_Shaded_de
c);
    V1 = round(V1*100)/100;
    I1 = round(I1*100)/100;
    P1 = round(P1*100)/100;
    I1(I1<0)=0;
    P1(P1<0)=0;

%Locate actual MPPT using incremental

%method starting from panel spec MPPT
P1_Pmp = 0;
    if max(I1) > Imgs1;
        index = find( I1( : ) == Imgs1 );
    else
        index = length(I1) - 1;
    end

```

```

while P1_Pmp == 0;

    if (P1(index-1)<=P1(index) & P1(index)>=P1(index+1));
        P1_Pmp = P1(index);
    elseif (P1(index-1)>=P1(index) & P1(index)>=P1(index+1) );
        index = index - 1;
    elseif (P1(index-1)<=P1(index) & P1(index)<=P1(index+1));
        index = index + 1;
    else
        P1(index) = 0;
        index = index - 1;
    end
end

%Model Panel 2: Solar panel model_Ser
[V2,I2,P2] =
Solar_panel_model_Ser(I_Step,G2,T,Vmps2,Vocs2,Imps2,Iscs2,P2_Shaded_de
c);
V2 = round(V2*100)/100;
I2 = round(I2*100)/100;
P2 = round(P2*100)/100;
I2(I2<0)=0;
P2(P2<0)=0;

%Locate actual MPPT using incremental

%method starting from panel spec MPPT
P2_Pmp = 0;
if max(I2) > Imps2;
    index = find( I2( : ) == Imps2 );
else
    index = length(I2) - 1;
end
while P2_Pmp == 0;
    if (P2(index-1)<=P2(index) & P2(index)>=P2(index+1));
        P2_Pmp = P2(index);
    elseif (P2(index-1)>=P2(index) & P2(index)>=P2(index+1));
        index = index - 1;
    elseif (P2(index-1)<=P2(index) & P2(index)<=P2(index+1));
        index = index + 1;
    else
        P2(index) = 0;
        index = index - 1;
    end
end

difference = abs(length (I1) - length (I2));
%Standardise vector lengths
zero_vector = zeros(1,difference);
if length (I1) < length (I2);
    I1 = I2;
    V1 = [V1,zero_vector];
    P1 = [P1,zero_vector];
end
if length (I1) > length (I2);
    I2 = I1;
    V2 = [V2,zero_vector];
    P2 = [P2,zero_vector];
end

```



```

%%%%%
if P2_Angle == 0;
K=K+1;
print('-djpeg',sprintf('IV_SER%d',K));
end;

if P2_Angle == 10;
K=K+1;
print('-djpeg',sprintf('IV_SER%d',K));
end;

if P2_Angle == 20;
K=K+1;
print('-djpeg',sprintf('IV_SER%d',K));
end;

if P2_Angle == 30;
K=K+1;
print('-djpeg',sprintf('IV_SER%d',K));
end;

if P2_Angle == 40;
K=K+1;
print('-djpeg',sprintf('IV_SER%d',K));
end;

if P2_Angle == 50;
K=K+1;
print('-djpeg',sprintf('IV_SER%d',K));
end;

if P2_Angle == 56;
K=K+1;
print('-djpeg',sprintf('IV_SER%d',K));
end;

%%%%%%%%%%%%%%%%%%%%%%%%%%%%%%%%%%%%%%%%%%%%%%%%%%%%%%%%%%%%%%%%%%%%%%%%
%%%%%
%CALCULATE MAX POWER AND EFFICIENCY VECTORS
%%%%%%%%%%%%%%%%%%%%%%%%%%%%%%%%%%%%%%%%%%%%%%%%%%%%%%%%%%%%%%%%%%%%%%%%
%%%%%
MP_Seperate = P1_Pmp + P2_Pmp; %Non
connected panel MP
MP_Series = Series_Pmp; %Series
connected panel MP

%Efficiency vector
Percent_Eff_to_Seperate(P2_Angle+1) = Series_Pmp / (P1_Pmp + P2_Pmp) *
100;

P2_Angle_Vector = [P2_Angle_Vector,P2_Angle]; %Panel
angle vector
P2_Angle = P2_Angle + 1; %Increment
panel 2 angle

MP_Sep_Vector = [MP_Sep_Vector , MP_Seperate]; %Non
connected panel MP vector
MP_Ser_Vector = [MP_Ser_Vector , MP_Series];

```



```

%%%%%%%%%%%%%%%%%%%%%%%%%%%%%%%%%%%%%%%%%%%%%%%%%%%%%%%%%%%%%%%%%%%%%%%%
%
[V,I,P,C1,C2] = Solar_panel_model(G,T,Vmps,Vocs,Imps,Iscs)

%Set Irradiance vector
G = 0:1000;

%Calculate value for modified open circuit voltage
Vocm = C2 * Vocs * reallog(1+(1-G/Gs)/C1)
%Calculate open circuit voltage change
deltaV = Vocs-Vocm

%%%%%%%%%%%%%%%%%%%%%%%%%%%%%%%%%%%%%%%%%%%%%%%%%%%%%%%%%%%%%%%%%%%%%%%%
%
%PLOT CALCULATED IV CURVE VALUES
%%%%%%%%%%%%%%%%%%%%%%%%%%%%%%%%%%%%%%%%%%%%%%%%%%%%%%%%%%%%%%%%%%%%%%%%
%
plot (G , Vocm , 'r')
xlabel('Irradiance (W/m²)')
ylabel('Open circuit voltage (V)')
set(gca, 'XTick', [0:100:1000])
set(gca, 'YTick', [0:5:60])

```

D.6. Script: Varied_Irradiance_Plot

```

%Script file Varied_Irradiance_Plot.m
%Name Christopher Kirby
%Student No 0050093295
%Subject ENG4111
%Assignment Engineering research project: Part 1
%Last Revised 14/06/2015 10:30
%
%Define panel specifications and standard test conditions
T = 25
Vmps = 35.4
Vocs = 44.6
Imps = 4.95
Iscs = 5.30

%%%%%%%%%%%%%%%%%%%%%%%%%%%%%%%%%%%%%%%%%%%%%%%%%%%%%%%%%%%%%%%%%%%%%%%%
%
%MODEL IV CURVE
%%%%%%%%%%%%%%%%%%%%%%%%%%%%%%%%%%%%%%%%%%%%%%%%%%%%%%%%%%%%%%%%%%%%%%%%
%
[V1000,I1000,P1000] = Solar_panel_model_Par(0.1,1000,T,Vmps,Vocs,Imps,Iscs,0)
I1000(I1000<0)=0

[V800,I800,P800] = Solar_panel_model_Par(0.1,800,T,Vmps,Vocs,Imps,Iscs,0)
I800(I800<0)=0

[V600,I600,P600] = Solar_panel_model_Par(0.1,600,T,Vmps,Vocs,Imps,Iscs,0)
I600(I600<0)=0

```

```
[V500,I500,P500] =
Solar_panel_model_Par(0.1,500,T,Vmps,Vocs,Imps,Isocs,0)
I500(I500<0)=0

[V400,I400,P400] =
Solar_panel_model_Par(0.1,400,T,Vmps,Vocs,Imps,Isocs,0)
I400(I400<0)=0

[V200,I200,P200] =
Solar_panel_model_Par(0.1,200,T,Vmps,Vocs,Imps,Isocs,0)
I200(I200<0)=0

[V100,I100,P100] =
Solar_panel_model_Par(0.1,100,T,Vmps,Vocs,Imps,Isocs,0)
I100(I100<0)=0
```

```
%%%%%%%%%%%%%%%%%%%%%%%%%%%%%%%%%%%%%%%%%%%%%%%%%%%%%%%%%%%%%%%%%%%%%%%%
%PLOT CALCULATED IV CURVE VALUES AT VARIOUS TEMPERATURE
%%%%%%%%%%%%%%%%%%%%%%%%%%%%%%%%%%%%%%%%%%%%%%%%%%%%%%%%%%%%%%%%%%%%%%%%
%PLOT
plot(V1000 , I1000 , 'r',V800 , I800 , 'g',V600 , I600 , 'b',V500 , I500
 , 'm',V400 , I400 , 'r--',V200 , I200 , 'g--',V100 , I100 , 'b--')
legend('1000W / m²', '800W / m²', '600W / m²', '500W / m²', '400W / m²', '200W
 / m²', '100W / m²')
xlabel('Voltage (V)')
ylabel('Current (A)')
set(gca, 'XTick', [0:5:60])
set(gca, 'YTick', [0:0.5:100])
```

D.7. Script: Varied_Temperature_Plot

```
%Script file Varied_Temperature_Plot.m
%Name Christopher Kirby
%Student No 0050093295
%Subject ENG4111
%Assignment Engineering research project: Part 1
%Last Revised 14/06/2015 10:35
%
%Define panel specifications and standard test conditions
G = 1000
Vmps = 35.4
Vocs = 44.6
Imps = 4.95
Isocs = 5.30

%%%%%%%%%%%%%%%%%%%%%%%%%%%%%%%%%%%%%%%%%%%%%%%%%%%%%%%%%%%%%%%%%%%%%%%%
%MODEL IV CURVE
%%%%%%%%%%%%%%%%%%%%%%%%%%%%%%%%%%%%%%%%%%%%%%%%%%%%%%%%%%%%%%%%%%%%%%%%
[Vn10,In10,Pn10] = Solar_panel_model_Par(0.1,G,-
10,Vmps,Vocs,Imps,Isocs,0)
In10(In10<0)=0
```

```

[V0,I0,P0] = Solar_panel_model_Par(0.1,G,0,Vmps,Vocs,Imps,Iscs,0)
I0(I0<0)=0

[V10,I10,P10] = Solar_panel_model_Par(0.1,G,10,Vmps,Vocs,Imps,Iscs,0)
I10(I10<0)=0

[V20,I20,P20] = Solar_panel_model_Par(0.1,G,20,Vmps,Vocs,Imps,Iscs,0)
I20(I20<0)=0

[V25,I25,P25] = Solar_panel_model_Par(0.1,G,25,Vmps,Vocs,Imps,Iscs,0)
I25(I25<0)=0

[V45,I45,P45] = Solar_panel_model_Par(0.1,G,45,Vmps,Vocs,Imps,Iscs,0)
I45(I45<0)=0

[V65,I65,P65] = Solar_panel_model_Par(0.1,G,65,Vmps,Vocs,Imps,Iscs,0)
I65(I65<0)=0

%%%%%%%%%%%%%%%%%%%%%%%%%%%%%%%%%%%%%%%%%%%%%%%%%%%%%%%%%%%%%%%%%%%%%%%%%%%%%%
%%%%%%%%%%%%%%%%%%%%%%%%%%%%%%%%%%%%%%%%%%%%%%%%%%%%%%%%%%%%%%%%%%%%%%%%%%%%%%
%PLOT CALCULATED IV CURVE VALUES AT VARIOUS TEMPERATURE
%%%%%%%%%%%%%%%%%%%%%%%%%%%%%%%%%%%%%%%%%%%%%%%%%%%%%%%%%%%%%%%%%%%%%%%%%%%%%%
%%%%%%%%%%%%%%%%%%%%%%%%%%%%%%%%%%%%%%%%%%%%%%%%%%%%%%%%%%%%%%%%%%%%%%%%%%%%%%
plot (Vn10 , In10 , 'r',V0 , I0 , 'g',V10 , I10 , 'b',V20 , I20 , 'm',V25 ,
I25 , 'r--',V45 , I45 , 'g--',V65 , I65 , 'b--')
legend('-10°C', '0°C', '10°C', '20°C', '25°C', '45°C', '65°C')
xlabel('Voltage (V)')
ylabel('Current (A)')
set(gca, 'XTick', [0:5:600])
set(gca, 'YTick', [0:0.5:100])

```

Appendix E. Modelling results

E.1. Optimum installation plots

E.1.1. Brooklyn Park.

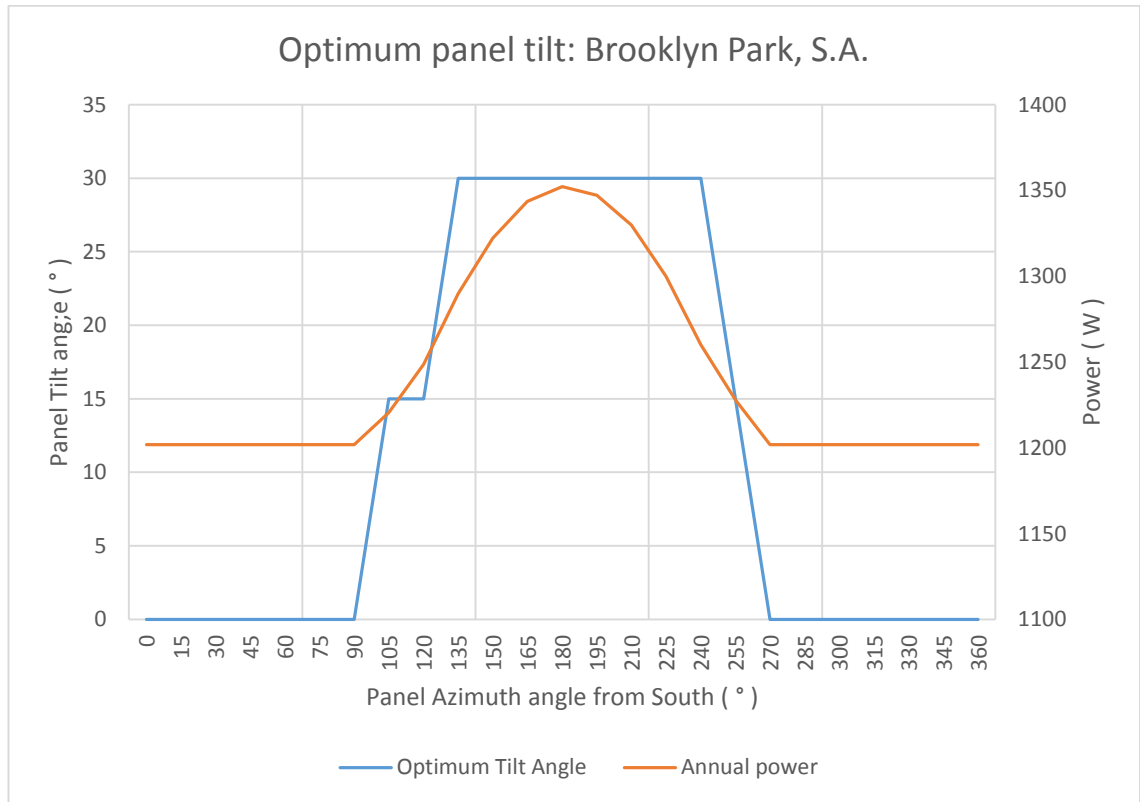


Figure E.1 – Brooklyn Park optimum tilt angle & generated power: 15° resolution

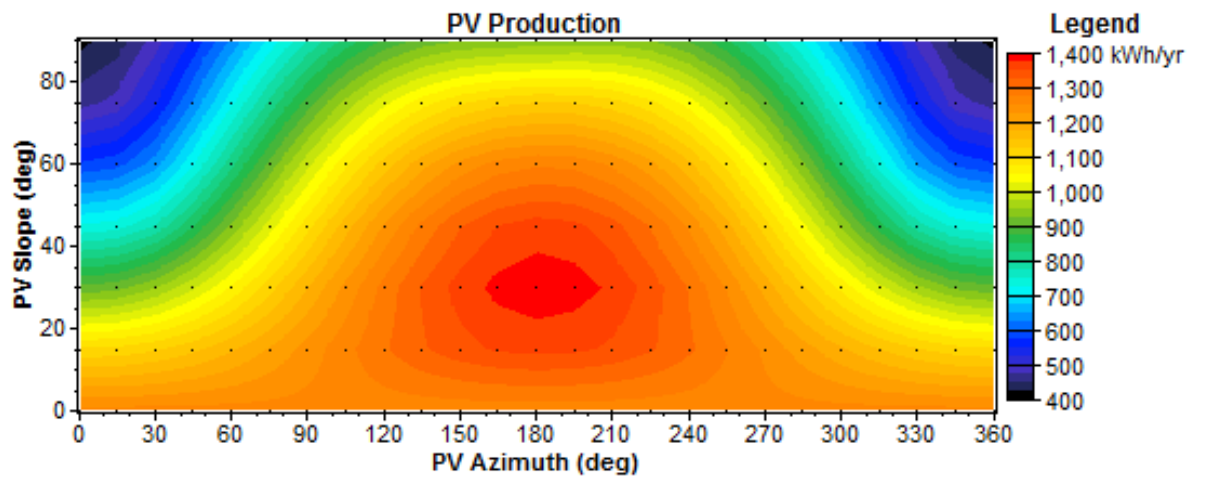


Figure E.2 – Brooklyn Park generated power surface plot: 15° resolution

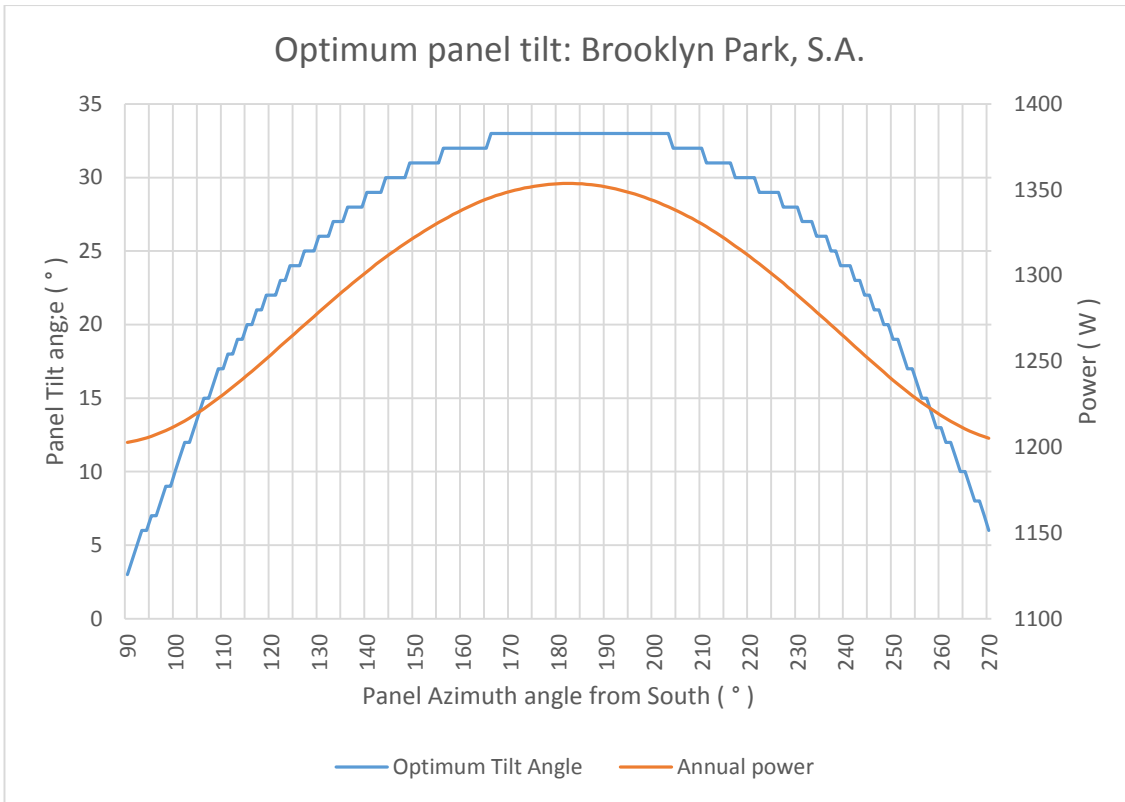


Figure E.3 – Brooklyn Park optimum tilt angle and generated power: 1° resolution

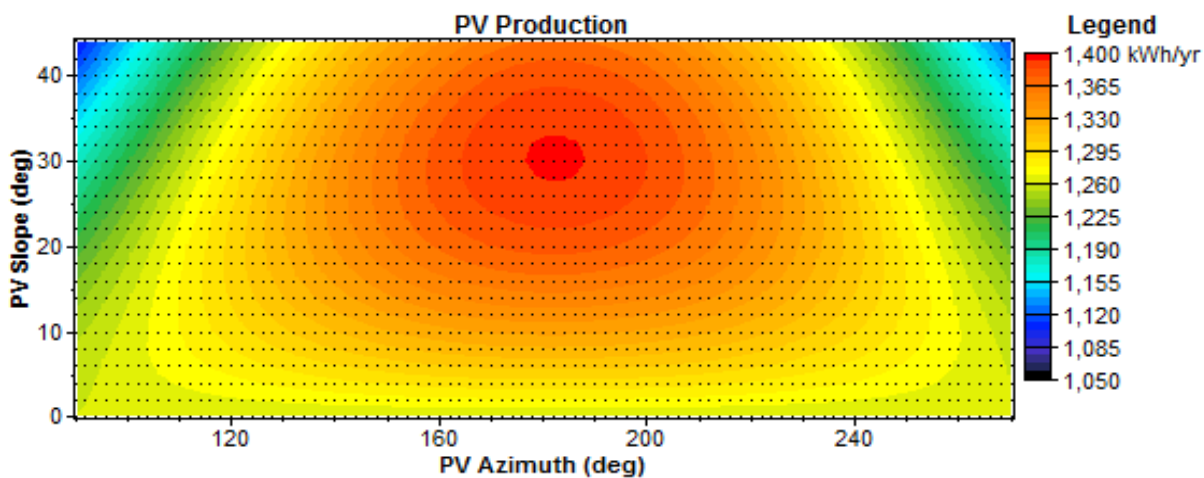


Figure E.4 – Brooklyn Park generated power surface plot: 2° resolution

E.1.2. Toowoomba

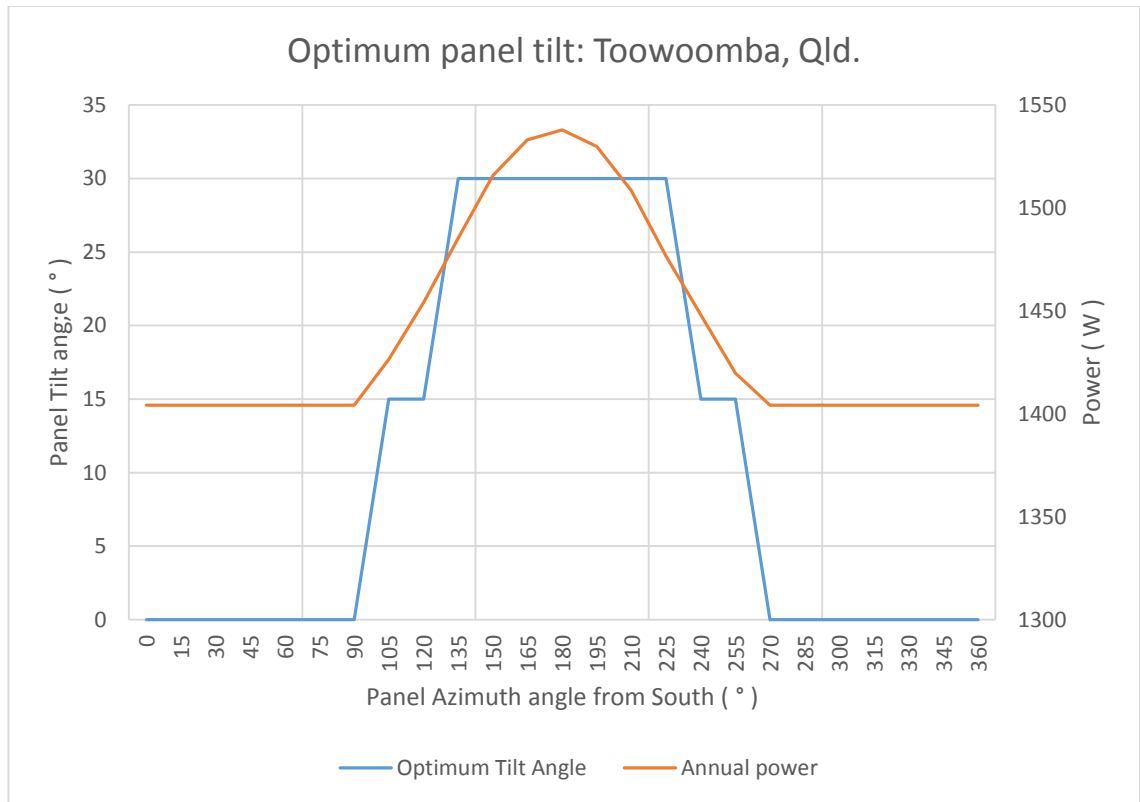


Figure E.5 – Toowoomba optimum tilt angle and generated power: 15° resolution

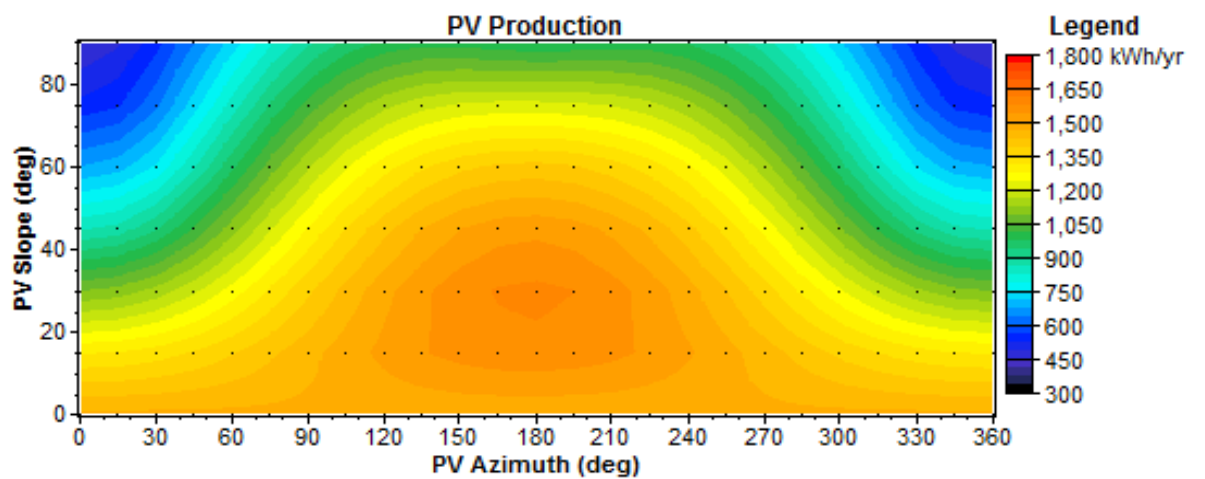


Figure E.6 – Toowoomba generated power surface plot: 15° resolution

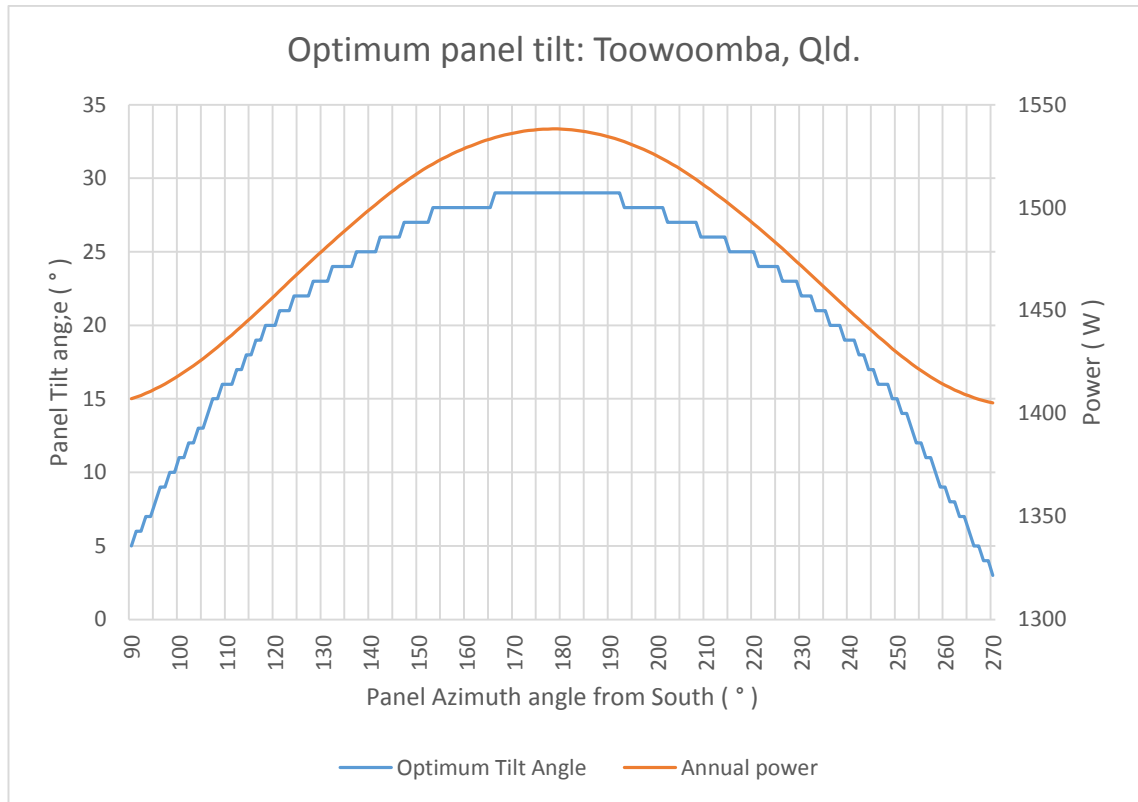


Figure E.7 – Toowoomba optimum tilt angle and generated power: 1° resolution

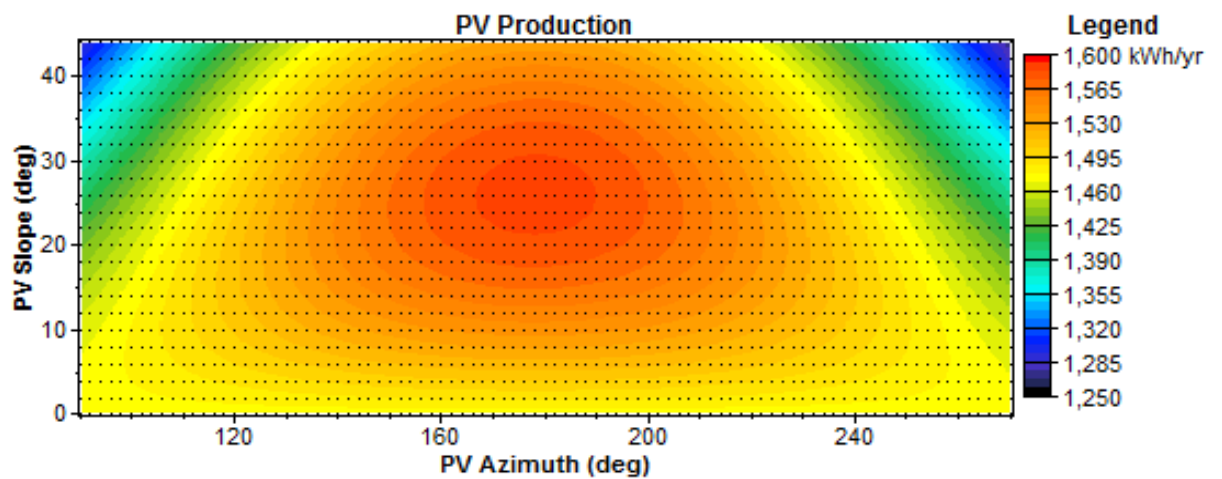


Figure E.8 – Toowoomba generated power surface plot: 2° resolution

E.1.3. Darwin.

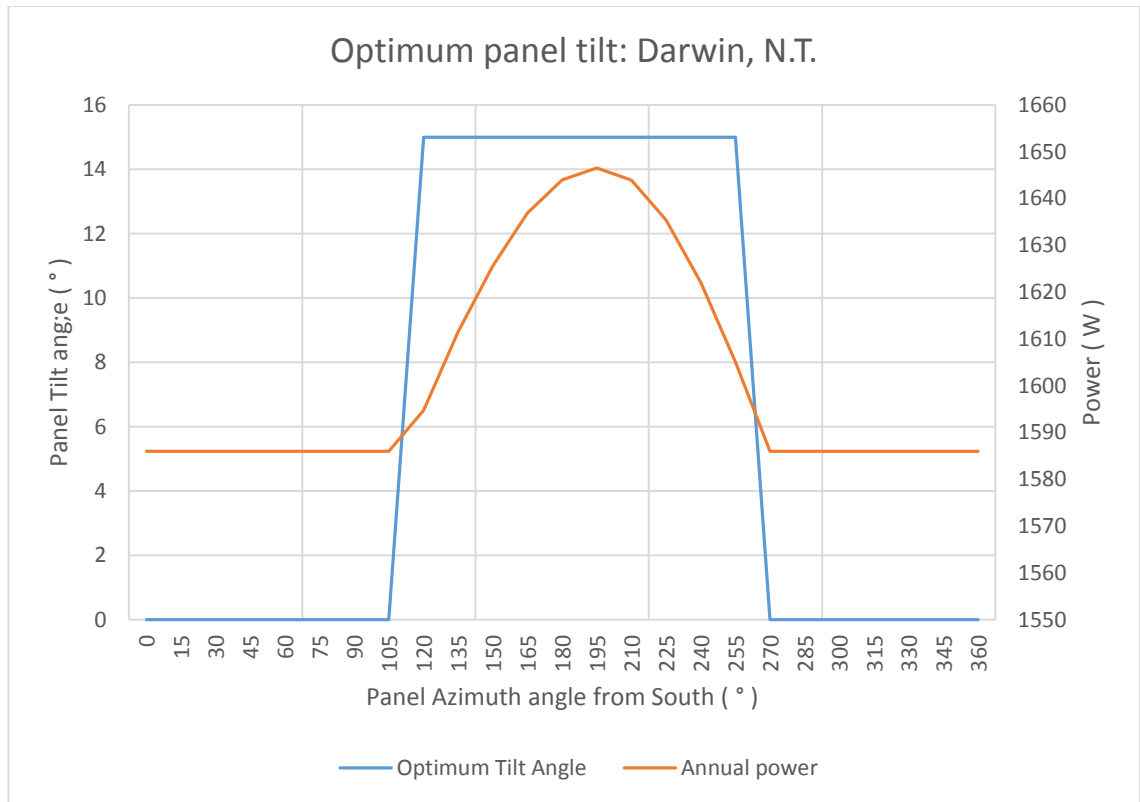


Figure E.9 – Darwin optimum tilt angle and generated power: 15° resolution

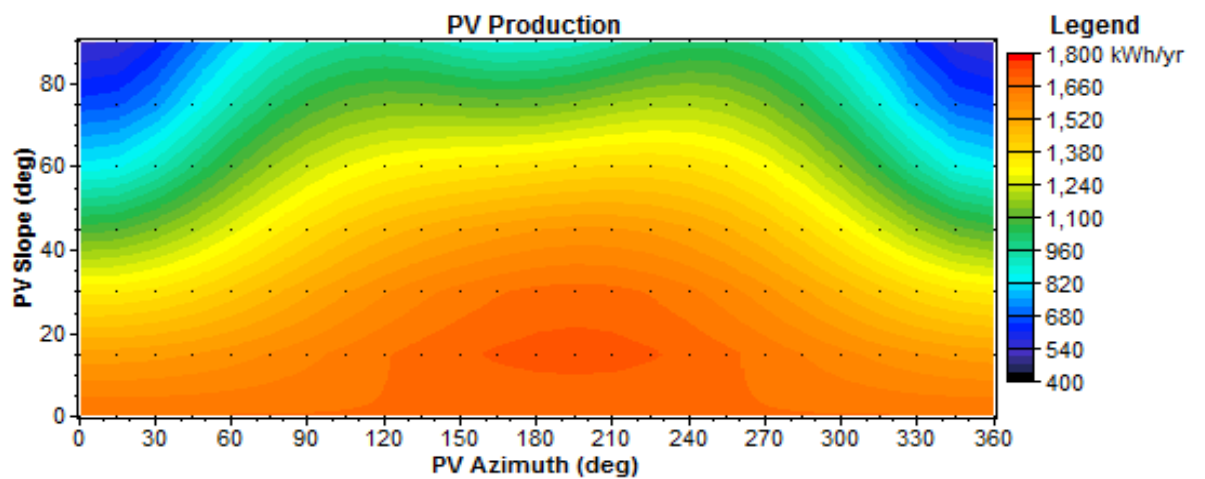


Figure E.10 – Darwin generated power surface plot: 15° resolution

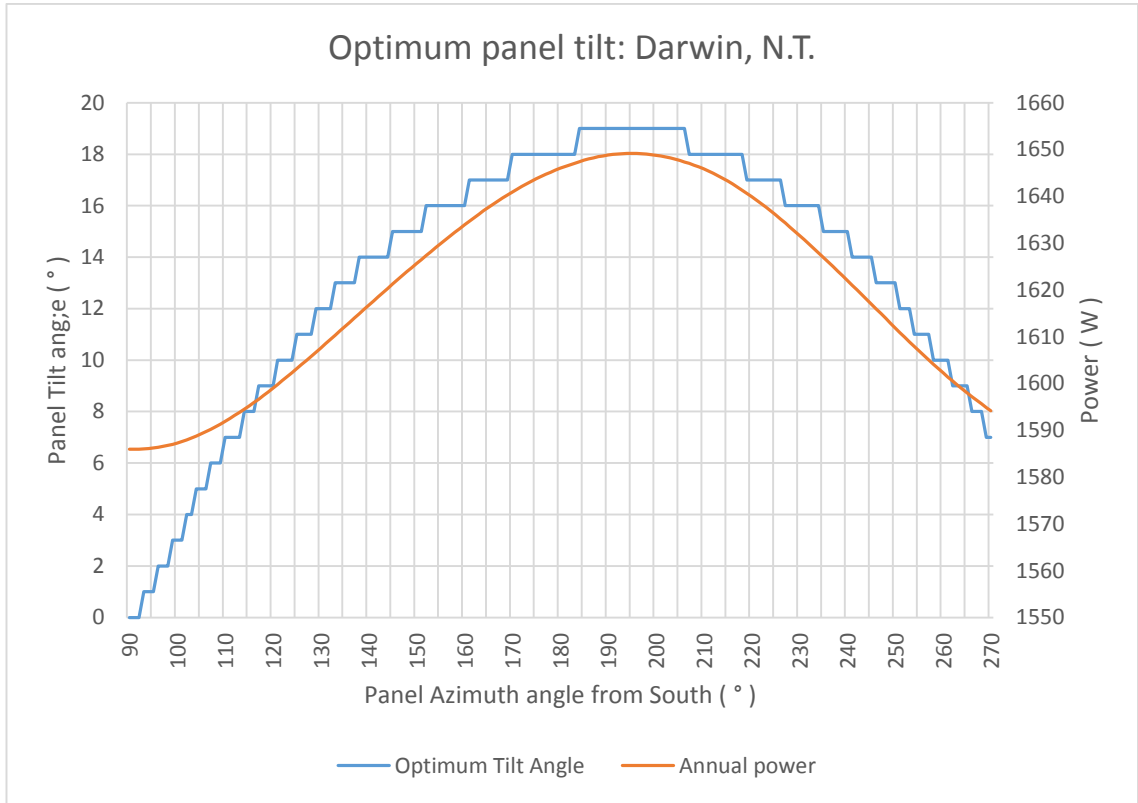


Figure E.11 – Darwin optimum tilt angle and generated power: 1° resolution

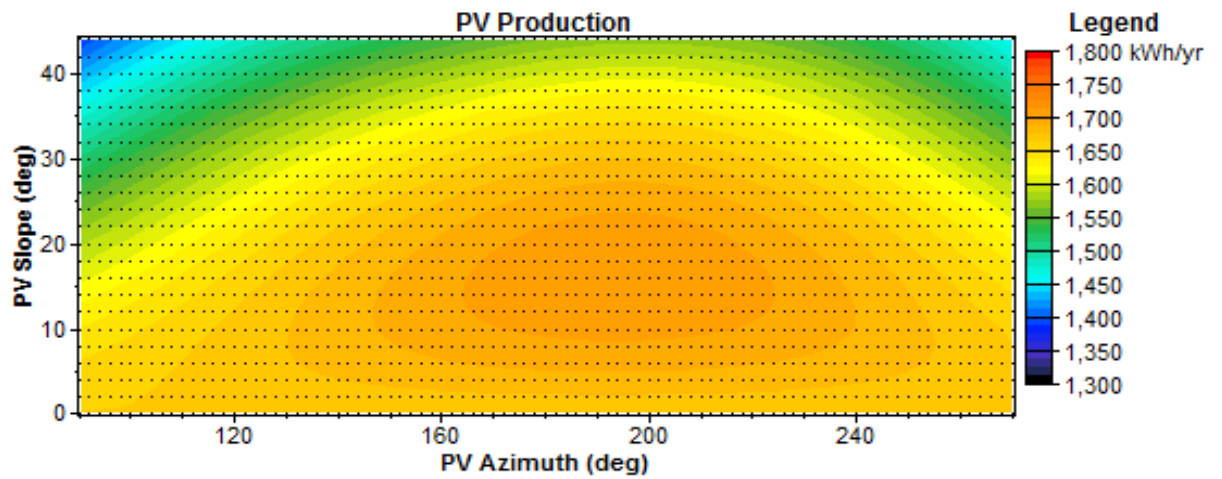


Figure E.12 – Darwin generated power surface plot: 2° resolution

E.1.4. **Hobart.**

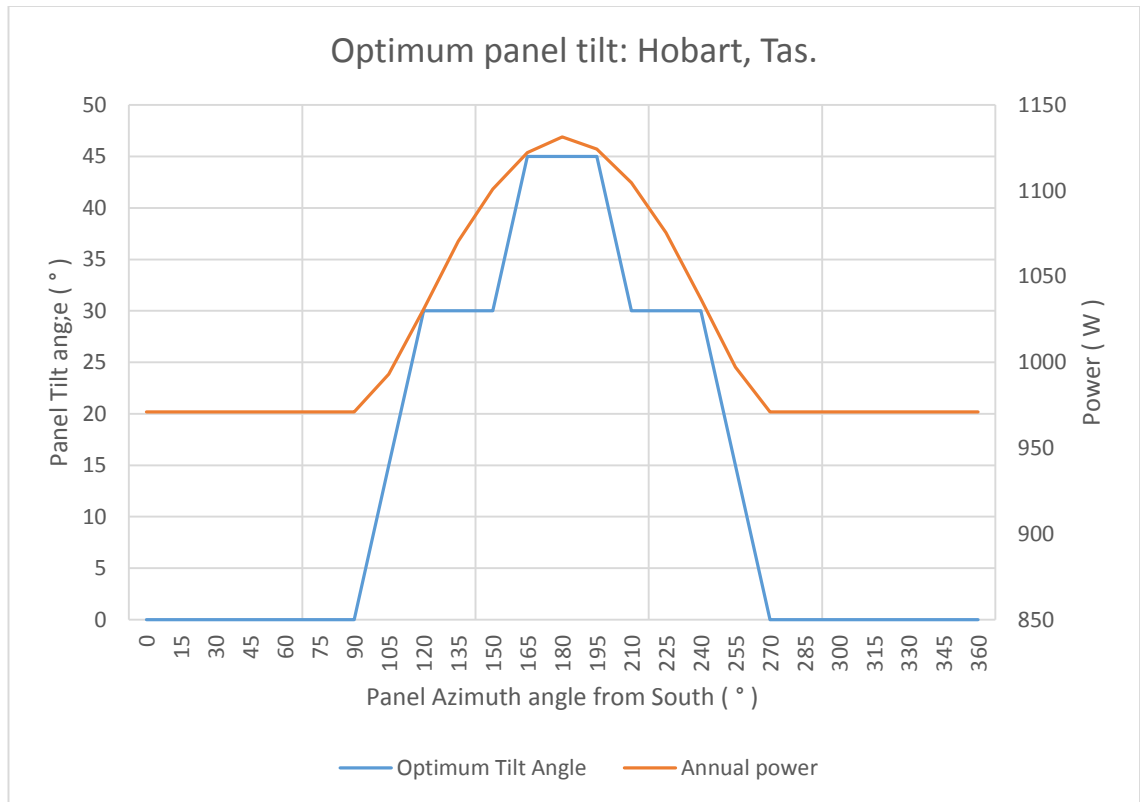


Figure E.13 – Hobart optimum tilt angle and generated power: 15° resolution

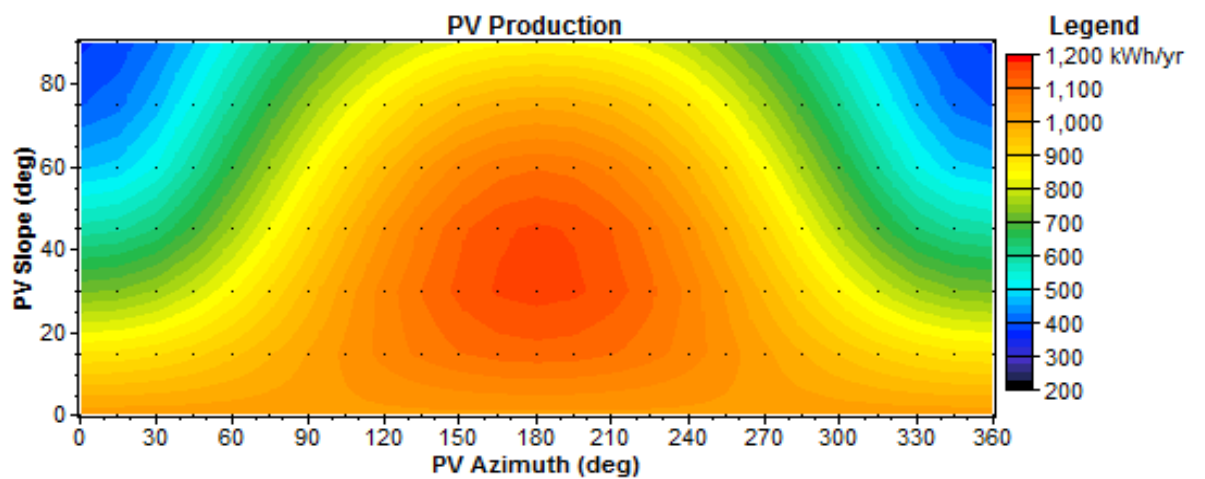


Figure E.14 – Hobart generated power surface plot: 15° resolution

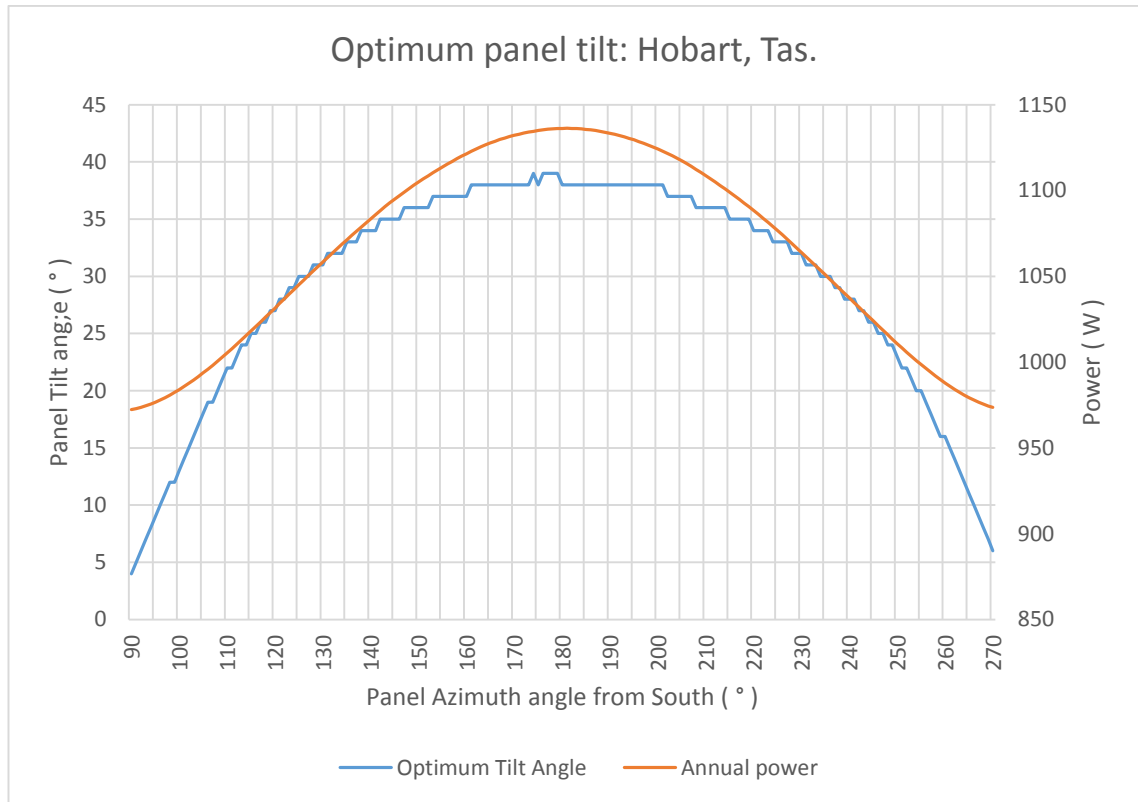


Figure E.15 – Hobart optimum tilt angle and generated power: 1° resolution

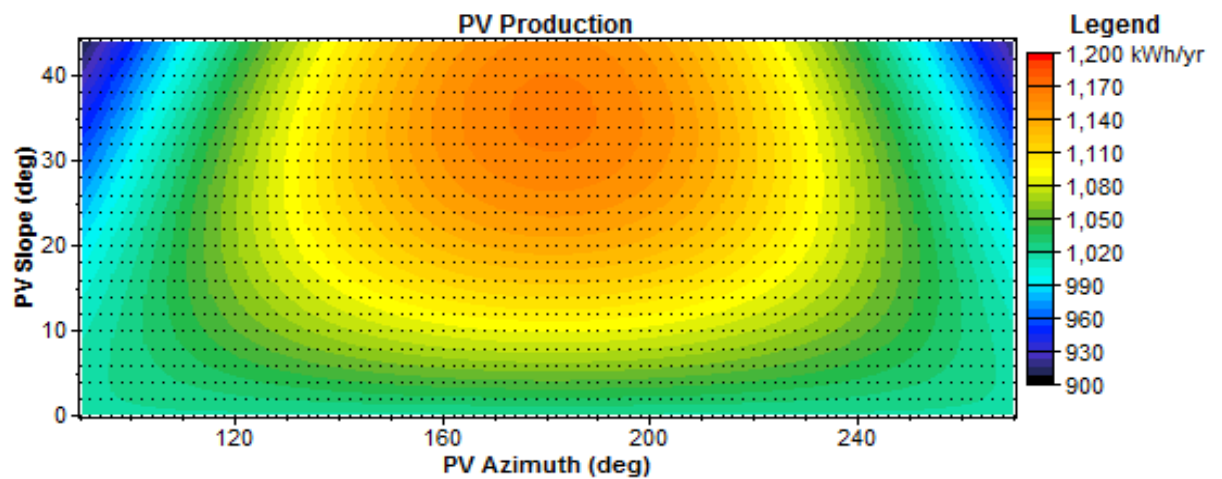


Figure E.16 – Hobart generated power surface plot: 2° resolution

E.2. Location offset plots

E.2.1. Brooklyn Park.

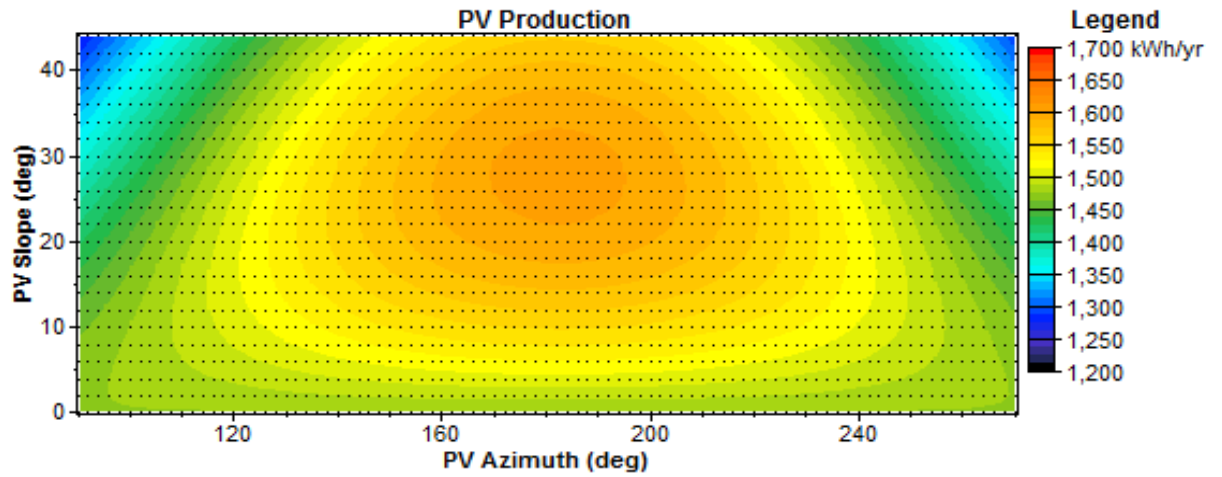


Figure E.17 – Brooklyn Park 5°N generated power surface plot: 2° resolution

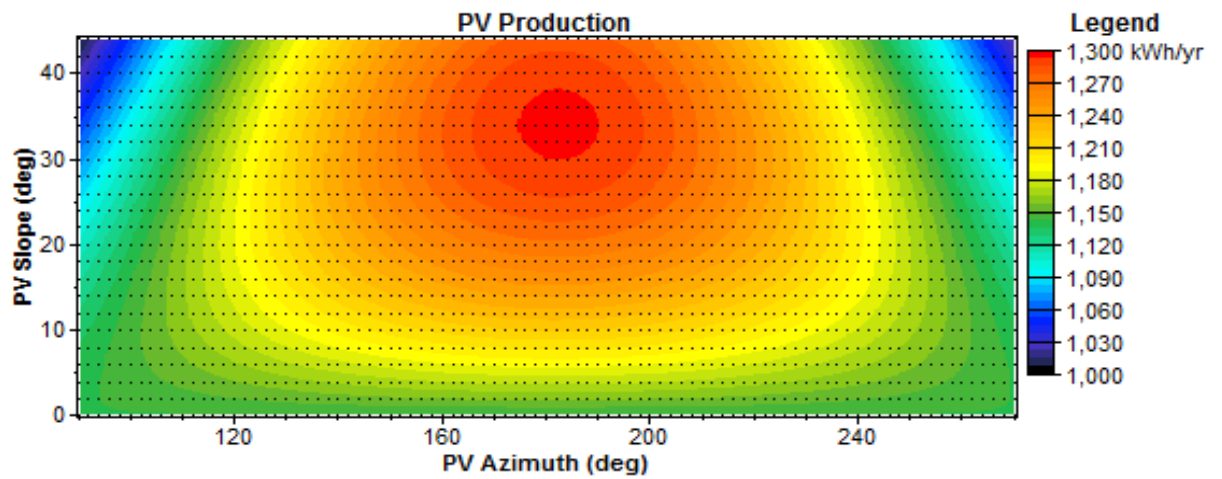


Figure E.18 – Brooklyn Park 5°S generated power surface plot: 2° resolution

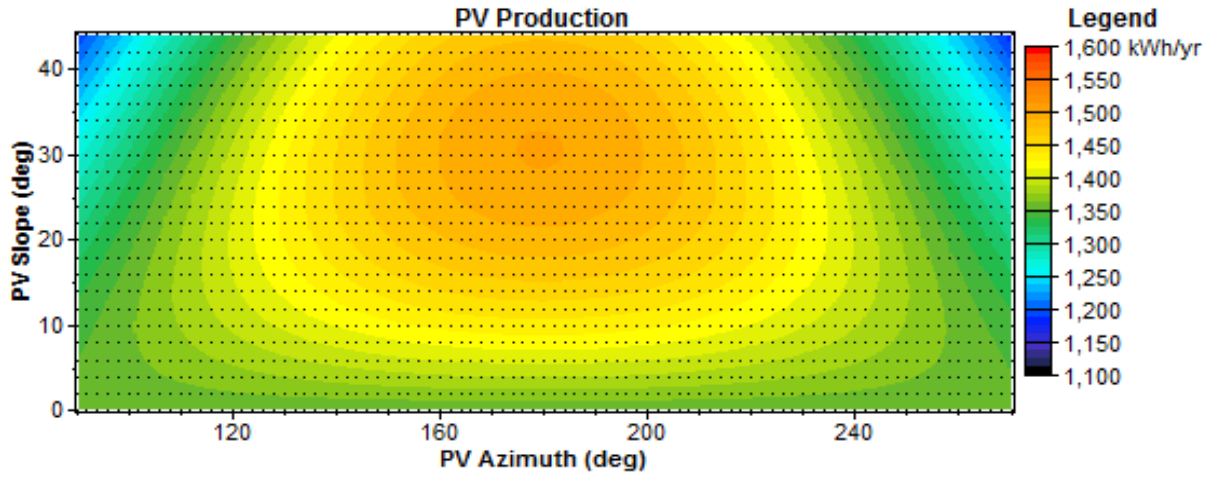


Figure E.19 – Brooklyn Park 5°E generated power surface plot: 2° resolution

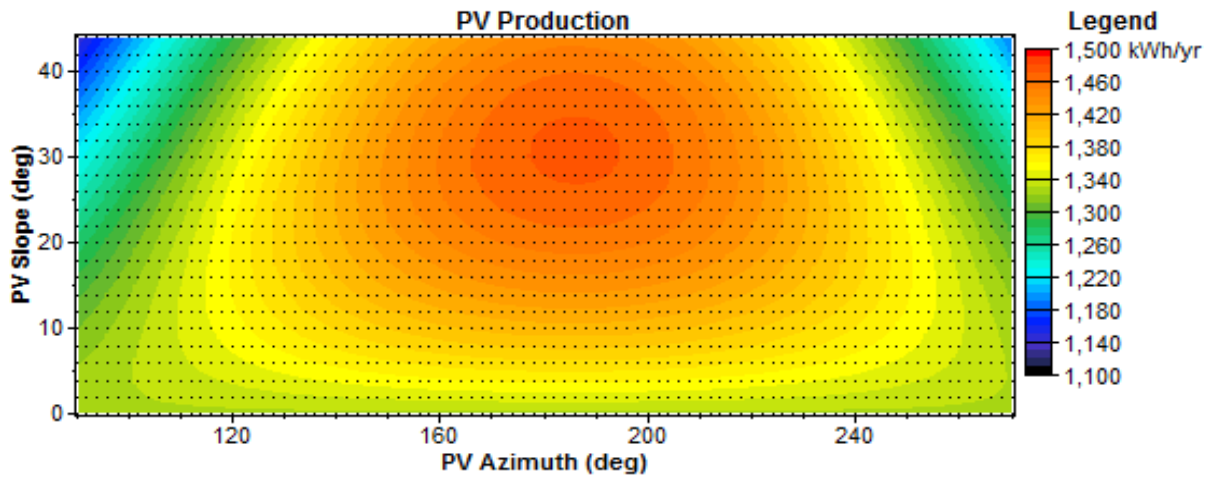


Figure E.20 – Brooklyn Park 5°W generated power surface plot: 2° resolution

E.2.2. Toowoomba

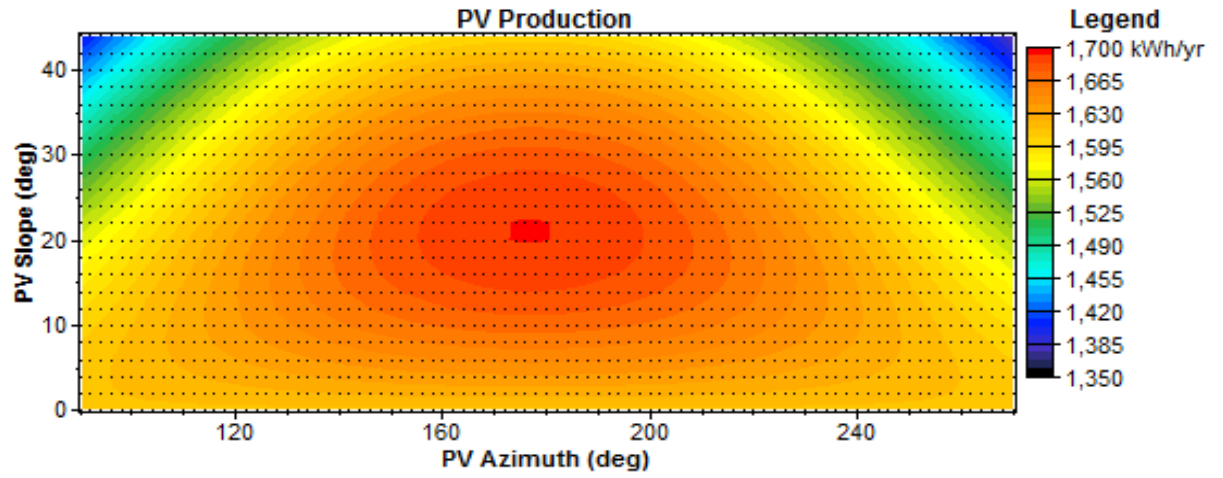


Figure E.21 – Toowoomba 5°N generated power surface plot: 2° resolution

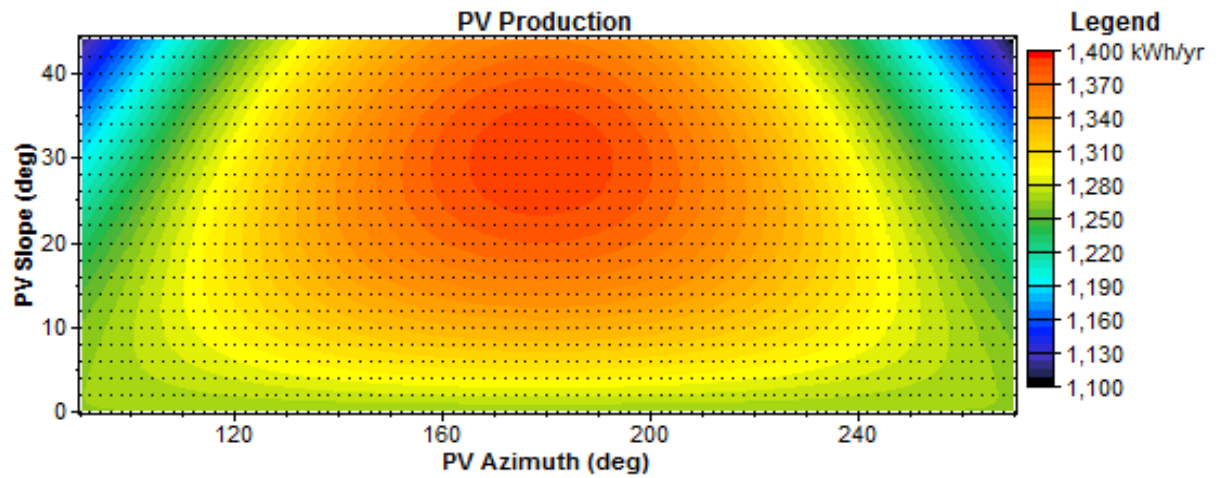


Figure E.22 – Toowoomba 5°S generated power surface plot: 2° resolution

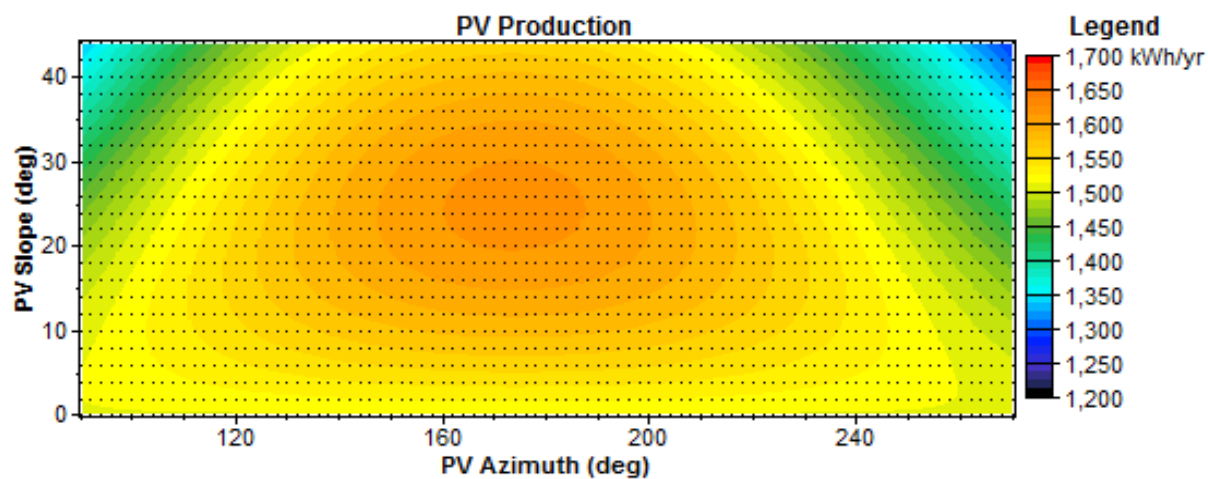


Figure E.23 – Toowoomba 5°E generated power surface plot: 2° resolution

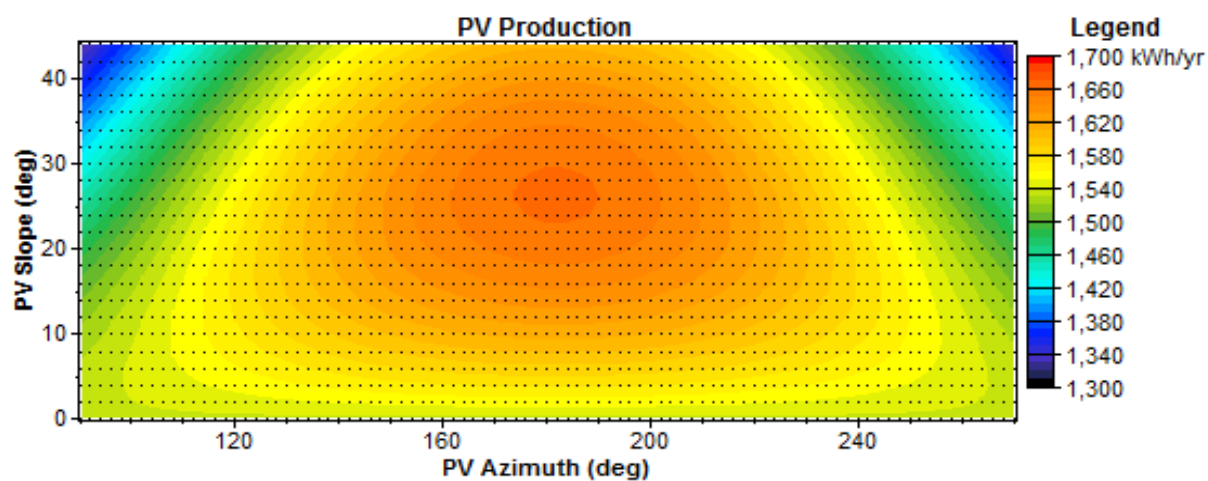


Figure E.24 – Toowoomba 5°W generated power surface plot: 2° resolution

E.2.3. Darwin.

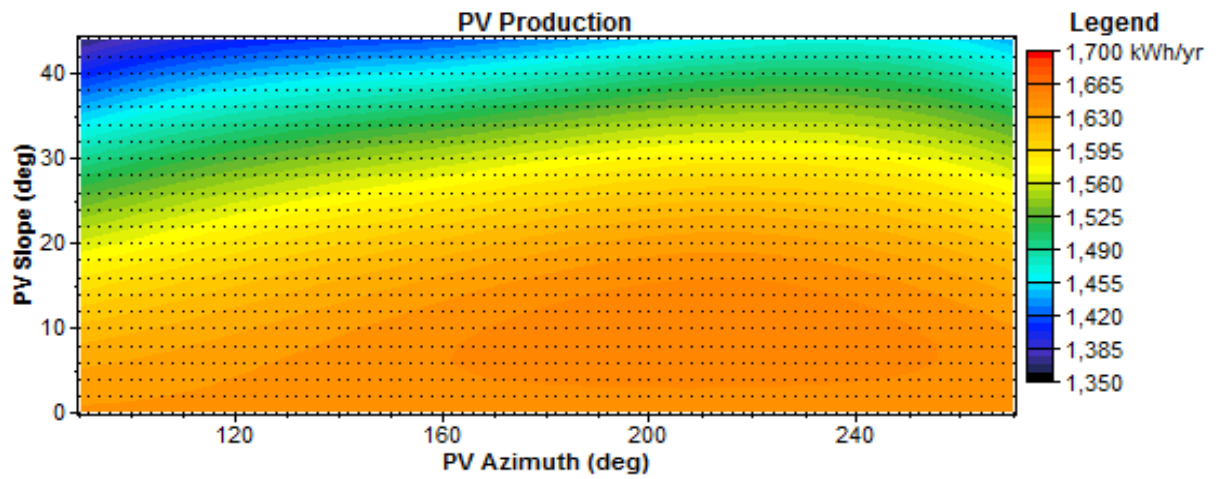


Figure E.25 – Darwin 5°N generated power surface plot: 2° resolution

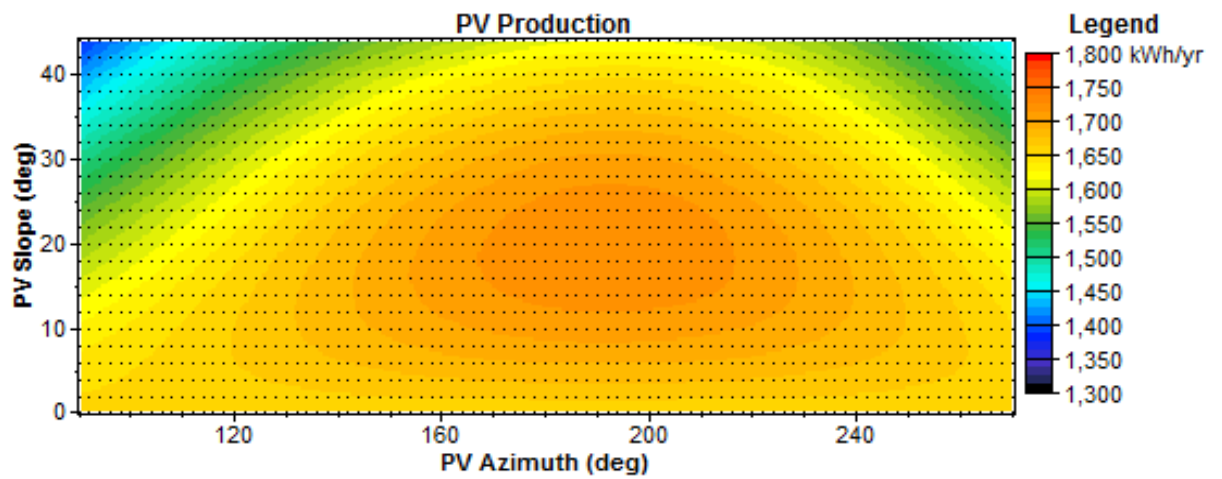


Figure E.26– Darwin 5°S generated power surface plot: 2° resolution

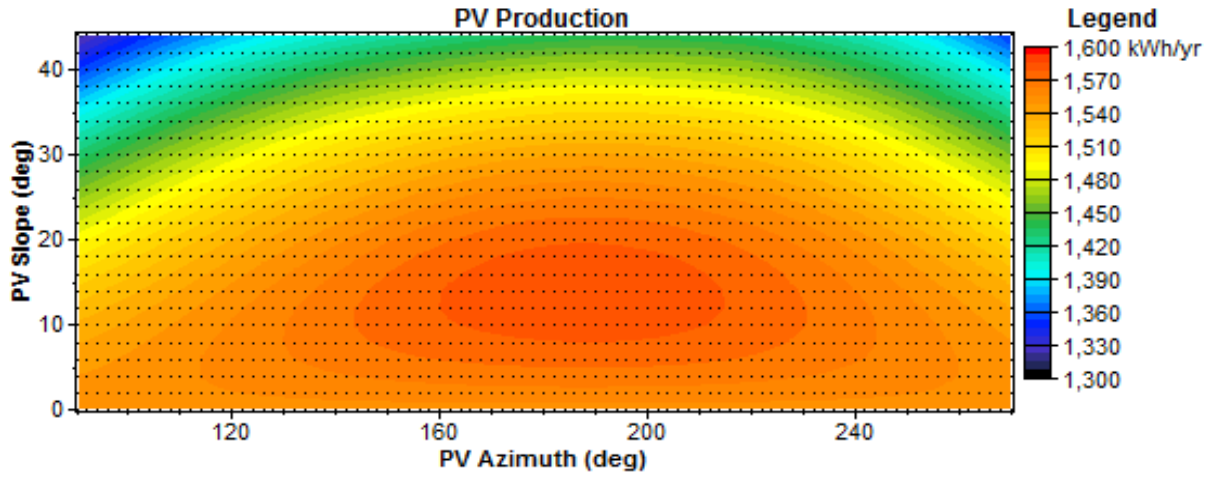


Figure E.27 – Darwin 5°E generated power surface plot: 2° resolution

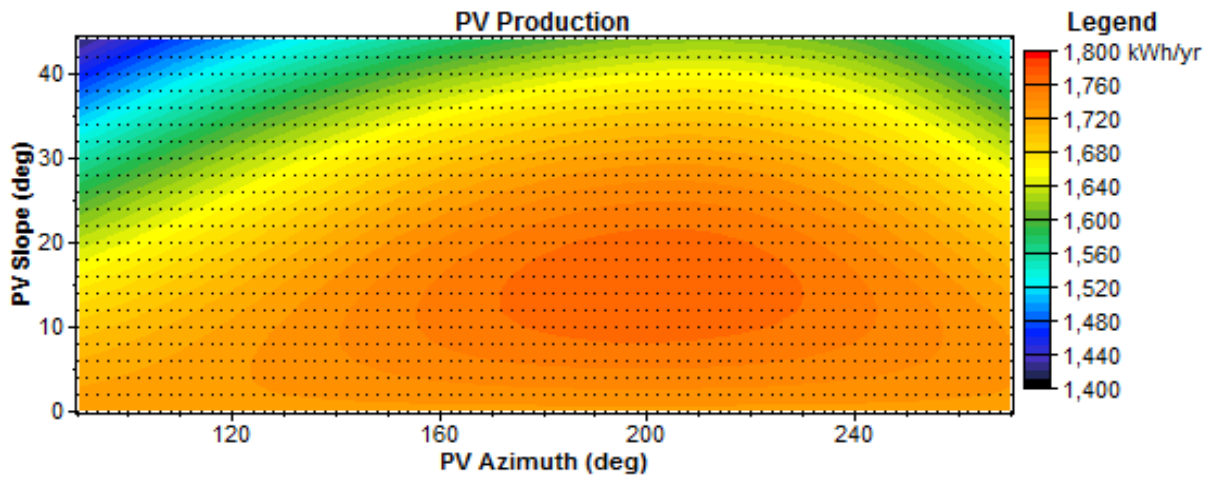


Figure E.28 – Darwin 5°W generated power surface plot: 2° resolution

E.2.4. Hobart.

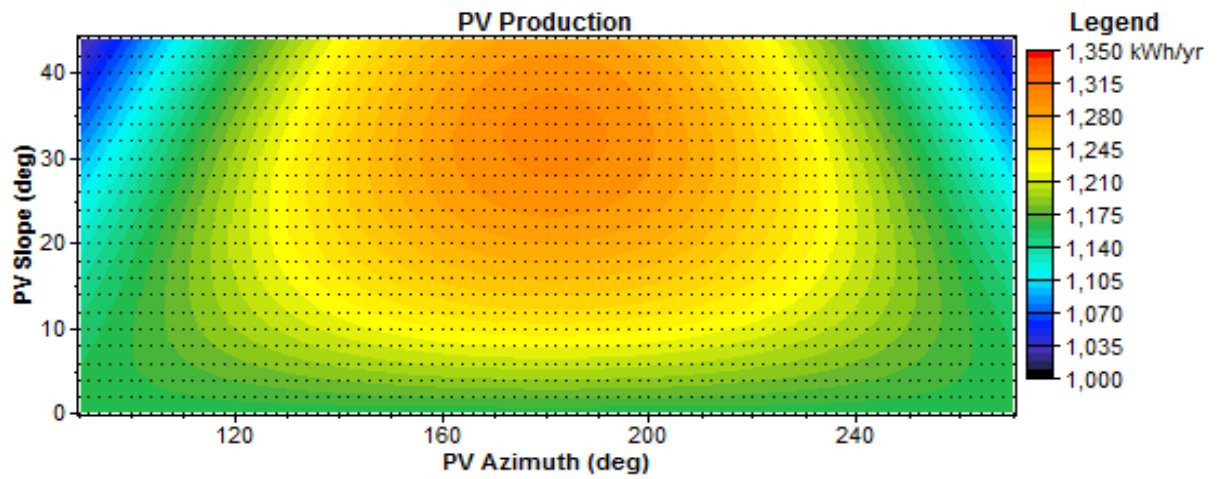


Figure E.29 – Hobart 5°N generated power surface plot: 2° resolution

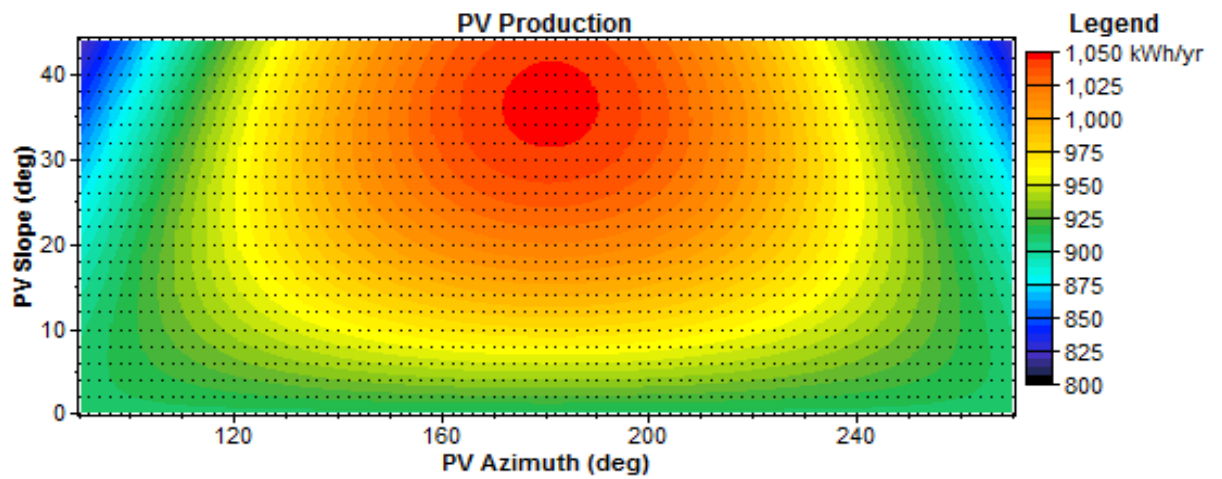


Figure E.30 – Hobart 5°S generated power surface plot: 2° resolution

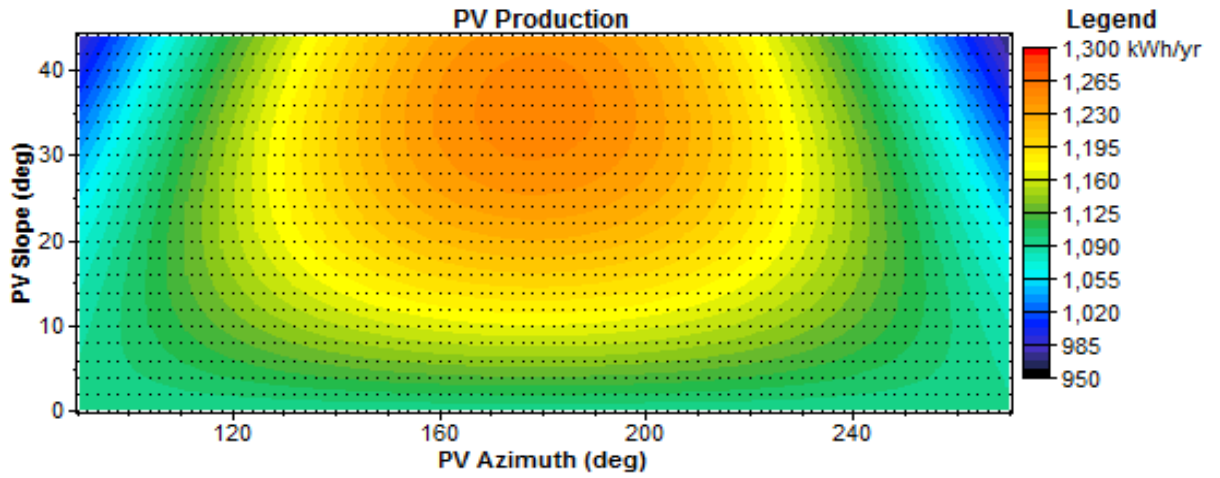


Figure E.31 – Hobart 5°E generated power surface plot: 2° resolution

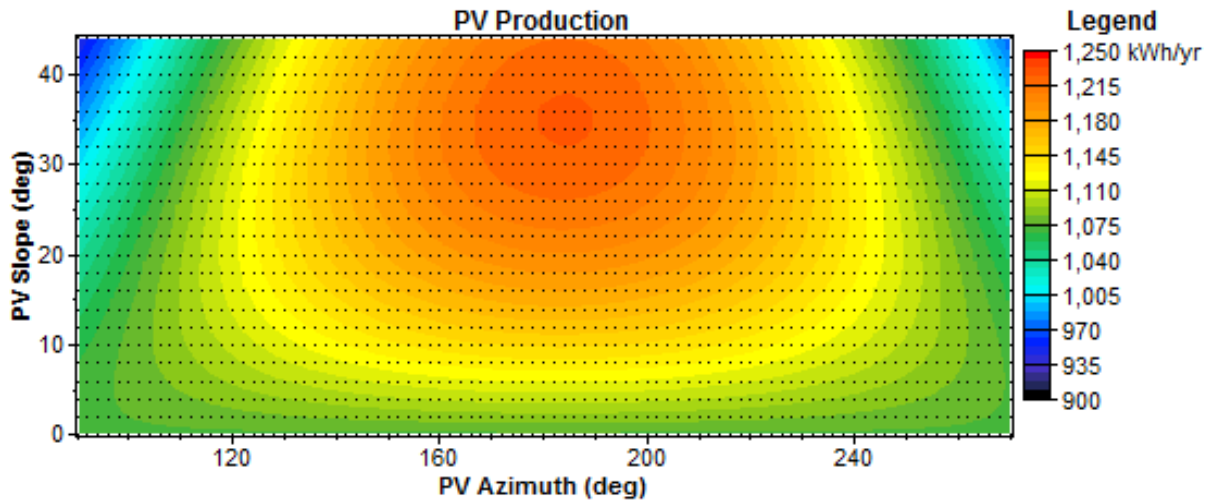


Figure E.32 – Hobart 5°W generated power surface plot: 2° resolution

Appendix F. Hazard identification and risk assessments

F.1. **Hazard identification.**

F.1.1. **Solar installations**

- Is there adequate information relating to,
 - Existing electrical installation,
 - Existing solar installation. (Applicable to site with existing solar system only)
- Does the following exist,
 - Safe working procedure,
 - Installers certified to work at heights,
 - Installer licensed to perform work on mains electrical installation,
 - Installer licensed to install solar systems.
- Have the following factors been considered during this risk assessment,
 - Input from installation workers,
 - Work related stress factors,
 - Requirements of different worker groups,
 - Requirement for PPE.
- Can risk be minimised by the following,
 - Isolating power prior to connection to mains,
 - Avoid working alone.
- Is there a risk of injury or illness due to the following,
 - Falling from heights,
 - Slipping or falling on unsuitable working surface,
 - Slipping or falling due to holes or skylights,
 - Suitability of ladder to assess working surface,
 - Tools or equipment being dropped from heights,
 - Lifting heavy items,
 - Water present around electrical work,
 - Failure to maintain minimum electrical clearance from HV power lines,
 - Electrical hazard from PV generated power,
 - Repetitive work process,
 - Prolonged kneeling or squatting.
- Any other items which have not been covered.

F.1.2. **Project.**

- Has the following been considered throughout this hazard identification.
 - Work related stress factors,
 - Risk of data loss
- Is there a risk of injury or illness due to the following,
 - Eye strain,
 - Repetitive movements,
 - Adequate lighting on the work surface,
 - Sitting for extended period of time,
 - Any other items which have not been covered.

(European Agency for Safety and Health at Work, n.d.)

F.2. **Risk matrix scores.**

The relative priority of each identified item within the risk assessment is determined using a numerical scoring process. Values for this process are detailed in table F.1, and overall risk level is detailed in table F.2. (University of Melbourne, 2004)

Table F.1 – Risk management score.

| Likelihood | | Exposure | | Consequence | |
|------------|------|------------|----|---|----|
| Certain | 1 | Permanent | 10 | Fatality / Destruction of infrastructure | 10 |
| Likely | 0.6 | Frequent | 6 | Injury requiring hospitalisation or irreversible damage / Major damage | 6 |
| Possible | 0.3 | Occasional | 3 | Injury requiring medical treatment / Minor damage to Infrastructure | 3 |
| Unlikely | 0.1 | Infrequent | 2 | Injury requiring first aid treatment / Minimal damage to Infrastructure | 2 |
| Rare | 0.05 | Rare | 1 | Negligible injury / Negligible damage to Infrastructure | 1 |

Table F.2 – Risk score.

| Risk Score | |
|------------|----------------|
| Extreme | ≥ 20 |
| High | ≥ 10 < 20 |
| Medium | ≥ 3 < 10 |
| Low | < 3 |

F.3. Risk assessment.

F.3.1. Solar installations

Date: 23/05/2015

Location: Brooklyn Park, S.A.

Table F.3 – Risk assessment: Solar installation.

| Hazard | Assessment of risk level | | | Risk level | | Control measures |
|--|--------------------------|-----|------|------------|--------|---|
| | L/hood | Exp | Conc | Score | Rating | |
| No safe working procedure | 0.3 | 6 | 10 | 18 | H | Ensure S.W.P in place before work commencing. |
| Input required by installation staff for the risk assessment | 0.1 | 6 | 6 | 3.6 | M | Consult installers for further input for the risk assessment and hazard identification. |
| Installers working alone | 0.3 | 6 | 10 | 18 | H | Installers to be within contact of another trained person at all times. |
| Working at heights / Risk of falling | 0.6 | 10 | 10 | 60 | E | Barriers installed at all roof edges prior to work commencement. |
| Lifting of heavy objects. | 0.6 | 10 | 3 | 18 | H | Mechanical lifting aids to be used, or multiple person lift. |
| Main switchboard not shielded from rain when open. | 0.3 | 6 | 6 | 10.8 | H | Cover to be installed above main switchboard. |
| Kneeling for extended time | 0.6 | 3 | 3 | 5.4 | M | Limit working time while kneeling and provide knee protection. |
| Mobile phone communication equipment located on roof. | 0.3 | 10 | 6 | 18 | H | Access to roof space to be coordinated with mobile communications providers. (Required on this site.) |

F.3.2. **Project.**

Date: 22/05/2015

Location: Home office.

Table F.4 – Risk assessment: Project.

| Hazard | Assessment of risk level | | | Risk level | | Control measures |
|---|--------------------------|-----|------|------------|--------|---|
| | L/hood | Exp | Conc | Score | Rating | |
| Stress due to heavy workload | 0.3 | 6 | 2 | 3.6 | M | Schedule time for rest away from study |
| Risk of data loss | 0.1 | 10 | 10 | 10 | H | Backup Copies of assignment on separate storage devices. |
| Eye strain from long periods looking at a computer screen | 0.3 | 3 | 2 | 1.8 | L | Limit computer usage. Utilise written sources of information where possible. |
| Repetitious movements | 0.3 | 3 | 6 | 5.4 | M | Limit computer usage. |
| Inadequate lighting in study | 0.6 | 3 | 2 | 3.6 | M | Install desk light to increase lighting. |
| Sitting for long time | 0.3 | 3 | 2 | 1.8 | L | Limit working period. |

Appendix G. Specification sheets

G.1. Hareon Solar specification sheet

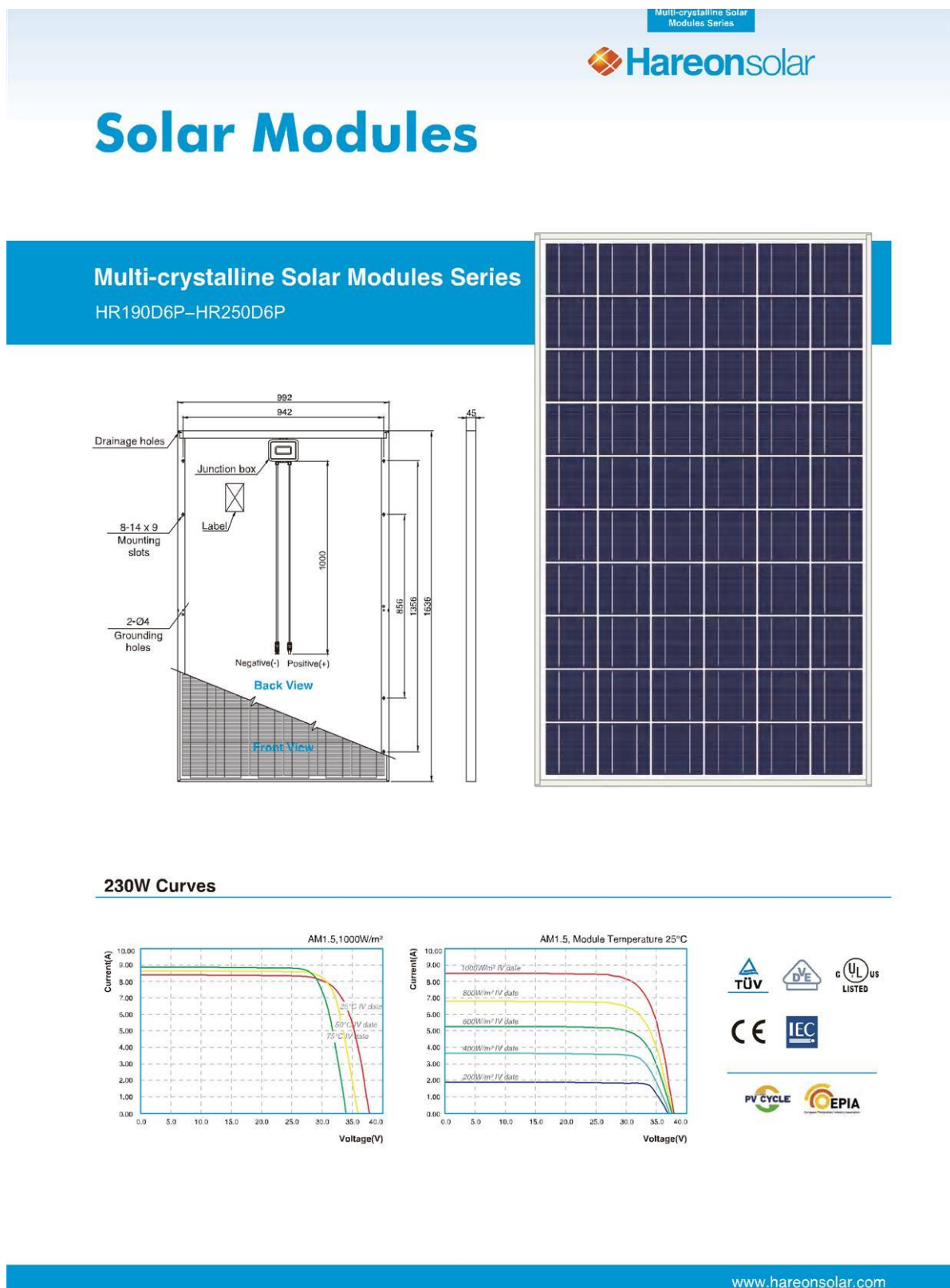


Figure G.1a – Hareon solar specification sheet

Jiangyin Hareon Power Co Ltd, n.d.

Jiangyin Hareon Power Co., Ltd.

■ Performance

| | |
|----------|--|
| Warranty | 90% power output over 12 years 80% power output over 25 years |
| | Free from defects in materials and workmanship for 10 years |

■ Qualification Test

| | |
|-----------------------------|--|
| Temperature cycling range | - 40°C to +85°C for 200 cycles |
| Damp heat test | 85°C and 85 relative humidity for 1000 h |
| Front & rear wind load test | 2400 Pa |
| Hot spot free | 100% EL inspection before and after lamination |

■ Electrical Characteristics

| Cell Type(mm) | 156 X 156 Poly Solar Cell | | | | | | | | | | | | | |
|------------------------------------|---------------------------|---------|---------|---------|---------|---------|---------|---------|---------|---------|---------|---------|---------|--|
| Item | HR-190W | HR-195W | HR-200W | HR-205W | HR-210W | HR-215W | HR-220W | HR-225W | HR-230W | HR-235W | HR-240W | HR-245W | HR-250W | |
| Max power (Wp) | 190 | 195 | 200 | 205 | 210 | 215 | 220 | 225 | 230 | 235 | 240 | 245 | 250 | |
| Max power voltage (Vm) | 28.80 | 28.80 | 28.90 | 29.00 | 29.10 | 29.20 | 29.30 | 29.40 | 29.50 | 29.60 | 29.70 | 29.80 | 29.90 | |
| Max power current (Im) | 6.60 | 6.78 | 6.93 | 7.07 | 7.22 | 7.37 | 7.51 | 7.66 | 7.82 | 7.94 | 8.08 | 8.22 | 8.36 | |
| Open circuit voltage (Voc) | 36.00 | 36.00 | 36.10 | 36.20 | 36.30 | 36.40 | 36.50 | 36.60 | 36.70 | 36.80 | 36.90 | 37.00 | 37.10 | |
| Short circuit current (Isc) | 6.94 | 7.13 | 7.29 | 7.45 | 7.61 | 7.77 | 7.93 | 8.08 | 8.25 | 8.38 | 8.52 | 8.67 | 8.81 | |
| Module eff (%) | 11.71 | 12.01 | 12.32 | 12.63 | 12.94 | 13.25 | 13.56 | 13.86 | 14.17 | 14.48 | 14.79 | 15.10 | 15.40 | |
| Max series fuse | | | | | | | | | | | | | | 15 A |
| Number of diode | | | | | | | | | | | | | | 3 |
| Number of cells | | | | | | | | | | | | | | 60 |
| Max system voltage | | | | | | | | | | | | | | 600 VDC |
| Temperature coefficients of Pm | | | | | | | | | | | | | | -0.44%/°C |
| Temperature coefficients of Voc | | | | | | | | | | | | | | -0.32%/°C |
| Temperature coefficients of Isc | | | | | | | | | | | | | | 0.055 %/°C |
| Nominal operating cell temperature | | | | | | | | | | | | | | 45 °C ± 3 °C |
| Output tolerance | | | | | | | | | | | | | | 0 ~5W, +/-3% |
| Standard test conditions | | | | | | | | | | | | | | STC: AM1.5, 1000 W/m ² , Module Temperature 25 °C |

■ Mechanical Characteristics

| | |
|---|--|
| Dimensions (mm) | 1636x 992x 45 |
| Weight (kg) | 19.5 |
| Solar Cells | 60 cells(156 mm x 156 mm) configured geometrically for a 6 x 10 matrix connected in series |
| Output cables lengths (mm) | 1000 |
| Cable cross section size (mm ²) | 4 |
| Construction | Front: High transmission 3.2mm tempered glass. Rear: White backsheet; Encapsulant: EVA. |

G.2. **Tindo Solar specification sheet**



The image is a promotional graphic for the Tindo Solar Karra 260 solar panel. It features a blue background with a white border. In the top right corner, there is a faint 'tindo' logo with a sun icon. The main text 'tindo solar' is in orange and grey. Below it, 'Karra 260' is in large white font, followed by 'The most powerful panel in the Tindo range' in smaller white font. A worker in an orange shirt and yellow hard hat is shown working on a solar panel. A circular logo with a kangaroo silhouette and the text 'Australian Made' is positioned in the lower left. The bottom of the graphic has an orange banner with the text 'Engineered For Australian Conditions'.

tindo
solar

Karra 260
The most powerful panel in the Tindo range

Australian Made

Engineered For Australian Conditions

Figure G.2a – Tindo solar specification sheet

Data Sheet Karra Model

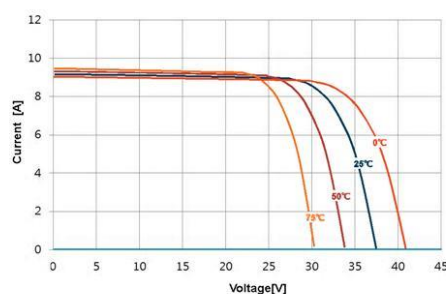
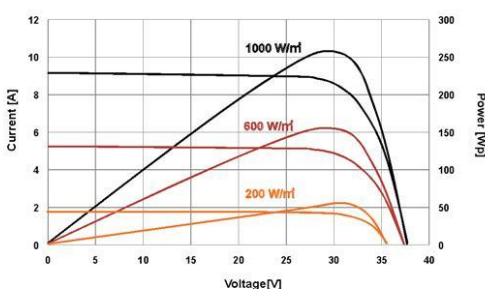
Electrical Characteristics

| 60Cells Panel Description | | Karra-240 | Karra-245 | Karra-250 | Karra-255 | Karra-260 |
|-----------------------------|------|-----------|-----------|-----------|-----------|-----------|
| Item | Unit | | | | | |
| Max. Power (Pmax) | Wp | 240 | 245 | 250 | 255 | 260 |
| Max. Power voltage (Vmp) | V | 29.6 | 29.8 | 30 | 30.2 | 30.4 |
| Max. Power current (Imp) | A | 8.1 | 8.2 | 8.3 | 8.4 | 8.6 |
| Open circuit voltage (Voc) | V | 37.3 | 37.5 | 37.7 | 37.9 | 38.1 |
| Short circuit current (Isc) | A | 8.7 | 8.7 | 8.8 | 8.8 | 8.8 |
| Panel efficiency | % | 14.3 | 14.6 | 15.0 | 15.3 | 15.6 |
| Power tolerance | % | ±3 | | | | |

*STC(Standard Test Condition) : 1,000W/m², AM 1.5, 25°C



Irradiance & Temperature Curves



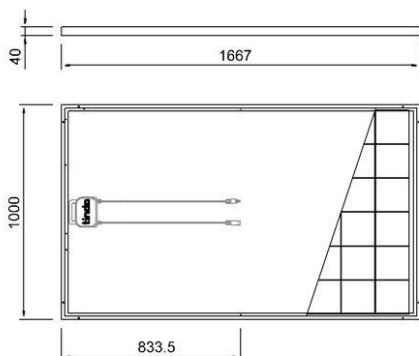
Mechanical Characteristics

| | |
|-----------------------------|---|
| Cells per Panel | 60 Cells (6 x 10) |
| Cell Type | 156 x 156 mm Multi-crystalline |
| Panel Dimension (L x W x H) | 1,667 x 1,000 x 40 mm |
| Panel Weight | 18.5 kg (without inverter / 2.3 kg) |
| Front Glass | 3.2 mm Tempered Glass |
| Back Sheet | DuPont Tedlar film-based |
| Junction Box | Rated Current 18A / Rated Voltage 1000V(IEC) / IP65 |
| Frame | Anodized Aluminum |
| Output cable | 600mm / 4mm ² cable |
| Edge seal & J-box Sealant | Dow Corning |

Qualification Tests & Warranty

| | |
|----------------------------|--|
| Front load test | 2400 Pa (Snow) |
| Rear static load test | 5400 Pa (Wind) |
| Safety application class | Class A |
| Fire Safety Classification | Class C |
| Certifications | IEC 61215, IEC 61730 |
| Hallstone impact test | 25mm hallstone at 23m/s from 1m distance |
| Warranty | 10 years limited product warranty |
| Performance guarantee | 25 years limited warranty 80% power |
| PID Resistance | Yes as tested by Fraunhofer Institute |

Panel Drawing



Tindo Solar
tindosolar.com Phone 1300 846 367 6 Second Avenue Mawson Lakes SA 5095